COMPOSITION AND MOLECULAR MECHANISMS OF ROYAL JELLY'S ACTIVE INGREDIENTS: PROTECTIVE EFFECTS ON HUMAN LYMPHOCYTES, CYTOTOXIC EFFECTS ON MCF-7 BREAST CANCER CELL LINE

BY

MISS WANTHA JENKHETKAN

A DISSERTATION SUBMITTED IN PARTIAL FULFILLMENT OF THE
REQUIREMENTS FOR THE DEGREE OF DOCTOR OF PHILOSOPHY
PROGRAM IN BIOCHEMISTRY AND MOLECULAR BIOLOGY
FACULTY OF MEDICINE
THAMMASAT UNIVERSITY
ACADEMIC YEAR 2017
COPYRIGHT OF THAMMASAT UNIVERSITY

COMPOSITION AND MOLECULAR MECHANISMS OF ROYAL JELLY'S

ACTIVE INGREDIENTS: PROTECTIVE EFFECTS ON HUMAN LYMPHOCYTES,

CYTOTOXIC EFFECTS ON MCF-7 BREAST CANCER CELL LINE

BY

MISS WANTHA JENKHETKAN

A DISSERTATION SUBMITTED IN PARTIAL FULFILLMENT OF THE

REQUIREMENTS FOR THE DEGREE OF DOCTOR OF PHILOSOPHY

PROGRAM IN BIOCHEMISTRY AND MOLECULAR BIOLOGY

FACULTY OF MEDICINE

THAMMASAT UNIVERSITY

ACADEMIC YEAR 2017

COPYRIGHT OF THAMMASAT UNIVERSITY

THAMMASAT UNIVERSITY

FACULTY OF MEDICINE

DISSERTATION

BY

MISS WANTHA JENKHETKAN

ENTITLED

COMPOSITION AND MOLECULAR MECHANISMS OF ROYAL JELLY'S ACTIVE
INGREDIENTS: PROTECTIVE EFFECTS ON HUMAN LYMPHOCYTES,
CYTOTOXIC EFFECTS ON MCF-7 BREAST CANCER CELL LINE

was approved as partial fulfillment of the requirements for

the degree of Doctor of Philosophy

on July 11, 2018

Chairman _____

(Professor Maitree Suttajit, Ph.D.)

Member and Advisor _____

(Associate Professor Treetip Ratanavalachai, Ph.D.)

Member and co-advisor _____

(Assistant Professor Supranee Kongkham, Ph.D.)

Member _____

(Associate Professor Arunporn Itharat, Ph.D.)

Member _____

(Assistant Professor Pintusorn Hansakul, Ph.D.)

Dean _____

(Associate Professor Dilok Piyayotai, M.D.)

Dissertation Title	COMPOSITION AND MOLECULAR MECHANISMS OF ROYAL JELLY'S ACTIVE INGREDIENTS: PROTECTIVE EFFECTS ON HUMAN LYMPHOCYTES, CYTOTOXIC EFFECTS ON MCF-7 BREAST CANCER CELL LINE
Author	Miss Wantha Jenkhetkan
Degree	Doctor of Philosophy
Major Field/Faculty/University	Biochemistry and Molecular Biology Faculty of Medicine Thammasat University
Dissertation Advisor	Associate Professor Treetip Ratanavalachai, Ph.D.
Dissertation Co-Advisor	Assistant Professor Supranee Kongkham, Ph.D.
Academic Year	2017

ABSTRACT

Royal jelly (RJ), a nutritious natural product from bees, is used as a traditional medicine for health promotion and longevity. 10-hydroxy-2-decenoic acid (10-H2DA), the unique fatty acid in RJ, also has anti-angiogenic and anti-tumor activities. However, molecular mechanisms on their cancer prevention and anti-cancer properties are still inconclusive. The study aimed to elucidate the cytogenetic effects and molecular mechanisms of RJ and its ingredients as chemopreventive and chemotherapeutic agents. Genotoxic and antigenotoxic effects against doxorubicin (DXR) of RJ, ethereal extract (EE), defatted material (DM), and 10-H2DA were investigated by the *in vitro* sister chromatid exchange (SCE) assay. Cytotoxic and antiproliferative effects of 10-H2DA alone and 10-H2DA co-treatments with DXR against MCF-7 breast cancer cells were evaluated by the MTS tetrazolium assay.

Gene expression modulations were detected by Western blot analysis. Cell cycle distribution, cell apoptosis were determined by flow cytometry. Morphological changes were detected by Hoechst 33258/propidium iodide double staining. We revealed that RJ treatments (0.0005-0.5 mg/mL) were not genotoxic nor cytotoxic on

human lymphocytes by the *in vitro* SCE assay. The lowest dose of RJ maximally enhanced cell proliferation, cell survival, longevity, and antioxidative response through induction of c-MYC/BAX, BCL2/BAX, h-TERT/BAX and NRF2/BAX. It activated G1/S, G2/M progression through increased cyclin E1 and cyclin B1.

On the contrary, the highest dose at 5 mg/mL RJ significantly increased SCE level. Nevertheless, pretreatment of 5 mg/mL RJ significantly decreased DXR-induced SCE levels. RJ (5 mg/mL) co-treatment with DXR protected human cells through reduction of cell apoptosis, increased antioxidative response and enhanced longevity. It delayed G2/M cell cycle through decreased cyclin B1, possibly allowing cells to repair.

Moreover, 125 μg/mL 10-H2DA significantly inhibited MCF-7 cell proliferation through induction of cell cycle arrest (decreased cyclin D1 and CDK4), cell apoptosis (decreased BCL2/BAX), shortened lifespan (decreased hTERT), and inhibited oncoprotein c-MYC. The co-treatment of DXR with 125 μg/ml 10-H2DA potentiated DXR-induced antiproliferative effects against MCF-7 cells. It enhanced cell apoptosis, cell cycle arrest and inhibited cell proliferation (decreased c-MYC). Unpredictably, all above treatments increased NRF2, the antioxidative response.

Therefore, RJ is a promising candidate as a chemopreventive agent by stimulating human cell growth, longevity and antioxidative response; with correct doses, it protects cells from genotoxic damage. Also, 10-H2DA is a promising candidate for chemotherapy by inhibiting breast cancer cells through enhancing cell apoptosis, inducing cell cycle arrest, shortening lifespan and inhibiting cell proliferation; adding DXR enhanced antiproliferative properties. Further *in vitro* and *in vivo* studies are needed to confirm the evidence.

ACKNOWLEDGMENTS

TABLE OF CONTENTS

LIST OF TABLES

LIST OF FIGURES

LIST OF ABBREVIATIONS

Symbols/Abbreviations	Terms
%	Percent
μL	Microliter
μg	Microgram
μM	Micromolar
°C	Degree Celsius
10-H2DA	10-Hydroxy-2-decenoic acid
BAX	BCL2 associated X protein
BCL2	B-cell lymphoma 2
CDK4	Cyclin-dependent kinase 4
CO_2	Carbon dioxide
DMSO	Dimethyl sulphoxide
DM	Defatted material
DNA	Deoxyribonucleic acid
DXR	Doxorubicin
EE	Ethereal extract
et al.	et alibi, and other
FCS	Fetal calf serum
g	Gram
GPx	Glutathione peroxidase
h	Hour
HO-1	Heme oxygenase-1
HPLC	High performance liquid chromatography
hTERT	Human telemorase revese transcriptase
IC_{50}	50% Inhibitory concentration
LC_{50}	50% lethal concentration
M	Molar (concentration)

mg	Milligram
mL	Milliliter
mM	Millimolar
mole	Mole
nm	Nanometer
NRF2	Nuclear factor erythroid-2 related factor2
O.D.	Optical density
PBS	Phosphate buffered saline
PI	Propidium iodide
PVDF	Polyvinylidene fluoride
RJ	Royal jelly
ROS	Reactive oxygen species
Rpm	Revolutions per minute
SD	Standard deviation
SDS	Sodium dodecyl sulfate
SDS-PAGE	Sodium dodecyl sulfate polyacrylamide gel electrophoresis
TBS	Tris- buffered saline
TGI	Total growth inhibition

CHAPTER 1

INTRODUCTION

Cancer is a major public health problem in Thailand as well as worldwide: in 2012, there were about 8.2 million cancer deaths and 32.6 million cancer cases. New cases are expected to reach 14.1 million in 2035, and the incidence will increase to 24 million in 2078 (1). Globally, the most common types of cancer in order of frequency for men are prostate (25%), colorectal (13%), and lung (9.3%); in contrast, for women, the most frequent cancers are breast (35%), colorectum (9.5%) and cervix uteri (9.1%). In Thailand, World Health Organization reported that cancer caused about 84,981 deaths in 2012 (2). The most common cancer found in Thai women is breast cancer (31%), whereas colorectum cancer (16%) is most common in Thai men (1).

Cancer is the uncontrolled growth of abnormal cells due to over-activation of oncogenes coupled with under-activation of tumor suppressor genes. Hanahan and Weinberg, 2011 (3) have summarized the characteristics of multi-step cancer progression into six general capabilities which composed of 1) self-sufficiency in growth signals 2) insensitivity to growth inhibitory signals 3) evasion of programmed cell death (apoptosis) 4) limitless replicative potential 5) sustained angiogenesis and 6) tissue invasion and metastasis.

There are many kinds of cancer treatment such as surgery, chemotherapy, and radiation therapy. However, all have side effects and for chemotherapy, these include hair loss, fatigue, vomiting, diarrhea and heart attack. Doxorubicin (DXR), one of the most effective anthracycline anticancer drugs, intercalates into DNA, inhibits DNA DNA topoisomerase II-mediated DNA repair and generates free radicals inducing membrane damage (4). It can cause cardiotoxicity and hematotoxic effects (5). Another chemotherapeutic agent, mitomycin C (MMC), also was demonstrated to increase DXR-induced cardiotoxicity when administered with DXR (6).

Due to these perilous side effects, natural and safer products are being explored. Dietary agents not only have the potential for use in therapy but also in chemoprevention. Various foods have long been associated with either causing or

preventing cancer. Epidemiology studies suggest that, in general, diet plays a significant role for 1/3 to 2/3 of all modifiable risk factors on human cancer development (7). Substances in medicinal herbs have also been studied for use as chemoprevention and chemotherapy. For example, *Azadirachta indica* (neem) showed chemopreventive and antitumor effects in many types of cancer. The substance extracted from neem has a pivotal role in anti-cancer control by inhibition of cell proliferation, stimulation of cell death, suppression of cancer angiogenesis and balance of cellular reduction/oxidation (8, 9). Resveratrol, a natural product found in grapes, also has anti-cancer effects and chemopreventive properties (10, 11). It suppressed cell proliferation of various tumor cells such as breast, ovarian, prostate, and lymphoid cancers. The growth-inhibitory effect of resveratrol was mediated through cell-cycle arrest and cell apoptosis. It also blocked carcinogen activation by inhibiting aryl hydrocarbon-induced CYP1A1 expression and activity, therefore suppressed tumor initiation, promotion and progression. Lee et al., 2013 reported that the combination of resveratrol and chemotherapeutic agent, clofarabine, showed the synergistic antiproliferative effect against human malignant mesothelioma MSTO-211H cells (12).

Royal jelly, a nutritious natural product from bees, is commonly used as a traditional medicine in Asia, Europe, America, Canada, and Australia for health promotion and longevity. It has numerous biological properties: anti-inflammation (13), antioxidant activity (14), antifatigue (15), neurogenesis promotion (16), bone formation stimulation (17) and cancer cell growth inhibition (18). Moreover, 10-hydroxy-2-decenoic acid (10-H2DA), the most abundant fatty acid in RJ, also has several pharmacological properties such as anti-angiogenic activity , anti-inflammatory activity (19), antibiotic activity , lifespan extension (20) and anti-tumor activity (21). However, understanding on molecular mechanisms of RJ and its special fatty acid, 10-H2DA in cancer chemoprevention and cancer therapy is limited. Therefore, studies on molecular mechanisms of RJ and 10-H2DA for cancer prevention and chemotherapy are required to be more elucidated. Nevertheless, there are reports on the side effect of RJ consumption. Ingestion of RJ can cause anaphylaxis in allergic individuals (22, 23). Furthermore, the consumption of RJ in combination with the prolonged administration of warfarin (a blood coagulant) can increase bleeding (24). Thus the

exact composition and toxicity of RJ should be known before a thorough examination of its chemoprevention and chemotherapy properties on human cells.

The present study aimed to elucidate the effectiveness of Thai RJ and its extracts as chemopreventive and chemotherapeutic agents. Chemical compositions of RJ were analyzed for carbohydrate, lipid, protein, ash and moisture contents by standard AOAC method. RJ was extracted by diethyl ether as a solvent using Soxhlet apparatus for 24 h. Then, the ethereal extract (EE) and defatted material (DM) were collected. All phenolic and flavonoid contents and antioxidant activities of RJ were determined by chemical-based assays to evaluate its antioxidative potential. In addition, 10-H2DA contents in RJ and EE were also determined by high-performance liquid chromatography (HPLC) (25).

To evaluate biosafety of RJ, EE,DM and 10-H2DA, their genotoxicity were evaluated on human lymphocytes using *in vitro* sister chromatid exchange (SCE) assay. SCE is an exchange of DNA fragments of sister chromatids on the same loci of a homologous chromosome: the result of DNA repair mechanism. It is a valuable tool for the quantitative and qualitative evaluation of DNA damage caused by physical (e.g. radiation), chemical (e.g. mutagens and carcinogens) and biological factors (e.g. virus and bacteria) (26).

In addition, pretreatments of RJ, EE, DM and 10-H2DA followed by doxorubicin (DXR), a genotoxic chemotherapeutic agent, were performed to evaluate the antigenotoxicities of RJ, EE, DM and 10-H2DA against DXR on human lymphocytes by SCE assay. These procedure determined the chemopreventive activities of RJ and its ingredients.

Furthermore, to evaluate the chemotherapeutic activities, various concentrations of 10-H2DA were treated against MCF-7 breast cancer cell line and MTS tetrazolium assay was performed to determine the cytotoxic effects of 10-H2DA treatements against breast cancer cells. Additionally, the antiproliferative activities of 10-H2DA in combination with DXR treatments on MCF-7 cells were evaluated by MTS assay. These procedures determined the chemotherapeutic activities of 10-H2DA itself and 10-H2DA in adjunct with DXR against MCF-7 breast cancer cell line.

Moreover, the molecular mechanisms underlying the genotoxicity of RJ alone and antigenotoxicity of RJ against DXR on human lymphocytes as well as the cytotoxicity of 10-H2DA alone on MCF-7 breast cancer cells and antiproliferative effects of 10-H2DA in combination with DXR were evaluated. Detecting of pivotal regulatory proteins that the chemoprevention and chemotherapy regularly share such as cell cycle regulators (cyclin E1, cyclin B1, cyclin D1, cyclin dependent kinase 4), oncogene (c-MYC), tumor suppressor gene (p53), telomerase (hTERT), antioxidative response (NRF2, HO-1), and apoptosis markers (BCL2, BAX) were quantified by Westen blot analysis.

In addition, effects on kinetics of cell cycle progression determined as a percentage of early G1, G1, S, and G2 phases were evaluated by flow cytometry using propidium iodide staining. Effects on kinetics of cell apoptosis determined as the percentages of live, early apoptosis, late apoptosis and necrosis were quantified by flow cytometry using annexin V and propidium iodide double staining. Lastly, effects on nuclear morphological changes were assessed by fluorescence microscope using Hoechst 33258 and propidium iodide double staining.

Objectives

1. To analyze the general chemical compositions of Thai RJ and its antioxidative potential including flavonoid content, total phenolic content and antioxidative activity

2. To examine the genotoxic effects of RJ and its ingredients (EE, DM and 10-H2DA) treatments on human lymphocytes

3. To examine the antigenotoxic effects of RJ and its ingredients (EE, DM and 10-H2DA) treatments on human lymphocytes

4. To examine the molecular mechanisms of genotoxic effects of RJ treatments alone and antigenotoxic effects of RJ pretreatments against DXR on human lymphocytes

5. To examine the cytotoxic and proliferative effects of 10-H2DA treatments against MCF-7 breast cancer cells

6. To examine the antiproliferative effects of 10-H2DA in combination with DXR treatments against MCF-7 breast cancer cells

7. To examine the molecular mechanisms of antiproliferative effects of 10-H2DA treatment alone and antiproliferative effects of 10-H2DA in combination with DXR treatments against MCF-7 breast cancer cells

Conceptual framework
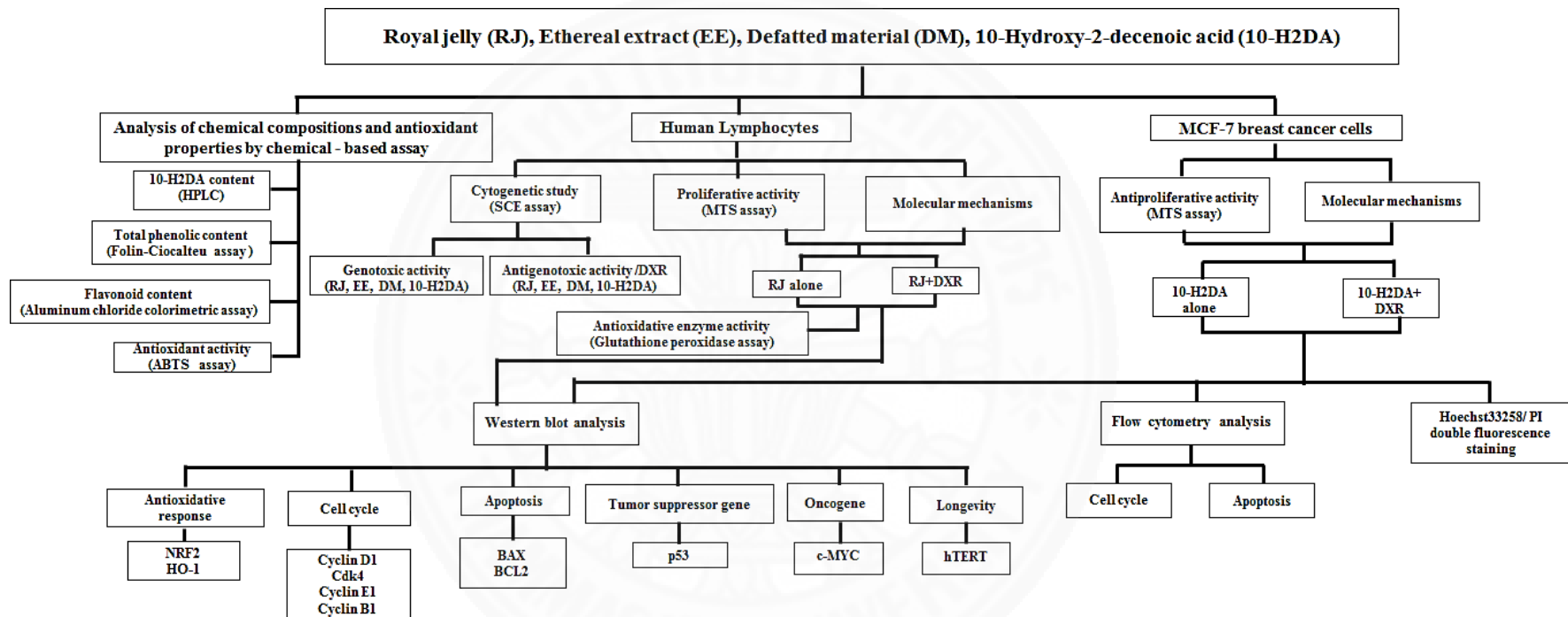
Figure 1   Schematic diagram of the analysis of royal jelly and its ingredients

CHAPTER 2
REVIEW OF LITERATURE

2.1 Breast Cancer

In 2012, breast cancer was estimated 1.67 million new cancer cases diagnosed (25% of all cancers), and ranks second overall. It is now the most common cancer both in developed and developing zones with approximately 690,000 new cases estimated for each area (population ratio 1: 4). Thailand is in the developing zone. Incidence rates of breast cancer vary from 19.3 per 100,000 women in Eastern Africa to 89.7 per 100,000 women in Western Europe, and are higher (greater than 80 per 100,000) in the developed zones of the world (except Japan) and lower (less than 40 per 100,000) in most of the developing zones . Breast cancer ranked as the fifth cause of death from cancer overall. It is the most frequent cause of cancer death in women in less developed regions. In more developed regions, breast cancer is the second cause of cancer death after lung cancer. However the survival rate of breast cancer in developed regions is higher (6 per 100,000 in Eastern Asia to 20 per 100,000 in Western Africa (2).

In Thailand, breast cancer is the most common found and accounts for 32% of all cancer in both sexes (Figure 2.1). It ranks as the fourth cause of death from cancer overall (6%), after the liver cancer (23%), lung cancer (21%) and colorectum cancer (8.1%) (Figure 2.2). The report of Kotepui et al., 2013 showed that breast cancer incidence under age 40 years was slightly low while the incidence in the age groups 40 and older was very high (27).
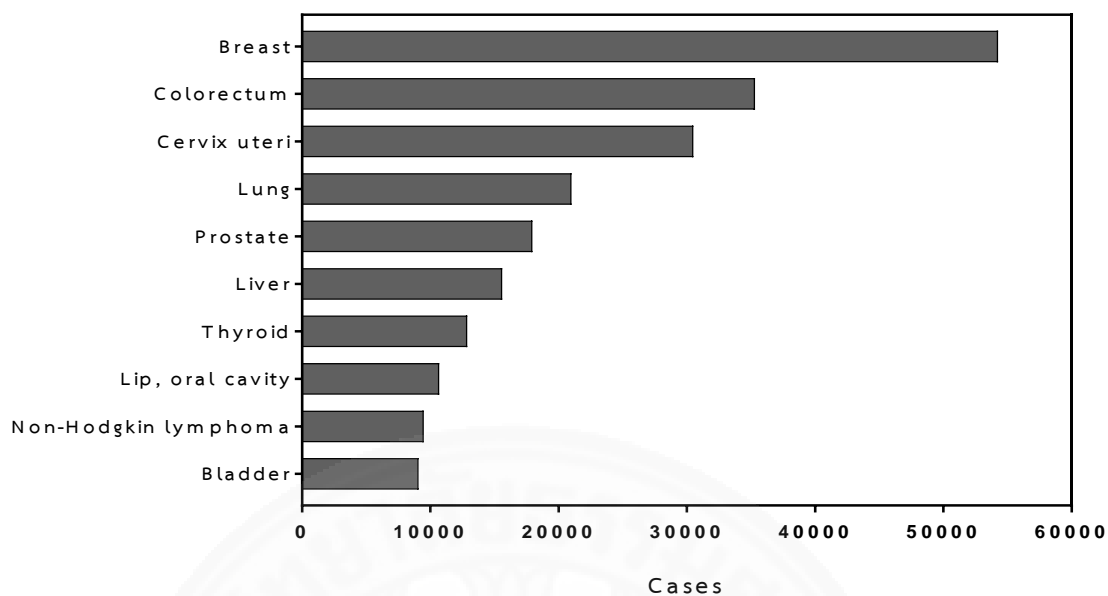
Figure 2.1 Estimated number of incident cases, both sexes of top 10 cancer sites, Thailand in 2012 (1). Data source: GLOBOCAN 2012,[©] International Agency for Research on Cancer 2018 (http://gco.iarc.fr/)
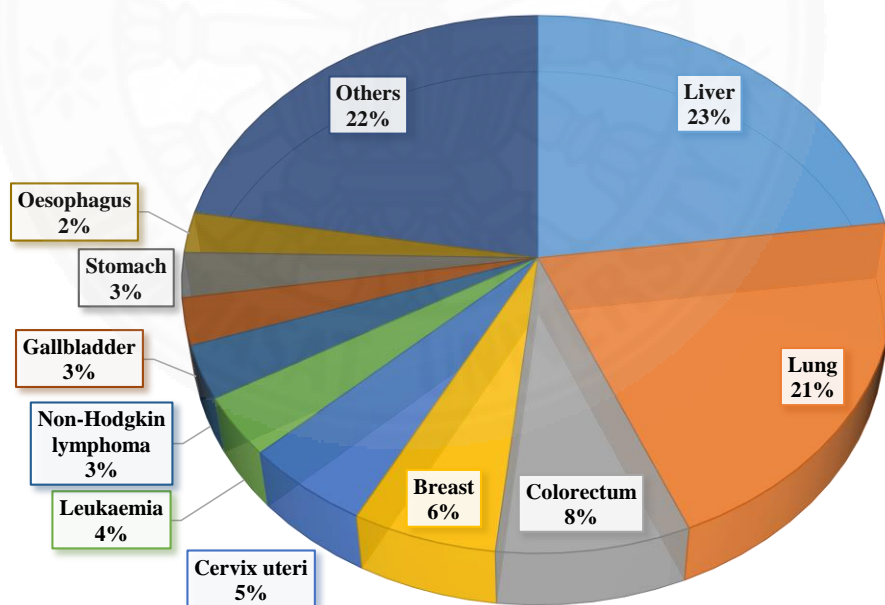
Figure 2.2 Estimated numbers of death of each cancer site, Thailand in 2012 (2). Data source: GLOBOCAN 2012, [©] International Agency for Research on Cancer 2018 (http://gco.iarc.fr/)

Breast cancer has different clinical properties, pathologic features, morphology, grade, and hormone receptors. It was classified into 5 subtypes depending on gene expression levels of estrogen receptor (ER), progesterone receptor (28), epidermal growth factor receptor-2 (Her-2), KI67 antigen, and basal marker (cytokeratin; CK5 or CK5/6) (31-33). Prevalence of each subtypes was shown in Table 1. The most prevalent types is luminal A and the least is Normal-like. Mavaddat et al., 2015 reported that the ER- negative disease rate is high in relatives and family under the age of 50 years.

Table 1 Summary of the molecular subtypes of breast cancer (modified from Dai X et al., 2015)

Intrinsic subtypes	Immunohistochemical status	Prevalence
Luminal A	[ER^+|PR^+] $HER2^-KI67^-$	23.7%
Luminal B	[ER^+|PR^+] $HER2^-KI67^+$	38.8%
	[ER^+|PR^+] $HER2^+KI67^+$	14.0%
HER2 over-expression	[ER^-PR^-] $HER2^+$	11.2%
Basal-like	[ER^-PR^-] $HER2^-$, basal marker$^+$	12.30%
Normal-like	[ER^+|PR^+] $HER2^-KI67^-$	7.8%

2.2 Natural products for chemoprevention and chemotherapy

Carcinogenesis is a multi-step process involving initiation, promotion and progression steps in order to transform normal cells into cancer cells. Its mechanisms of action comprise of various changes at genetic, epigenetic and cellular levels including abnormal cell divisions. The balance between cell proliferation and programmed cell death in the form of apoptosis is also important. In order to prevent carcinogenesis, many chemical compounds from natural products such as resveratrol in grape has been extensively studied to be used as chemoprevention and chemotherapy. Veroni et al., 2016 reported that resveratrol suppressed tumor initiation, promotion and progression and also blocked metabolic activation of procarcinogen (29). It had additive and/or synergistic effects when used in adjuvant

therapy associated with 5-fluorouracil or cisplatin but not with DXR (29). Azadirachtin and Nimbolide in neem (30, 31), catechin and epicatechin in green tea (32) and curcumin in turmeric (33) are also reported as potent cancer chemopreventive compounds.

2.3 Modulation of molecular mechanisms of carcinogenesis

2.3.1 Modulation through cell cycle regulators

Progression of the cell cycle is normally controlled by consecutive activation and inactivation of cyclins and cyclin-dependent kinases (cdks). The cdks belong to the family of serine/threonine protein kinases. Their kinase activity depends on the presence of cyclin proteins. In each cell cycle, specific cyclins increase specifically at each phase of the cell cycle. In early G1 phase, cyclin D participates with cdk4 and cdk6 proceeds cell cycle from G0/G1 to late G1 and passes through the restriction point in which cyclin D/cdk activity is no longer needed for cell cycle progression. Then, cyclin E stimulates cdk2 and activates G1 to early S phase transition. After that, cyclin A stimulates cdk2 and activates late S-to early G2 phase. Cyclin A also stimulates cdk2 and activates early G2 to late G2 phase. The cyclin B stimulates cdk complex and required during G2 to M phase transition (Figure 2.3) (34). Modulation of the cell cycle through cyclins or cdks could interfere cell proliferation.
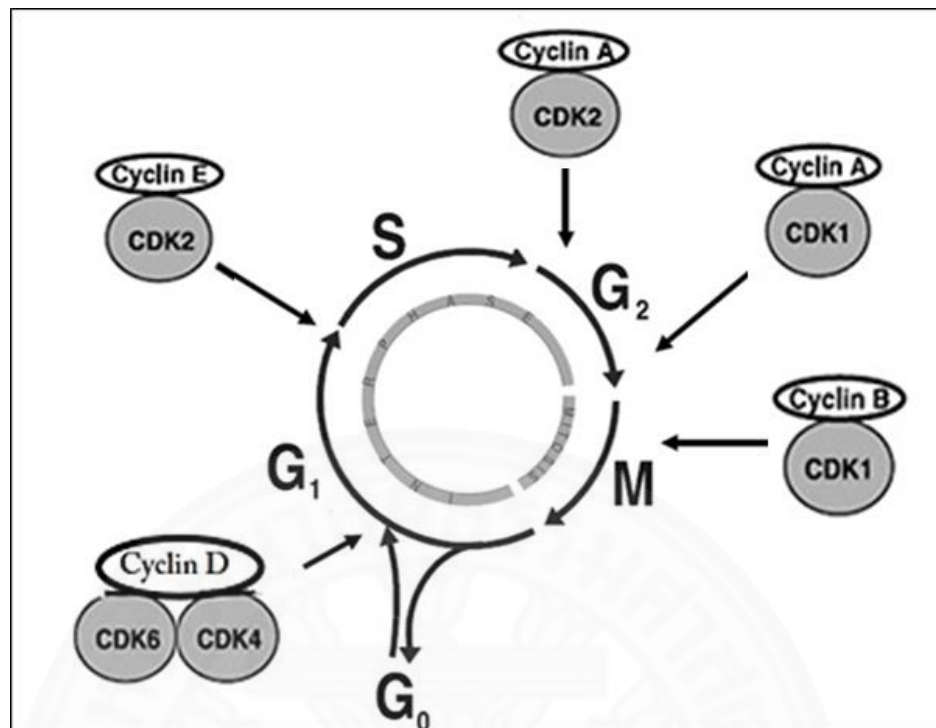
Figure 2.3 Schematic diagram of cell cycle progression (modified from Vermeulen et al., 2003 (34)

2.3.2 Modulation through c-MYC

c-MYC, a proto-oncogene transcription factor, plays a critical role in a diversity of cellular proliferation, differentiation, metabolism and apoptosis (35). Under normal condition, its expression is strictly controlled. It stimulates in response to extracellular activation from growth factors (36). Overexpression of c-MYC is a hallmark of many human cancers. Therefore, inhibition of c-MYC can cause tumor regression and cell differentiation and can be used for cancer therapy (37). In addition, a transcription factor of c- MYC activates aryl hydrocarbon (Ah) receptors and stimulates expression of heme oxygenase-1 (HO-1). HO-1 is an inducible antioxidative enzyme induced by oxidative stress (38). c-MYC also activates human telomerase (hTERT) (39). Human telomerase is an RNA-dependent DNA polymerase that synthesizes telomeric DNA sequences and provides the molecular basis for unlimited proliferative potential.

2.3.3 Modulation through p53

p53, a transcription factor and a tumor suppressor, is a crucial regulator in numerous cellular procedures including cell signal transduction, cell cycle regulator, cellular response to DNA-damage, genomic stability, and apoptosis (22). It stimulates the transcription genes such as p21WAF1 and Bax to induce the apoptotic process, hindering the cell growth with damaged DNA or cancer cells (40, 41). In the case of mutant p53, it loses the capability to bind DNA efficiently, and as a result, the p21 protein is not made available to control cell division. Thus, cells divide uncontrollably and develop cancer. Dietetic agents such as curcumin, resveratrol, and indole-3-carbinol can modulate p53 action (42-44). Both DXR and 5-fluorouracil (5-FU), potent chemotherapeutic agents also increases accumulation of p53 (45).

2.3.4 Modulation through human telomerase reverse transcriptase (hTERT)

Telomere, the ends of human chromosomes, is composed of tandemly repeated G-rich DNA sequences on humans, which protects chromosome ends (46). During DNA replication, the leading strand of DNA is replicated as one continuous strand, while the lagging strand is replicated by use of RNA primers and small Okazaki fragments. After the RNA primers are removed and the fragments are ligated together, the lagging strand is left with DNA on the end that do not get replicated. This results in telomere shortening (47). Telomere shortening finally can cause cell cycle arrest, senescence and mortality (48). To avoid this situation, human telomerase, a ribonucleoprotein complex, adds TAGGG repeats to the ends of the chromosomes. The complex contains essence enzyme (human telomerase reverse transcriptase (hTERT) and a template site for DNA elongation (human telomerase RNA: hTR). hTERT is the catalytic subunit of telomerase and is associated with the rate-limiting step in the activation of telomerase (49). The high-level expression of hTERT was observed in embryonic stem cells and germ cells. However, hTERT is expressed at a low level and eventually silenced in differentiated somatic cells (50). The over-expression of hTERT lets cells to continue proliferating. It has been found to be associated with DNA repair mechanism. (51). The aberrant expression of hTERT is found

in 80-95% of cancer (50). Moreover, it defends cells from signaling into cell cycle arrest and/or apoptosis which can lead to cancer cells resistant against radiation therapy or chemotherapeutic agents (52-54). Therefore, it is a one of a molecular target for cancer therapy. Many studies show inducible dominant-negative hTERT mutants were able to reduce endogenous telomerase activity in cancer cells which lead to telomere shortening and rapid cell death (55, 56).

2.3.5 Modulation through programmed cell death: apoptosis

Cancer therapies, such as chemotherapy, radiotherapy, and immunotherapy could induce apoptosis in cancer cells allowing cells to commit suicide (57). It also occurs in normal cells through development and aging process to maintain cell populations in tissues. The two major process of apoptosis is an intrinsic or mitochondrial pathway and extrinsic or death receptor pathway which both mechanisms can link to each other (Figure 2.4) (58).

The intrinsic pathway affects mitochondrial membrane permeability leading to release cytochrome c, the pro-apoptotic molecules, into the cytoplasm. The cytochrome c binds with CED-4/Apaf-1 and procaspase-9 forming apoptosome. Consequently, apoptosome activates procaspase-9 to form caspase-9 which will stimulate degradation of caspase-3 and induce apoptosis. On the contrary, Bcl-2 (B-cell lymphoma protein 2) can inhibit the cytochrome c releasing from mitochondria into the cytoplasm and inhibits the apoptosome formation (59).

The extrinsic pathway initiates when death ligands attach to death receptors. The death receptor, the type 1 TNF receptor (TNFR1) and Fas protein receptor, will bind to their ligands called TNF and Fas ligand (FasL) recruiting adapter proteins such as TNF receptor-Associated Death Domain (TRADD) and Fas-Associated Death Domain (FADD). FasL triggers Fas protein which initiates the recruitment of caspase-8 via an adapter molecule FADD to the formation of Death-Inducing Signaling Complex (DISC). Then, DISC stimulates caspase 8 and serially activates caspase 3 which triggers apoptosis (60).
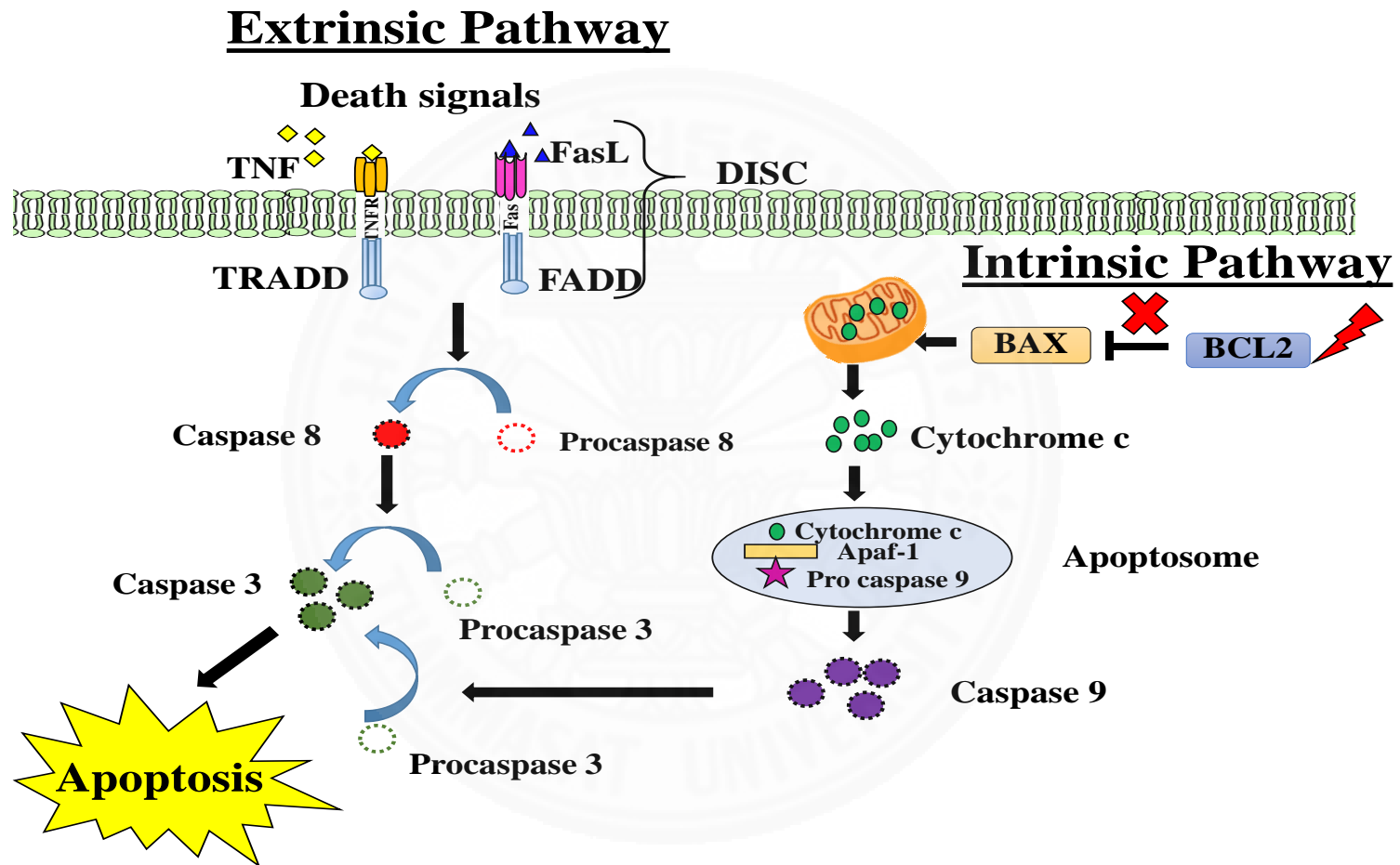
Figure 2.4 Apoptosis pathway (modified from Wong et al., 2011 (59))

2.3.6 Modulation of antioxidative response: NRF2 and HO-1

Normally, cells have a production of free radicals, called reactive oxygen species in balance with antioxidative response producing antioxidative enzymes and antioxidants (61). However, during oxidative stress, there is an imbalance in the production and elimination of free radicals, leading to the damage of biomolecules such as lipids, proteins, and DNA. These may finally leads to mutations and ultimately to the development of cancer (62). Therefore, chemopreventive agents which possess antioxidative activities could interfere in the process of this carcinogenesis (63).

Most of the antioxidative enzymes are in phase II conjugating enzymes such as heme oxygenase-1 (HO-1), glutathione peroxidase (GPx), and catalase (CAT). At the transcriptional level, phase II enzymes are largely regulated by the transcription factor known as nuclear factor-erythroid 2–related factor 2 (NRF2) (64).

NRF2, a transcription factor that naturally binds to Keap1 and does not express/function (65). The levels of NRF2 are, therefore, low under the normal condition, but under oxidative stress, NRF2 is released from Keap1 and moves from cytosol into the nucleus to activate various transcription of phase II enzymes and antioxidants e.g. HO-1 (Figure 2.5) (66).
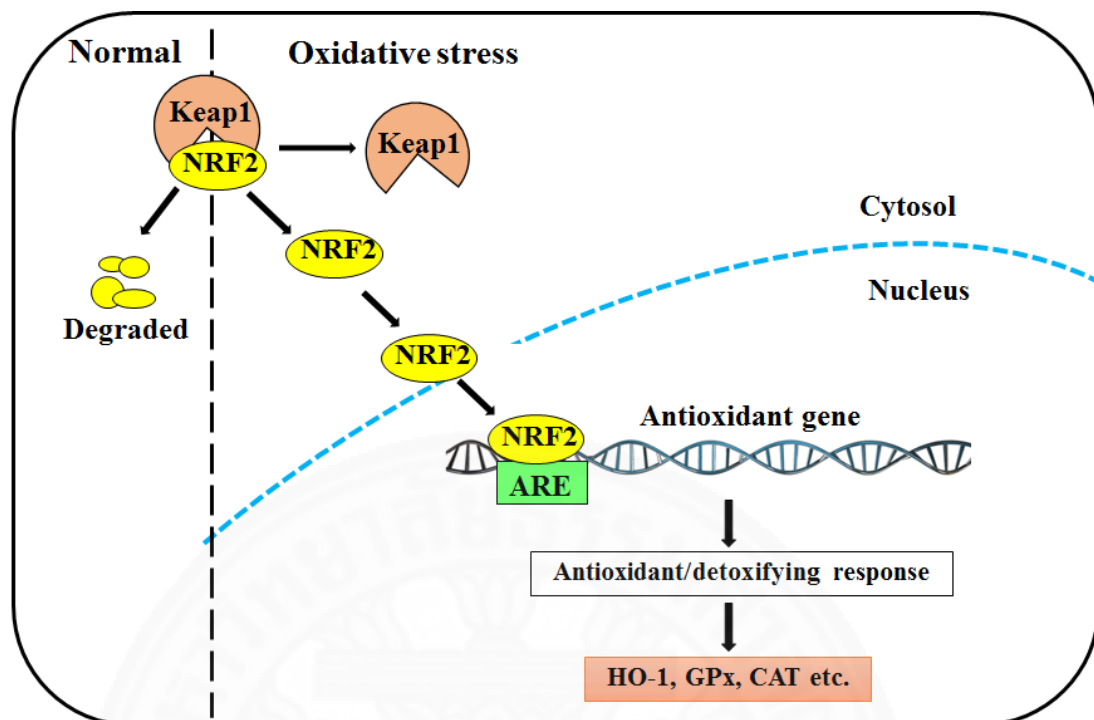
Figure 2.5 Antioxidative gene expression via the ARE/NRF2 pathway (modified from Amma Owusu-Ansah et al., 2015 (61). ARE: Antioxidant response element, NRF2: Nuclear factor erythroid 2-related factor 2, Keap1: Kelch-like ECH-associated protein 1, HO-1: Heme oxygenase 1, GPx: Glutathione peroxidase, CAT: Catalase

2.3 Royal jelly and its properties

RJ is only a particular food for queen bee throughout her life while the other bees in a hive have bee pollen and honey as food after three days of life. The queen bee has twice the size of worker bees and is only a fertile female in a hive. Whereas there are about 20,000-30,000 worker bees, who are infertile females and hundreds for the drone, a fertile male. The only queen bee can lay approximately 2,000 eggs per day and it has a long life (about 5-8 years), 40 times more than worker bees (67). RJ generally is composed of 60% water, 30% carbohydrate, 3-8% lipids, 27-40% proteins and 0.8-3% ash, of dry matter (68). Special fatty acids found specifically in RJ are 10-H2DA and 10-hydroxydecanoic acid figure (10-HDA) (Figure 2.7). Moreover, RJ is compose of important flavonoids such as quercetin, kaempherol and galangin (69).
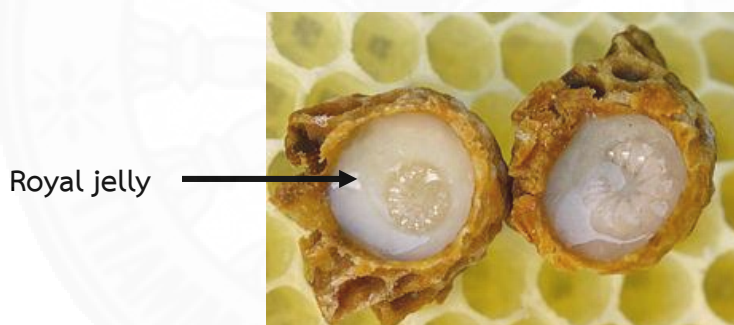
Figure 2.6 Royal jelly. The black arrow indicates royal jelly in the cell (https://en.wikipedia.org/wiki/Royal_jelly)

10-Hydroxy-2-decenoic Acid
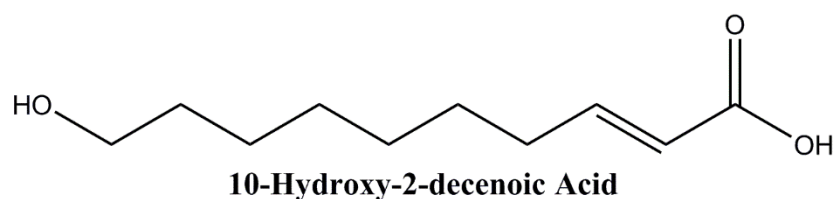
Figure 2.7 Structure of 10-hydroxydecenoic acid (10-H2DA)

2.4.1 Antibacterial activity

Blum et al., 1959 reported that 10-H2DA had an antibacterial activity (70). Our previous studied using RJ from northern Thailand also demonstrated that the crude RJ, EE and DM had antibacterial activities against both gram positive and gram negative bacteria such as *Sarcina lutia*, *Salmonella typhi*, *Staphylococcus aureus* and *Shigella flexneri*, whereas bacteriostatic action was shown against *Bacillus cereus, Escherichia coli, Proteus vulgaris* and *Pseudomonas aeruginosa* (71). Fujiwara et al., 1990 demonstrated that there was a potent antibacterial peptide namely royalisin in RJ. Royalisin had potent antibacterial activity against gram-positive bacteria including Streptococcus, Staphylococcus*, Micrococcus luteus, Sarcina lutea*, Clostridium, Corynebacterium, *Lactobacillus helveticus*, and Leuconostoc, but not against gram-negative bacteria (72). Fontana et al., 2004 reported that jelleine, a peptide with 8-9 amino acids showed antibacterial activity against gram-positive cocci (*S. aureus*, *S. saprophyticus*, and *B. subtilis*) and gram-negative rods (*E. coli, E. cloacae*, *K. pneumoniae*, and *P. aeruginosa*), and yeast (*C. albicans*) (73).

2.4.2 Antioxidant activity

The antioxidant of RJ was evaluated in yeast *Saccharomyces cerevisiae* by cultivated in YEPD medium with 1, 2 and 5 g/L of RJ and estimated intracellular oxidation by 20, 70-dichlorofluorescein measuring (74). The results revealed that RJ decreased intracellular oxidation in a dose-dependent manner. RJ pretreatements protected albino rats from gamma irradiation-induced oxidative stress (75). RJ intake in type 2 diabetic patient significantly increased serum total antioxidant capacity, compared to placebo group (76).

2.4.3 Estrogenic activity

RJ stimulated the proliferation of mouse osteoblast-like MC3T3-E1 cells, possibly involving with estrogenic activity of RJ (17). Using reporter gene expression assay, RJ could bind to estrogen receptor and transcribed a reporter gene through estrogen response element and treatment of RJ in ovariectomized rat restored vascular endothelial growth factor (VEGF) in uterus, demonstrating estrogenic acitivity

of RJ *in vitro* and *in vivo* (77). 10-H2DA binds to β-estrogen receptor but not α-estrogen receptor and it induced MCF-7 breast cancer cell proliferation (78).

2.4.4 Antitumor activity

Townsend et al., 1960 reported that RJ and 10-H2DA inhibited carcinogenesis in transplantable mouse leukemia and 3 lines of ascites tumors cells: 6CSHED lymphosarcoma, TA3 mammary carcinoma and Ehrlich carcinoma (18). In addition, RJ inhibited the growth-promoting effect of bisphenol A, a xenoestrogen, on MCF-7 breast cancer cell lines (79). The treatment with 10-H2DA inhibited VEGF-induced proliferation, migration and tube formation on human umbilical vein endothelial cells (HUVECs) (80). Salazar-Olivo, L. and Paz-Gonzalez, P. (2005) reported that protein extract (RJP30) from RJ was cytotoxic for HeLa human cervicouterine carcinoma cells (80). In addition, using mouse tumor model, intravenous but not intraperitoneally or subcutaneously administration of RJ pretreatment before tumor cell (mammary carcinoma and colon carcinoma) inoculation significantly inhibited mice metastasis formation (81).

CHAPTER 3

RESEARCH METHODOLOGY

3.1 Equipments

Materials	Model	Company
Autosampler spectra system	AS3500	Thermo Fisher Scientific, USA
Autopipette	Pipetman	Gilson, France
Biosafety cabinet	Power wave XS	BioTek, USA
Centrifugal evaporator	Concentrator5301	Eppendorf, Germany
CO_2 incubator	Series II water jacket	Thermo Fisher Scientific, USA
Corning cell culture flask	25 and 75cm^2	Sigma, USA
High-performance liquid chromatography (HPLC)	Spectra system P400	Thermo Fisher Scientific, USA
Hotplate stirrer	SB162	Stuart, UK
Incubator	UNB500	Memmert, Germany
Magnetic stirrer	500P-2	PMC, USA
McFarland Densitometer	DEN-1	Grant-bio, England
Microcentrifuge	Legend Micro17	Thermo Fisher Scientific, UK
Microplate spectrophotometer	PowerWave™ XS	Bio-Tek, USA
Microscope cover slips 24x60 mm	50-949-493	Thermo Fisher Scientific, USA
Microscope slide	7105	Sail Band, China
Mini-Gel electrophoresis unit	Mini protein	Bio-Rad, USA
Nanodrop spectrophotometer	Nanodrop 2000	Thermo Fisher Scientific, USA

Materials	Model	Company
Odyssey Fc Imager	Li-Core Biosciences	Li-Core Biosciences, USA
pH meter	PHS-3BW	BANTE instrument, China
Phase contrast microscope	AXIO	Zeiss, Germany
Fluorescence microscope	Eclipse-Ci	Nikon, USA
Power supply	Power PACTM Basic	Bio-Rad, USA
Quick Spin	C1301B-230	Labnet, Korea
Rotating shaker	SSM4	Stuart, UK
Sonicator	Model	SONICS, USA
Spectrophotometer	UV-1601	Shinmadzu, Japan
Vortex mixer	Genie 2 G-560E	Scientific IndustriesTM, USA
Water bath	WNB Basic	Memmert, Germany

3.2 Chemicals

Chemicals	Catalog Number	Company
2-Mercaptoethanol	1610710	Bio-Rad, USA
4x Laemmli sample buffer	161-0747	Bio-Rad, USA
10-hydroxy-2E-decenoic acid	10976	Cayman Chemical, USA
Ammonium persulphate	7727-54-0	Sigma, USA
Actin antibody	4967	Cell signaling technology, USA
BAX antibody	2772	Cell signaling technology, USA
BCL2 antibody	2876	Cell signaling technology, USA

Chemicals	Catalog Number	Company
c-MYC antibody	9402	Cell signaling technology, USA
cdk4 antibody	MAB8879	Merck millipore, USA
Cyclin B1 antibody	4138	Cell signaling technology, USA
Cyclin D antibody	06-137	Merck miilipore, USA
Cyclin E1 antibody	04-222	Cell signaling technology, USA
hTERT antibody	ABE2075	Merck millipore, USA
HO-1 antibody	70081	Merck millipore, USA
NRF2 antibody	ABE829	Merck millipore, USA
p53 antibody	9282	Cell signaling technology, USA
Bio-Rad Protein Assay Kit II	5000002	Bio-Rad, USA
CellTiter 96® AQueous One Solution Cell Proliferation Assay Kit	G3582	Promega, USA
Coomassie® Brilliant Blue R-250	1610435	Bio-Rad, USA
Doxorubicin hydrochloride (Adriamycin)	S1208	Pfizer, USA
Diethyl ether	362551.1611	AppliChem Panreac, Germany
Giemsa stain set	RA-002-12	Biotech reagent, Thailand
Glycine	1610718	Bio-Rad, USA
GPx cumene hydroperoxide	703118	Cayman chemical, USA
Guava Instrument Cleaning Fluid (ICF)	4200-0140	Merck miilipore, USA
IRDye 680 mouse anti-rabbit	925-68071	LI-COR Biosciences, USA

Chemicals	Catalog Number	Company
MEM-non-essential amino acid (NAA)	1IVG2-11140-050	Thermo fisher scientific, USA
N, N'-Methylene-bis-acrylamide	1610158	Bio-Rad, USA
N, N, N', N'-Tetramethyl-1, 2-diaminoethane (TEMED)	1610800	Bio-Rad, USA
Nitrocellulose membrane	RPN303D	GE Healthcare, UK
Odyssey blocking buffer	927-50000	LI-COR Biosciences, USA
Percision Plus Protein Dual color Standard	1610374	Bio-Rad, USA
Permount, Fisher Sciencentific	SP15-500	Thermo fisher Sciencentific, USA
Phosphate buffered saline (PBS) tablet	E404-200TABS	Amresco, Canada
Propidium iodide/Ribonuclease	550825	BD Biosciences, USA
Protease inhibitor cocktail	539131-1VL	Merck Millipore, USA
RIPA lysis buffer	20-188	Merck Millipore, USA
Sodium dodecyl sulfate	1610301	Bio-Rad, USA
Sodium hydrogen carbonate	0865-1KG	VWR chemical, UK
Standard protein marker	1610377	Bio-Rad, USA
Sodium pyruvate solution	1IVG7-11360-070	Thermo fisher scientific, USA
Tris hydrochloride	PRO612	Promega, USA
Trypsin-EDTA	1IVG7-15400-054	Thermo fisher scientific, USA
Triton^{TM} X-100	A1287	ITW Companies, Germany
Tween 20	V900548-500ML	Sigma, USA

3.3 Analysis of general chemical compositions and pH of RJ

3.3.1 Extraction of RJ for EE and DM using Soxhlet apparatus

150 g RJ was extracted with 300 mL diethyl ether in Soxhlet apparatus at 45 °C for 36 h according to our previously described protocol (71). The EE and DM were separated and evaporated by a rotary evaporator at 50 °C and 50 rpm for 30 min. Then, EE and DM were evaporated in vacuum desiccator for 72 h, weighted and stored at minus 20 °C until use.

3.3.2 Determination of moisture content by thermal analysis (AOAC method (82))

Empty dish and lid were dried in the oven at 105 °C for 3 h and transferred to a desiccator to cool and weighed. Then, RJ sample was weighed to the dish and spreaded the sample to the uniformity. The dish with RJ sample was dried in the oven for 3 h at 105 °C. After drying, transferred the dish to the desiccator to cool and reweighed the dish and its dried sample. Then, the moisture content was calculated by the following formula (82).

$$\text{Moisture content (\%)} = \frac{W1 - W2}{W1} \times 100$$

W1 = weight of the sample before drying

W2 = weight of the sample after drying

3.3.3 Determination of protein content by Kjedahl apparatus

RJ sample (0.5-1.0 g) was added to the digestion flask and added 5 g Kjedahl catalyst and 200 ml of H_2SO_4. Then, the samples was boiled in the Kjeldahl apparatus. The flask was heated until all NH_3 was distilled, removed receiver, washed tip of the condenser and titrated excess standard acid distilled with standard NaOH solution and calculated as follows:

Protein (%) = $\underline{\text{(A-B)} \times \text{N} \times 1.4007 \times 6.25}$

W

Where A   = volume of 0.2 N HCl used in sample titration

 B   = volume of 0.2 N HCl used in blank titration

 N   = Normality of HCl

 W   = weight of sample

 14.007   = atomic weight of nitrogen

3.3.4 Determination of ash content by thermal analysis (AOAC method (82))

The crucible and lid were heated in the furnace at 550 °C overnight and cooled in the desiccator for 30 min. Then, RJ was weighed to the crucible with 3 decimal places. The RJ sample in crucible was heated at 550 °C overnight, cooled down in the desiccator. Then crucible with RJ sample was weighed and calculated with the following formula (82).

$$\text{Ash } (\%) = \frac{\text{weight of ash}}{\text{weight of sample}} \text{ x } 100$$

3.3.5 Quantitative analysis of 10-H2DA in RJ and EE by high performance liquid chromatography (HPLC)

RJ was dissolved in 55% V/V methanol: 45% distilled water (pH 2.5). The solution was vortexed, sonicated for 30 min, and filtered through a 0.22 µm membrane filter. A chemical fingerprint of RJ was carried out to examine 10-H2DA with an HPLC Spectra System P-4000 with reversed phase HPLC column and a UV detector at wavelength 215 nm. The mobile phase was composed of solvent A (water pH 2.5) and solvent B (methanol with gradient elution as follows: methanol at 55% solvent B from 0 to 30 min; flow rate: 0.5 mL/min, 10 µL autosampler injection. The data acquisition and processing were performed by Chrome quest software (25).

3.4 Analysis of antioxidant properties of RJ

3.4.1 Determination of total phenolic content by Folin-Ciocalteu method

Phenolic compounds are secondary metabolites found in plants. They contain benzene rings, with one or more hydroxyl substituents, and range from simple phenolic molecules to highly polymerized compounds. The phenolic substances contain numerous varieties of compounds: simple flavonoids, phenolic acids, complex flavonoids and colored anthocyanins (83). The polyphenolic components may act as antioxidants or as agents of other mechanisms contributing to anticarcinogenic or cardioprotective action (84) .

Total phenolic content in the RJ was determined by using Folin–Ciocalteu method (85, 86) with some modification. Briefly, 200 µl of different concentration of RJ was mixed with 100 µL Folin-Ciocalteu's reagent and 80 µL of sodium carbonate solution (0.7 M), then the mixture was allowed to stand for 30 min at room temperature. The absorbance was measured at 760 nm using a PowerWave™ XS Microplate spectrophotometer. The total phenolic content was calculated by using an equation obtained from the standard gallic acid calibration curve and expressed as gallic acid equivalents (GAE), in milligrams per gram of the sample.

3.4.2 Determination of flavonoid content by aluminum chloride colorimetric method

Total flavonoid content was estimated by aluminum chloride colorimetric method which adapted from Mella et al., 2013 (86). In brief, RJ (20, 40, 60, 80 and 100 µg/mL) were added to 5 % sodium nitrite ($NaNO_2$) and incubated at room temperature for 6 min. Then, 10 % aluminum chloride ($AlCl_3$) was added and incubated for 6 min. After that, 4% sodium hydroxide (NaOH) was added and continued to incubate for 15 min. The absorbance of the reaction mixture was measured at 510 nm. The flavonoid content was calculated by using an equation obtained from the rutin standard calibration curve and expressed as rutin equivalents,

in milligrams per gram of the sample (11). Rutin is the rutoside; quercetin 3-O-rutinoside.

3.4.3 Antioxidant capacity by ABTS assay

Antioxidant activity was measured by monitoring of the decay of the radical cation $ABTS^{•+}$ produced by the oxidation of 2,2′-azinobis (3-ethylbenzothiaziline-6-sulfonate) (ABTS) caused by free radicals. $ABTS^{•+}$ has strong absorption at 734 nm. Stock $ABTS^{•+}$ solution was prepared from 7 mM ABTS and 40 mM of potassium persulfate in distilled water. Briefly, $ABTS^{•+}$ solution was diluted with ethanol to achieve an absorbance of 0.75 at 734 nm. Four mL of $ABTS^{•+}$ working solution and 0.5 mL of sample solution of different concentrations were mixed and incubated at 30 °C in water bath for 6 min. Absorbance at 734 nm was measured. Trolox (6-hydroxy-2, 5, 7, 8-tetramethylchroman-2-carboxylic acid) is a water-soluble analog of vitamin E. Trolox standard calibration curve was used as positive control. Trolox equivalents are used to express the results (TEAC, Trolox Equivalent Antioxidant Capacity) (87).

3.5 Analysis of the effects of RJ, EE, DM and 10-H2DA on human lymphocytes

3.5.1 Genotoxic effects of RJ, DM, EE, and 10-H2DA treatments for 3 h on human lymphocytes detected by *in vitro* sister chromatid exchange (SCE) assay

Fresh blood samples for all experiments were obtained by venipuncture from 10 healthy volunteers, age 25-35 years with no recent exposure to radiation or drugs. These studies were approved by our institutional ethics committee MTU-EC-DS-2–067/56 and MTU-EC-DS-66077/60.

3.5.1.1 Preparation of RJ, EE and DM for culture

Crude RJ and EE fraction were each mixed with dimethylsulfoxide (DMSO) for an hour (5 mg/mL of RJ and 2.5 mg/mL of EE) and then

centrifuged. The supernatant was then mixed with RPMI for another hour resulting in the stock solution of crude RJ extract or ethereal EE. Ten-fold serial dilutions of RJ and EE in RPMI medium were freshly prepared. For DM, it was directly solubilized in RPMI medium. Ten-fold serial dilutions of DM were freshly prepared before initiating cell culture.

3.5.1.2 Cell cultures

One ml whole blood was cultured in a 5 mL culture medium (10% fetal bovine serum, 10% autologous plasma, 1% penicillin-streptomycin, 2% phytohemagglutinin and 1% L-glutamine) under standard blood culture conditions (88). Twenty-four hours after the initiation of the culture, lymphocytes were centrifuged to obtain packed cells. The supernatant medium was removed and saved for reuse.

3.5.1.3. Genotoxic studies of RJ, EE, DM and 10-H2DA treatments by *in vitro* SCE assay

The lymphocytes were treated with RJ (0.0005-5 mg/mL), EE (0.00025-2.5 mg/mL), DM (0.0005-5 mg/mL) and 10-H2DA (0.000125-1.25 mg/mL) in plain RPMI 1640 culture medium for three hours at 37 °C. Following centrifugation at 400 g for 10 min, the supernatant medium was discarded. Then, incubation of the treated cells was continued at 37 °C in the dark with the previously saved medium. Bromodeoxyuridine (BrdU) (Sigma-Aldrich, USA) was also added in the culture medium for the final concentration of 5 µM.

3.5.1.4 Cell culture harvesting and staining

Cells were harvested at 76 h after initiation and were continually treated with hypotonic solution and fixed with Carnoy's fixative solution. Slides were prepared and stained with the fluorescent plus Giemsa technique according to our previous protocol (89). First, slides were placed in aluminum foil covered Coplin jars containing 40 ml of 12.5 mg/mL Bisbenzimide (Hoechst 33258)

Aqueous solution (Sigma-Aldrich, USA) for 30 min. Then, they were rinsed serially through distilled water and mounted with a few drops of McIlvane's buffer using a coverslip for each slide. Slides were then placed on a slide heater and exposed to UV light for 30 min. After the UV exposure, the cover slips were removed. Slides were washed thoroughly with distilled water and then stained with a 10% aqueous solution of Giemsa (Biotech reagents, Thailand) for 10 min. Slides were air-dried and mounted with permount mounting medium.

3.5.1.5 Cell scoring

Twenty-five cells per dose per experiment showing the second metaphase-staining pattern were scored from the coded slides for frequencies of sister chromatid exchange (SCE) to determine the genotoxic effects. The proliferation index (P.I.) and mitotic index (M.I.) were evaluated for their cytotoxic effect. The M.I. was determined as the number of all mitotic cells/1,000 cells. The P.I. was determined as (MI+2MII+3MIII)/100 cells, where MI is the number of metaphase cells from the first phase of the cell cycle (homogeneously-stained chromatids), MII is the number of metaphase cells from the second phase of the cell cycle (heterogeneously-stained chromatids), and MIII is the number of metaphase cells from the third phase of the cell cycle (mixed homogenously-stained and heterogeneously-stained chromatids). Two to three independent experiments were performed for each concentration of the treated compounds.

3.5.1.6 Statistical analysis

A square root transformation of the SCE data was required to stabilize the variances, according to the procedures of Whorton et al., 1985 (90). The frequency of transformed SCE was expressed as a square root of SCE. Dunnett's t-test was performed to analyze the difference between the means of the treated groups and the means of the control groups using the transformed data. Transformed SCE was expressed with the equation:

$$\text{Transformed SCE (SCE}_T) = \sqrt{\text{SCE}}$$

3.5.2 Antiproliferative effects of RJ treatments for 24 h on human lymphocytes detected by MTS assay

Human lymphocytes, cells were cultured in RPMI medium containing 10% fetal calf serum, 1% of penicillin/streptomycin, 2% phytohaemagglutinin and 1% L-glutamine in a 5% CO_2 incubator at 37 °C for 24 h. Then, lymphocyte cells (50,000 cells) were treated with RJ (0.0005-5 mg/mL) for 24 h at 37 °C. To determine cell viability, the CellTiter 96® AQueous One Solution Cell Proliferation MTS Assay kit was used. Briefly, 20 µL of the MTS tetrazolium compound [3-(4,5-dimethylthiazol- 2-yl) - 5-(3-carboxymethoxyphenyl)-2-(4-sulfophenyl)-2H-tetrazoliumre agent was added to each cell culture well containing treated cells in 100 µL medium, incubated at 37 °C for 2 h in a humidified 5% CO_2 incubator. The MTS was reduced by NADH or NADPH which produced by metabolically active cells. The formazan products were formed and measured by the absorbance at 490 nm with a PowerWave™ XS microplate spectrophotometer and calculated for the % cell viability (91) (92).

$$\% \text{ cell viability} = \left[(At)/(Ac)\right] \times 100$$

At : the absorbance of the treated well

Ac : the absorbance of control well

The IC50 value which is the concentration of sample required to inhibit 50% of the cell proliferation, was calculated by using the GraphPad software.

3.5.3 Analysis of pivotal gene expression: h-TERT, c-MYC, BCL2, BAX, NRF2, HO-1, cyclin E1, and cyclin B1 induced by RJ treatments for 24 h on human lymphocytes detected by Western blot analysis

Human lymphocytes cells were treated with 0.0005-5 mg/mL of RJ for 24 h. Then, cells were washed twice with PBS buffer. The protein extracts were prepared by lysing 10^7 cells in RIPA lysis buffer containing protease inhibitor cocktail set I (500 µM 4-benzenesulfonyl fluoride hydrochloride (AEBFS), hydrochloride (HCl), 150 nM aprotinin, bovine lung, crystallin, 1 µM E-64 protease inhibitor, 0.5 nM disodium EDTA ($C_{10}H_{14}N_2Na_2O_8$), 1 µM leupeptin hemisulfate ($C_{20}H_{38}N_6O_4 \cdot 1/2H_2SO_4$)). The lysate was centrifuged at 10,000 xg for 10 min, and the supernatant was recovered. Protein

quantification was carried out following the Bradford protein assay kit (Bio-Rad, USA). Protein samples (50 µg) were boiled for 5 min in a sodium dodecyl sulfate (SDS) buffer and separated on 10% SDS-polyacrylamide denaturing gel electrophoresis (SDS-PAGE) according to the method of Laemmli (93). For Western blot analysis, the proteins were blotted onto nitrocellulose membrane. The blots were blocked by incubation in Odyssey blocking buffer for 1 h. After a brief rinse, blots were incubated overnight in TBST-blocking buffer with corresponding rabbit antibody e.g. rabbit anti-p53, anti-BAX, anti-BCL2, anti-c-MYC, anti-cyclin D1, anti cyclin-E1, anti-cyclin B1, anti-NRF2, anti-hTERT, and anti-HO-1. Rabbit anti-β-actin polyclonal antibody were used as an internal control. Blots were washed three times with TBST, incubated with LI-COR IRDye 680 mouse anti-rabbit (1:10,000) in TBST for 1h at room temperature and washed again. The protein bands were visualized using Odyssey Fc Imager (LI-COR, USA).

3.5.4 Analysis of glutathione peroxidase (GPx) activities induced by RJ treatments on human lymphocytes for 24 h

The activity of glutathione peroxidase (GPx) was measured by using glutathione Peroxidase (GPx) Assay kit (Cayman Chemical, USA). Human lymphocyte cells were treated with RJ (0.0005-5 mg/mL) for 24 h. The treated cells were washed in phosphate buffer. Then, the cells were homogenized in 1 mL cold buffer, which consisted of 50 mM Tris-HCl, pH 7.5, 5 mM EDTA, 1 nM dithiothreitol (DTT). The homogenate was centrifuged at 10,000x g for 15 min at 4 °C. The supernatant was removed for the assay. GPx activity was indirectly measured through a coupled reaction with glutathione reductase. Oxidized glutathione (GSSG) was produced upon reduction of hydroperoxide by GPx, and was recycled to its reduced state by glutathione reductase (GR) and NADPH. The oxidation of NADPH to NADP$^+$ is presented by a decrease in absorbance at 340 nm. Under conditions in which the GPx activity is rate limiting, the rate of decrease in the A340 is directly proportional to the GPX activity in the sample. The assay was performed according to the manufacturer's instructions and the GPx activity was be calculated using two formula.

$$\Delta A340/\min = \frac{(A_{340\ (Time\ 2)} - A_{340\ (Time\ 1)})}{(Time\ 2_{min} - Time\ 1_{min})}$$

Time 1 represents absorbance at 0 min, Time 2 is the absorbance at 5 min and ΔA340/min refers to the change in absorbance per minute obtained from the standard curve. Thus, the activities of GPx in the samples were determined by following formula:

$$GPx\ activity = \frac{\Delta A340\ /\min}{0.00373\ \mu M^{-1}} \times \frac{0.19\ ml}{0.02\ ml}\ x\ Sample\ dilution$$

One unit is defined as the amount of enzyme that caused the oxidation of 1.0 nmol of NADPH to NADP$^+$ per min at 25 $^\circ$C.

3.5.5 Antigenotoxic effects of RJ, DM, LE, and 10-H2DA treatments against DXR on human lymphocytes detected by *in vitro* sister chromatid exchange (SCE) assay

3.5.5.1 Cell culture

Twenty-four hours after the initiation of the culture, lymphocytes were centrifuged to obtain packed cells. The supernatant medium was removed and saved for reuse. The lymphocytes were pretreated with RJ (0.0005-5 mg/mL), EE (0.00025-2.5 mg/mL), DM (0.0005-5 mg/mL) and 10-H2DA (0.0125-125 µg/mL) in plain RPMI 1640 culture medium for two hours at 37 $^\circ$C. Following centrifugation, the supernatant medium was discarded. The incubation of the treated cells was then treated with 0.1 µg/mL DXR at 37 $^\circ$C for two hours. Then the treated medium was discarded after centrifugation and culturing of the treated cells were continued with the previously saved medium and with 5 µM BrdU in the dark. As a positive control, the lymphocytes were simultaneously treated with plain RPMI 1640 culture medium for two hours followed by DXR for two hours. As a solvent control, DMSO was cultured for two hours followed by DXR for two hours. As a negative control, treatments were made with either plain RPMI 1640 or DMSO for two hours followed by plain RPMI 1640 for two hours.

3.5.5.2 Cell harvesting and staining

Cells were harvested as described in 3.5.1.4 except that harvesting was done at 96 h after initiation because of cell cycle. The fluorescent plus Giemsa technique was also performed for staining as described in 3.5.1.4.

3.5.5.3 Cell scoring

Twenty-five cells per dose per experiment showing the second metaphase-staining pattern were scored from the coded slides for frequencies SCE to determine its antigenotoxic effect. The M.I. and P.I. were also determined as described in 3.5.1.5.

3.5.5.4 Statistical analysis

The frequency of transformed SCE was expressed as a square root of SCE. Dunnett's t-test was performed to analyze the difference between the means of the treated groups and the means of the control groups using the transformed data as described in 3.5.1.6.

3.5.6 Proliferative activities of RJ co-treatments with DXR for 24 h on human lymphocytes detected by MTS tetrazolium assay

Human lymphocytes, cells were cultured in RPMI medium containing 10% fetal calf serum, 1% of penicillin/streptomycin, 2% phytohaemagglutinin and 1% L-glutamine in a 5% CO_2 incubator at 37 $^\circ$C for 24 h. Then, lymphocyte cells (50,000 cells) were co-treated with RJ (0.0005-5 mg/mL) and 0.2 µg/mL for 24 h at 37 $^\circ$C. To determine cell viability, the CellTiter 96® AQueous One Solution Cell Proliferation MTS Assay kit (Promega, USA) was used as described in 3.5.2.

3.5.7 Analysis of pivotal gene expressions: h-TERT, c-MYC, BCL2, BAX, NRF2, HO-1, cyclin E1, and cyclin B1 induced by RJ co-treatments with DXR for 24 h on human lymphocytes by Western blot

Human lymphocytes cells were co-treated with RJ (0.0005-5 mg/mL) and 0.2 µg/mL DXR for 24 h. Then, cells were washed twice with PBS buffer and analysis of pivotal gene with procedure as described in 3.5.3.

3.5.8 Analysis of GPX activities induced by RJ co-treatments with DXR on human lymphocytes for 24 h

For glutathione peroxidase assay, human lymphocyte cells were co-treated with RJ (0.0005-5 mg/mL) with 0.2 µg/mL DXR for 24 h. The activity of GPx was measured by using glutathione peroxidase (GPx) Assay kit (Cayman Chemical, USA) as described in 3.5.4.

3.6 Analysis of the effects of 10-H2DA on MCF-7 breast cancer cells

3.6.1 Proliferative activities of 10-H2DA for 24 h on MCF-7 breast cancer cell line detected by MTS tetrazolium assay

The MCF-7 cells were cultured in MEM medium with glutamine containing 10% fetal calf serum, 1 mM sodium pyruvate, 1% of penicillin/ streptomycin at 37 $^{\circ}$C in a 5% CO_2 incubator. MCF-7 cells were seeded into 96-well plates at a density of 5×10^3 per well (100 µL) for 24 h then cells were treated with the 10-H2DA (1.25, 12.5 and 125 µg/mL) for 24 h at 37 $^{\circ}$C. Subsequently, the CellTiter 96® AQueous One Solution Cell Proliferation Assay kit (Pormega, USA) was applied following the manufacturer's instruction. Briefly, 20 µL of the MTS reagent was added to each well containing 100 µL of the medium. After that, the plate was incubated at 37 $^{\circ}$C for 2 h in a humidified and 5% CO_2 incubator. The absorbance was detected at 490 nm with a microplate spectrophotometer and calculated the percentage of cell viability as following formula.

$$\% \text{ cell viability} = \left[(At)/ (Ac)\right] \times 100$$

At : the absorbance of the treated well

Ac : the absorbance of control well

To investigate cytotoxic effects of 10-H2DA against MCF-7 breast cancer cells according to National Cancer Institute (NCI), USA (94) , further analysis of 50% growth inhibition (GI50), total growth inhibition (TGI), and 50% lethal concentration (LC50) values were determined according to the protocol by Holbeck, et al., 2010 (97).

In order to evaluate these GI50, TGI, and LC50 values, MCF-7 Cells were cultured for 24 h and called time zero density. Then, cells were treated with 10-H2DA (1.25, 12.5, 50, 125 and 250 µg/mL) for 24 h and measured the percentage of viable cells compared to the time zero density. Growth percent of 100 corresponds to growth seen in untreated cells. Growth percent of 50 corresponds to 50% growth (50% inhibition). Growth percent of 0 indicates no growth (TGI: total growth inhibition). Growth percent of -50 indicates lethality in 50% of the starting cells (LC50) (97).

The percentages of cell survival were calculated by following formular.

$$\% \text{ cell survival} \quad = [(T-T_0)/(C-T_0)] \times 100, \; T \geq T_0$$
$$= [(T-T0)/T_0] \times 100, \; T \leq T_0$$

T   = Average O.D. of treated with 10-H2DA for 24 h

T_0 = Avergae O.D. at 0 h

C   = Average O.D. of cells treated with only media for 24 h

3.6.2 Analysis of pivotal gene expressions: h-TERT, c-MYC, BCL2, BAX, NRF2, HO-1, cyclin E1, and cyclin B1 induced by 10-H2DA for 24 h on MCF-7 breast cancer cell line

MCF-7 cells were treated with various concentrations of 10-H2DA (1.25, 12.5 and 125 µg/mL). Then, the treated cells were washed twice with PBS buffer. The protein extracts were prepared by lysing 1×10^7 cells in RIPA lysis buffer containing protease inhibitor cocktail set I (500 µM 4-benzenesulfonyl fluoride hydrochloride (AEBFS), hydrochloride (HCl), 150 nM aprotinin, bovine lung, crystallin, 1 µM E-64 protease inhibitor, 0.5 nM disodium EDTA ($C_{10}H_{14}N_2Na_2O_8$), 1 µM leupeptin hemisulfate ($C_{20}H_{38}N_6O_4 \cdot 1/2H_2SO_4$)). The lysate was centrifuged at 10,000 xg for 10 min, and the supernatant was recovered. Protein quantification was carried out following the Bradford protein assay kit (Bio-Rad, USA). Protein samples (50 µg) were boiled for 5 min in a sodium dodecyl sulfate (SDS) buffer and separated by 10% SDS-polyacrylamide denaturing gel electrophoresis (SDS-PAGE) method of Laemmli. Then, the protein extracts were analyzed for the levels of h-TERT, c-MYC, BCL2, BAX, NRF2, HO-1, cylin E1, cylin B1 by Western blot as previously described in 3.5.3.

3.6.3 Analysis of cell cycle progression induced by 10-H2DA treatments for 24 h on MCF-7 breast cancer cells by flow cytometer

To determine the cell cycle distribution, 1×10^5 of MCF-7 cells were grown for 24 h at 37 °C with 5% CO_2. Then, the cells were treated with various concentrations of 10-H2DA (1.25, 12.5 and 125 μg/mL) for 24 h. Subsequently, the cells were harvested, washed with PBS and fixed in 70% cold ethanol at -20 °C. The cells were left to stand overnight and then collected by centrifugation at 500 rpm for min. Next, the cells were stained with propidium iodide/ribonuclease staining buffer and incubated at room temperature for 20 min. The cell cycle distribution were measured with Guava EasyCyteTM Flow Cytometer (Millipore) and the percentage of cells in the Sub G1, G0/G1, S, and G2/M phases of the cell cycle were determined using GuavaSoft software (95).

3.6.4 Analysis of cell apoptosis induced by 10-H2DA treatments for 24 h on MCF-7 breast cancer cells by flow cytometer

For apoptosis analysis, 1×10^5 MCF-7 breast cancer cells were seeded into 25 cm^2 flask overnight before treated with 10-H2DA (1.25, 12.5 and 125 μg/mL) for 24 h. Harvesting of cells included a collection of attached cells following trypsinization and floating cells, which were combined in the sample for processing. An Annexin V-FITC Apoptosis Detection kit I (BD Biosciences, USA) was applied as described by the manufacturer's protocol. Briefly, cells were washed twice with cold PBS and then resuspended cells in 1x binding buffer. The 10-H2DA treated cells were added with 5 μl FITC Annexin V and 5 μL PI and incubated at room temperature for 15 min in the dark. Then, cells were added with 400 μL of 1x binding buffer and analyzed immediately by Guava EasyCyteTM Flow Cytometer (Millipore, USA). Annexin V binds to the membrane phosphatidylserine(7) that flips from the inside to the surface of the membrane when apoptosis occurs. Propidium iodide stains the dead cells as it permeates damaged membrane. Annexin V and propidium iodide negative stained cells means viable cells. Annexin V positive and propidium iodide negative stained cells indicates early apoptosis with intact membranes. Annexin V and propidium iodide

positive stained cells shows end stage apoptosis and death. Annexin V negative and propidiumiodide positive stained cells demonstrates cell necrosis.

3.6.5 Morphological changes induced by 10-H2DA treatments for 24 h on MCF-7 breast cancer cells detected by Hoechst 33258 and propidium iodide double staining under fluorescence microscope

MCF-7 cells were grown on tissue culture plate and treated with MEM medium control, 1.25-125 µg/mL 10-H2DA and 1 µM DXR for 24 h. After 24 h, the cells were harvested, washed with cold PBS and adjusted to a density of 5×10^5 cells/mL. Then, treated cells were incubated with 10 µg/mL Hoechst 33258 staining solution at 37 °C in a CO_2 incubator for 7min and counterstained with 2.5 µg/mL PI for 15 min in the dark. Then aliquot of cell suspension was placed onto a glass microscopic slides. The slides were observed immediately under fluorescence microscope (Eclipse-Ci Nikon, USA) (96).

3.6.6 Proliferative activities of 10-H2DA in combination with DXR for 24 h on MCF-7 breast cancer cell line detected by MTS tetrazolium assay

The MCF-7 cells were cultured in MEM medium with glutamine containing 10% fetal calf serum, 1 mM sodium pyruvate, 1% of penicillin/streptomycin at 37 °C in a 5% CO_2 incubator. MCF-7 cells were seeded into 96-well plates at a density of 5×10^3 per well (100 µl) for 24 h then cells were treated with the 10-H2DA (1.25, 12.5 and 125 µg/mL) and 1 µM DXR for 24 h at 37 °C. Subsequently, the CellTiter 96® AQueous One Solution Cell Proliferation Assay kit (Promega, USA) was applied following the manufacturer's instruction. Briefly, 20 µl of the MTS reagent was added to each well containing 100 µl of the medium. After that, the plate was incubated at 37 °C for 2 h in a humidified in a 5% CO_2, humidified incubator. The absorbance was detected at 490 nm with a microplate spectrophotometer and calculated the percentage of cell viability as previously described in 3.6.1.

3.6.7 Analysis of pivotal gene expressions: h-TERT, c-MYC, BCL2, BAX, NRF2, HO-1, cyclin E1, and cyclin B1 induced by 10-H2DA in combination with DXR for 24 h on MCF-7 breast cancer cell line

MCF-7 cells were co-treated with 10-H2DA (1.25, 12.5 and 125 µg/mL) and 1 µM (0.54 µg/mL) DXR for 24 h. After treatment, cells were washed with PBS and extracted for proteins using RIPA lysis buffer. Then, the protein extracts were analyzed for the levels of h-TERT, c-MYC, BCL2, BAX, NRF2, HO-1, cylin E1, cylin B1 by Western blot as previously described in 3.6.2.

3.6.8 Analysis of cell cycle progression induced by 10-H2DA treatments in combination with DXR for 24 h on MCF-7 breast cancer cells by flow cytometer

To determine the cell cycle distribution, 1×10^{5} of MCF-7 cells were grown for 24 h at 37 °C with 5% CO_2. Then, the cells were co-treated with various concentrations of 10-H2DA (1.25, 12.5 and 125 µg/mL) and 1 µM DXR for 24 h. Subsequently, cell cycle progression was analyzed for the ratios of sub G1, G0/G1, S and G2/M phases by flow cytometer as previously described in 3.6.3.

3.6.9 Analysis of cell apoptosis induced by 10-H2DA treatments in combination with DXR for 24 h in MCF-7 breast cancer cells by flow cytometer using apoptosis assay kit (BD Bioscience, USA)

For apoptosis analysis, 1×10^{5} MCF-7 breast cancer cells were seeded into 25 cm^2 flask overnight before co-treated with 10-H2DA (1.25, 12.5 and 125 µg/mL) and 1 µM DXR for 24 h. Then, cells were harvested, washed and stained with FITC annexin V and PI. The percentages of live, early apoptosis, late apoptosis and necrosis were analyzed by flow cytometer as previously described in 3.6.4.

3.6.10 Morphological changes induced by co-treatments of 10-H2DA and DXR for 24 h on MCF-7 breast cancer cells detected by Hoechst 33258 and propidium iodide double staining under fluorescence microscope

MCF-7 cells were grown on tissue culture plate and co- treated with 1.25-125 µg/mL 10-H2DA and 1 µM DXR for 24 h. Then, all treated cells were harvested, washed and double stained with Hoechst 33258 and PI. Morphological changes were detected under fluorescence microscope as previously described in 3.6.5.

CHAPTER 4

RESULTS

4.1 Analysis of general chemical compositions and pH of RJ

Analysis RJ composition Frozen RJ produced by honeybees (*Apis mellifera*) was purchased from an apiary company (Chiang Mai, Thailand) certified by the Ministry of Industry, Thailand. Carbohydrate, protein, ash and moisture contents in RJ were measured using AOAC methods (82).

4.1.1 Analysis of general compositions in RJ

The frozen RJ samples from Chiangmai, northern Thailand had pH 4.0 with approximately 65% moisture, 2.5% lipids, 2.2% proteins, 0.2% fiber, no ash and 32% carbohydrates (%w/w). Our current samples had lower nutrient contents, especially proteins, lipids, and carbohydrates, compared to that of our previous report using fresh RJ from the same area, Chiangmai, northern Thailand, which had pH 3.5, 67.4% moisture, 12.1% carbohydrate, 4% lipid, 12% proteins and 1% ash (97). The compositions of RJ from Romania and Bulgaria also reported a higher amount of protein contents at 13% and 15.5%, respectively, and both had pH 3.9 (98).

4.1.2 Quantitative analysis of 10-H2DA in RJ and EE by HPLC

The retention times of 10-H2DA, RJ and EE were found to be about 20.38, 21.10 and 20.44 min respectively by our HPLC system (Figure 4.1 and 4.2). The amount of 10-H2DA in RJ and EE was 0.8% and 2.4% (w/w), respectively.
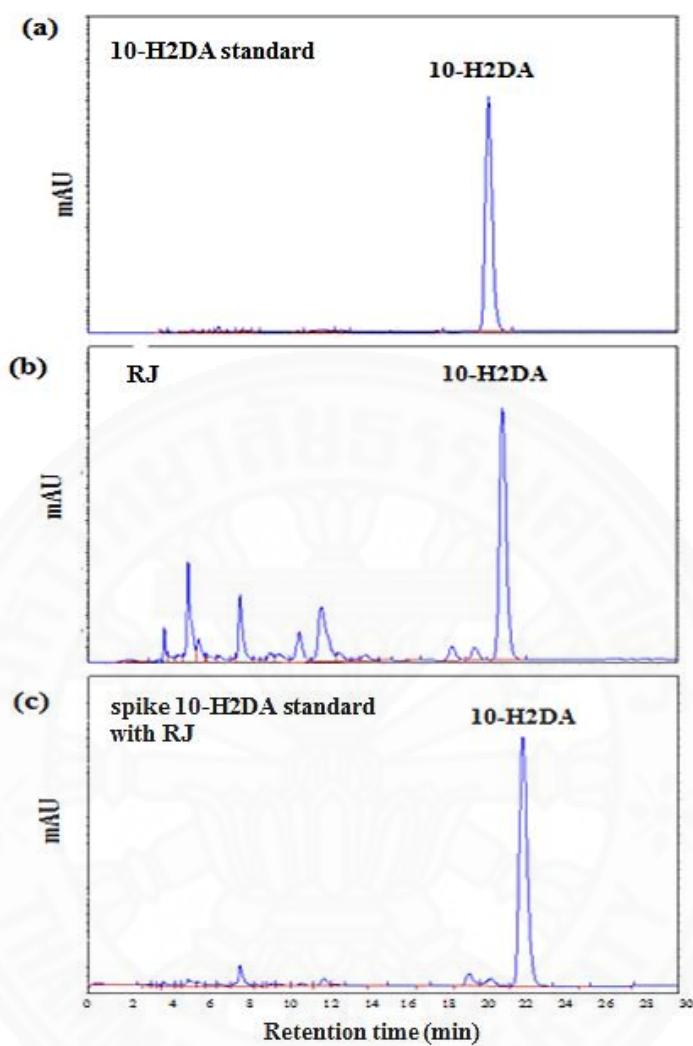
Figure 4.1 HPLC chromatogram. (a)10-H2DA standard, (b) a RJ sample (c) spike of 10-H2DA standard with RJ sample
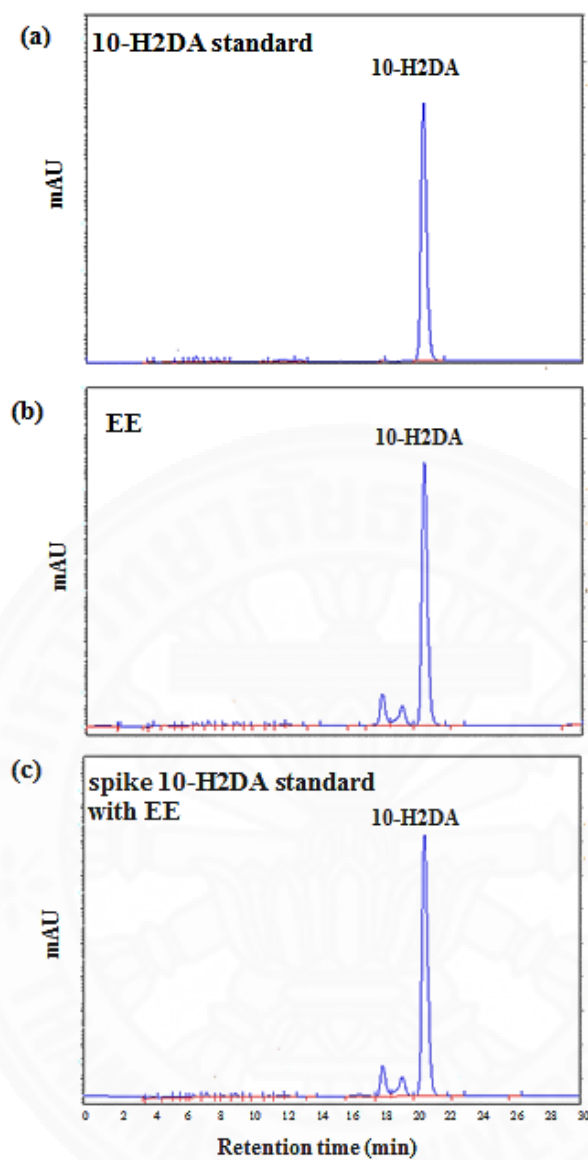
Figure 4.2 HPLC chromatogram. (a) 10-H2DA standard, (b) an EE sample (c) spike of 10-H2DA standard with EE sample

A standard curve of 10-H2DA was constructed from concentrations of 10-H2DA versus the peak area, as shown in the Figure 4.3. A linear relationship was found in the concentration of 10-H2DA ranging from 25 to 300 µg/mL (r^2=0.999).
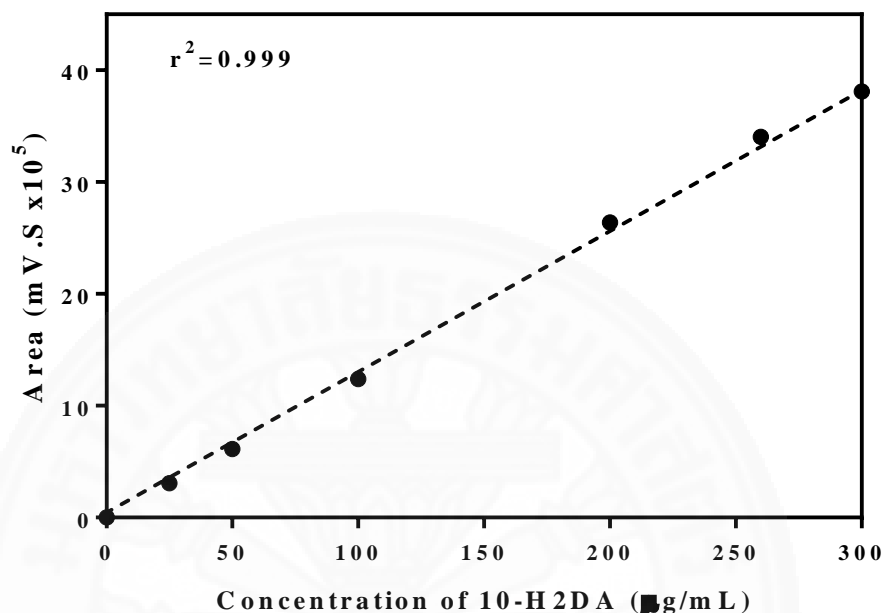
Figure 4.3 A standard curve of standard 10-H2DA determined by HPLC

The calculated area of 10-H2DA peak of RJ and EE showed that the amount of 10-H2DA in RJ and EE were 0.82% and 2.42% (w/w) respectively.

4.2 Analysis of antioxidant properties of RJ

4.2.1 Determination of total phenolic content, total flavonoid content and antioxidant activity in the RJ samples

Total phenolic acid of the RJ sample was 1.8 ± 0.5 mg gallic acid/g RJ. The results showed that the content of flavonoids was 0.9±0.08 mg gallic acid /g RJ. The antioxidant activity of the RJ sample was approximately 17.9 ± 1.9 µM Trolox equivalent antioxidant capacity (TEAC)/g RJ, Trolox EC50 = 1103 µM.

4.3 Effects of RJ, DM, EE, and 10-H2DA treatments on human lymphocytes

4.3.1 Genotoxic studies on human lymphocytes by *in vitro* SCE assay

4.3.1.1 Genotoxic and cytotoxic study of RJ, DM, EE, and 10-H2DA

(1) Genotoxic study of RJ treatments for 3 h

Treatments with RJ at 0.0005, 0.005, 0.05, and 0.5 mg/mL for 3 h were not genotoxic to human cells but the 5 mg/mL treatment induced genotoxicity by a 1.4-fold increase, compared to that of RPMI negative control ($p<0.05$) (Figure 4.4). Treatment of 2% V/V DMSO, a solvent control, showed a slight increase in SCE levels but there was no significant difference from that of the RPMI control. The SCE level induced by DXR treatment (0.1 µg/mL), a positive control, was a 2-fold increase ($p<0.05$). There was no significant difference between M.I. and P.I. among treatments (Table 4.1) indicating no cytotoxicity induced by all RJ treatments. However, there was a slight delay of cell cycle progression from MI to MII caused by the low dose of 0.0005 mg/mL RJ treatment (Figure 4.5). Cell cycle delay was also induced by 2% V/V DMSO solvent and DXR positive control. It is noteworthy that serial dilution of RJ (dissolved in DMSO) with RPMI solvent was prepared and therefore, the concentration of DMSO in RJ at 0.0005 mg/mL was 10,000 times diluted. Consequently, the effect of cell cycle delay resulted from RJ itself while the DMSO had little effect. RJ treatments at higher doses showed relatively higher cell cycle progression (higher MII cells than MI cells) as compared to that of the RPMI control.
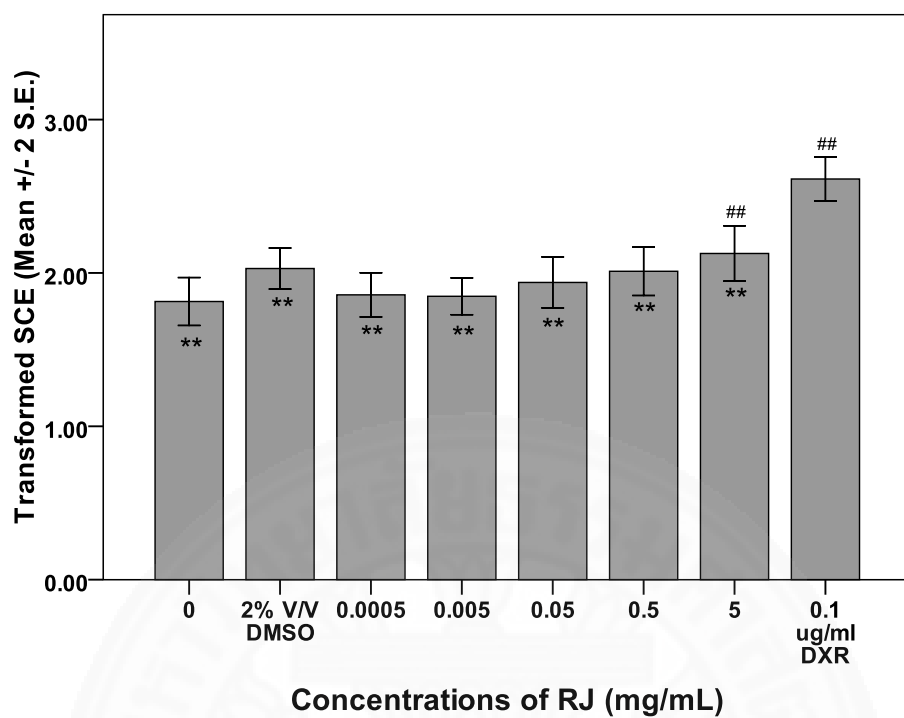
Figure 4.4 Transformed SCE induced by various concentrations of RJ treatments on human lymphocytes for 3 h

**p < 0.05 significantly different from the DXR-treated positive control

##p < 0.05 significantly different from the RPMI-treated negative control

Table 4.1. M.I. and P.I. induced by various concentrations of RJ treatments on human lymphocytes (n = 3)

RJ (mg/mL)	M.I. (mean ± SE)	P.I. (mean ± SE)
0	19.0 ± 2.0	2.7 ± 0.3
2% V/V DMSO	18.5 ± 0.5	2.4 ± 0.0
0.0005	21.0 ± 2.5	2.5 ± 0.0
0.005	18.0 ± 1.0	2.6 ± 0.2
0.05	17.5 ± 2.5	2.6 ± 0.2
0.5	14.0 ± 1.0	2.2 ± 0.2
5	17.0 + 4.0	2.6 ± 0.6
0.1 µg/mL DXR	12.0 ± 3.0	1.6 ± 0.3
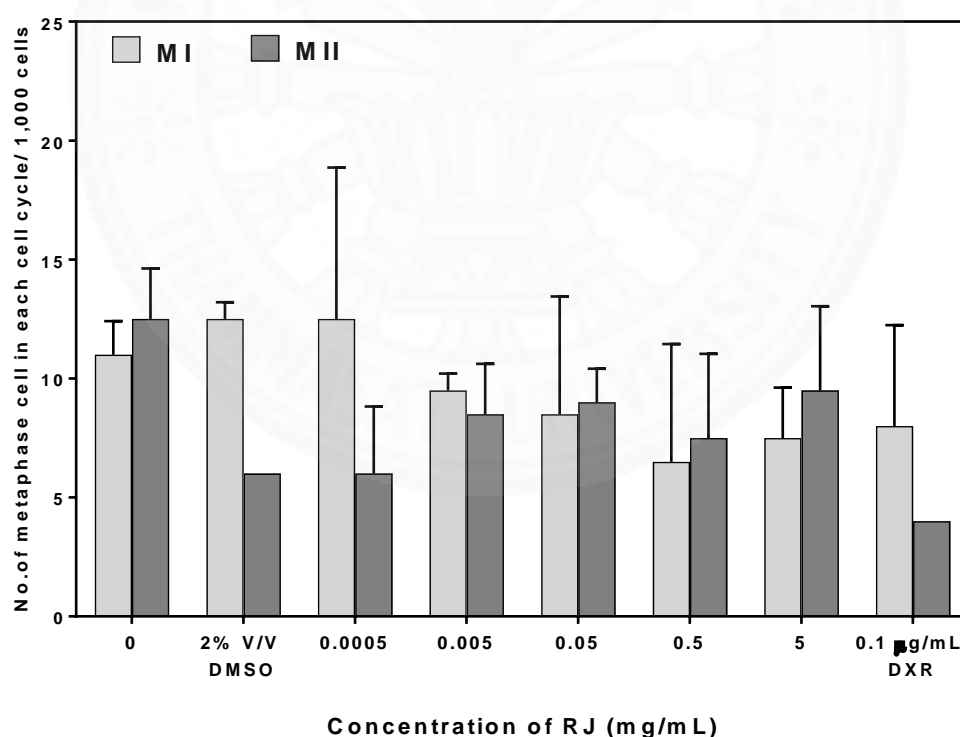
Figure 4.5 Effects on cell cycle progression induced by various concentrations of RJ treatments on human lymphocytes for 3 h (mean ± SE); MI and MII were the number of metaphase cells in the first and the second phase of the cell cycle, respectively (n = 3)

(2) Genotoxic study of DM treatments for 3 h

Treatments with DM at 0.0005, 0.005, and 0.05 mg/mL for 3 h had no genotoxicity to human cells but the 0.5 and 5 mg/mL treatments induced genotoxicity by a 1.4-fold increase compared to that of RPMI negative control ($p < 0.05$) (Figure 4.6). The SCE level induced by DXR treatment (0.1 μg/mL), a positive control, was a 2-fold increase ($p < 0.05$). There was no significant difference between M.I. and P.I. among treatments (Table 4.2) indicating no cytotoxicity was observed. However, there was a trend of enhancing cell cycle progression at 5 mg/mL (higher MII) whereas DXR treatment showed cell cycle delay (Figure 4.7).
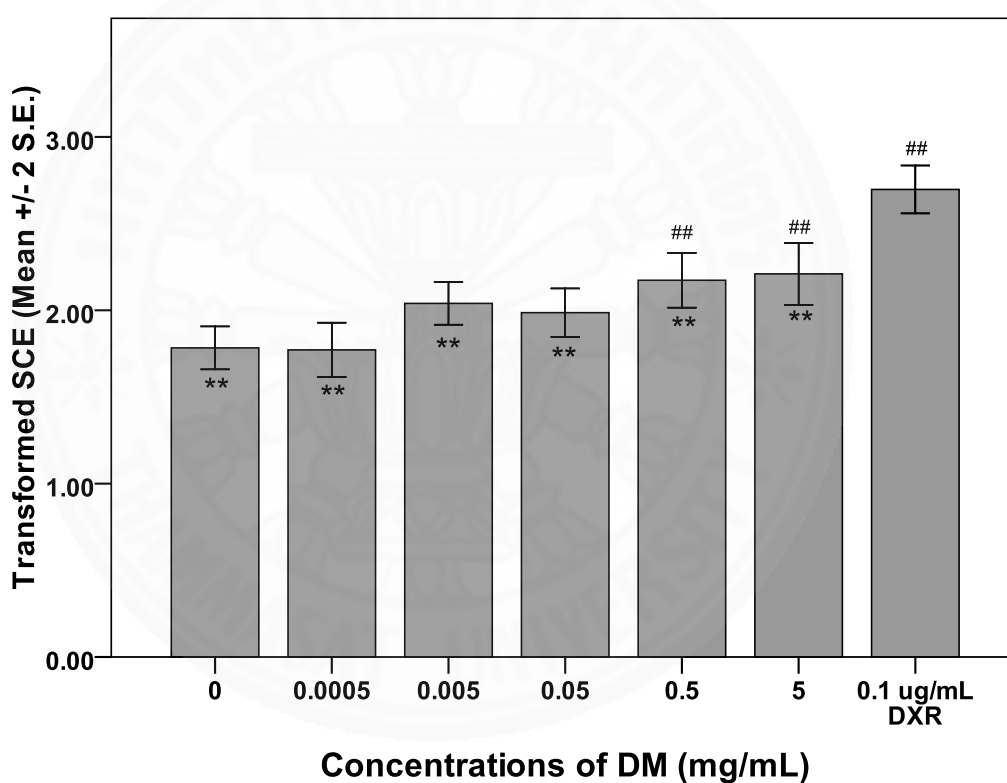
Figure 4.6 Transformed SCE induced by various concentrations of DM treatments on human lymphocytes for 3 h

[**]p < 0.05 significantly different from the DXR-treated positive control

[##]p < 0.05 significantly different from the RPMI-treated negative control

Table 4.2 M.I. and P.I. induced by various concentrations of DM treatments on human lymphocytes (n = 3)

DM (mg/mL)	M.I. (mean ± SE)	P.I. (mean ± SE)
0	19.0 ± 2.0	2.7 ± 0.3
0.0005	17.5 ± 0.7	2.9 ± 0.5
0.005	20.0 ± 4.2	2.9 ± 0.6
0.05	20.0 ± 5.6	3.1 ± 0.9
0.5	15.0 ± 0.0	2.3 ± 0.0
5	17.5 ± 6.3	2.9 ± 1.3
0.1 µg/mL DXR	12.0 ± 4.2	1.6 ± 0.4
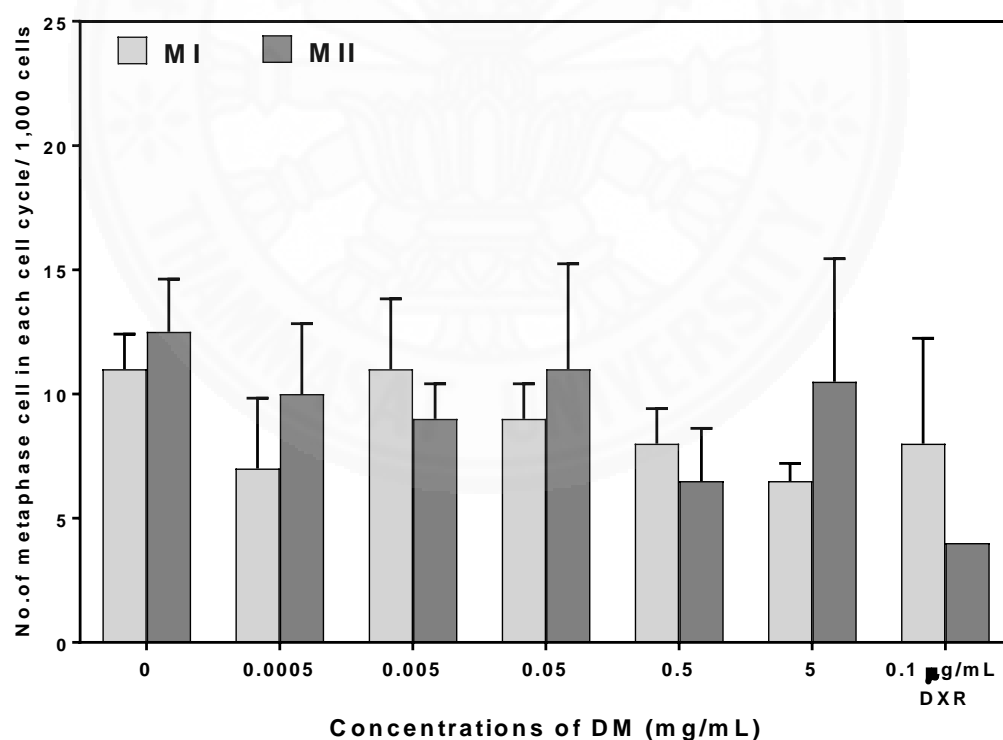
Figure 4.7 Effects on cell cycle progression induced by various concentrations of DM treatments on human lymphocytes for 3 h (mean ± SE); MI and MII were the number of metaphase cells in the first and the second phase of the cycle, respectively (n = 3)

(3) Genotoxic study of EE treatments for 3 h

Treatments with EE at 0.00025, 0.0025, 0.025, and 0.25 mg/mL for 3 h had no genotoxicity to human cells but the 2.5 mg/mL treatment slightly induced genotoxicity by a 1.2-fold increase compared to that of RPMI negative control ($p<0.05$) (Figure 4.8). The SCE level induced by DXR treatment (0.1 μg/mL), a positive control, was a 2-fold increase ($p<0.05$). There was no significant difference between M.I. and P.I. among treatments (Table 4.3) indicating no cytotoxicity was observed. However, there was a trend of enhancing cell cycle progression at the doses of (0.025-2.5 mg/mL) but not at the highest dose of 2.5 mg/mL. DXR treatment showed cell cycle delay (Figure 4.9).
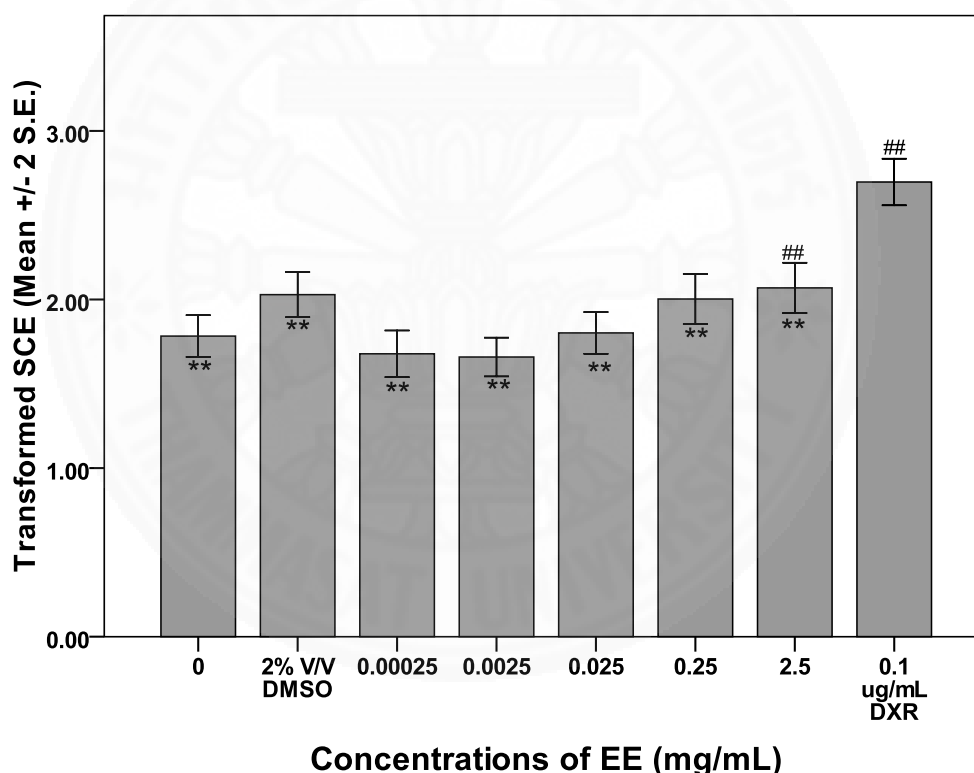
Figure 4.8 Transformed SCE induced by various concentrations of EE treatments on human lymphocytes for 3 h

[**]$p < 0.05$ significantly different from the DXR-treated positive control

[##]$p < 0.05$ significantly different from the RPMI-treated negative control

Table 4.3 M.I. and P.I. induced by various concentrations of EE treatments on human lymphocytes (n = 3)

EE (mg/mL)	M.I. (mean ± SE)	P.I. (mean ± SE)
0	19.0 ± 2.0	2.7 ± 0.3
2% V/V DMSO	18.5 ± 0.7	2.4 ± 0.0
0.00025	23.5 ± 6.3	3.6 ± 1.2
0.0025	16.5 ± 4.9	2.3 ± 0.6
0.025	17.5 ± 6.3	2.6 ± 0.9
0.25	25.0 ± 2.8	4.0 ± 0.7
2.5	22.5 ± 2.1	3.3 ± 0.4
0.1 µg/mL DXR	12.0 ± 4.2	1.6 ± 0.4
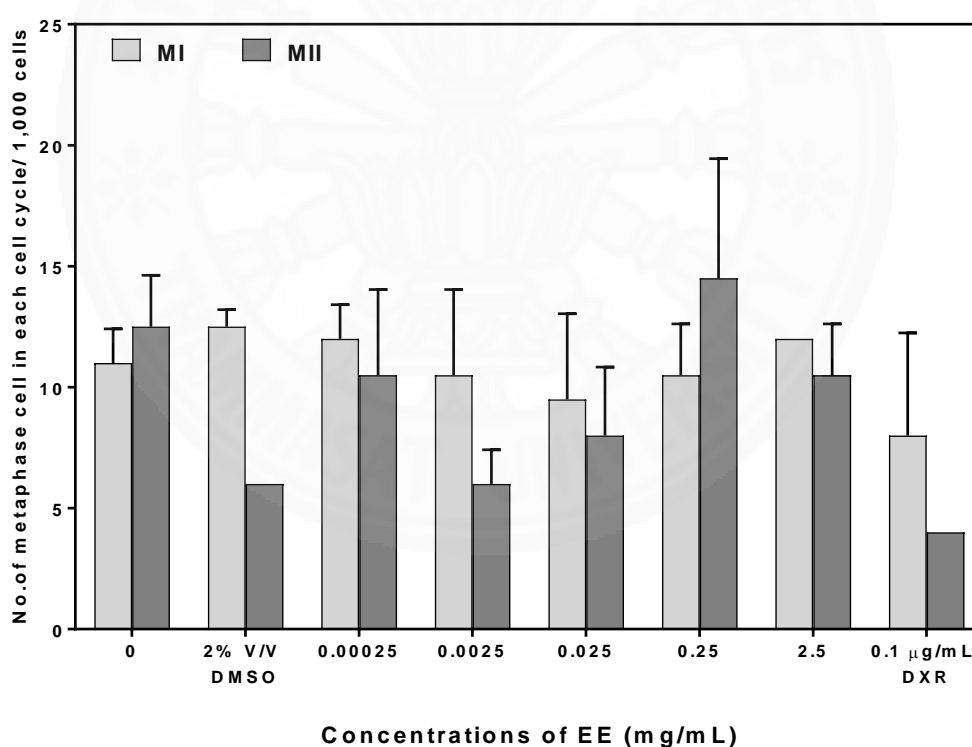
Figure 4.9 Effects on cell cycle progression induced by various concentrations of EE treatments on human lymphocytes for 3 h (mean ± SE); MI and MII were the number of metaphase cells in the first and the second phase of the cell cycle, respectively (n = 3)

(4) Genotoxic study of 10-H2DA treatments for 3 h

Treatments with 10-H2DA at 0.125, and 1.25 µg/mL for 3 h did not induce genotoxicity but 12.5 and 125 mg/mL treatments slightly induced genotoxicity by 1.3 and 1.6-fold increase (p<0.05). The SCE level induced by DXR treatment (0.1 µg/mL), a positive control, was a 2-fold increase (p<0.05) (Figure 4.10). There was no significant difference between M.I. and P.I. among treatments, however, there was a trend of dose-dependent decrease in M.I. and P.I. (Table 4.4). The number of metaphase cells in MII was lower than in MI especially at the lowest dose, of 0.125 µg/mL and at the highest dose, of 125 µg/mL 10-H2DA treatments as well as the DXR control treatment indicating effects on cell cycle delay (Figure 4.11).
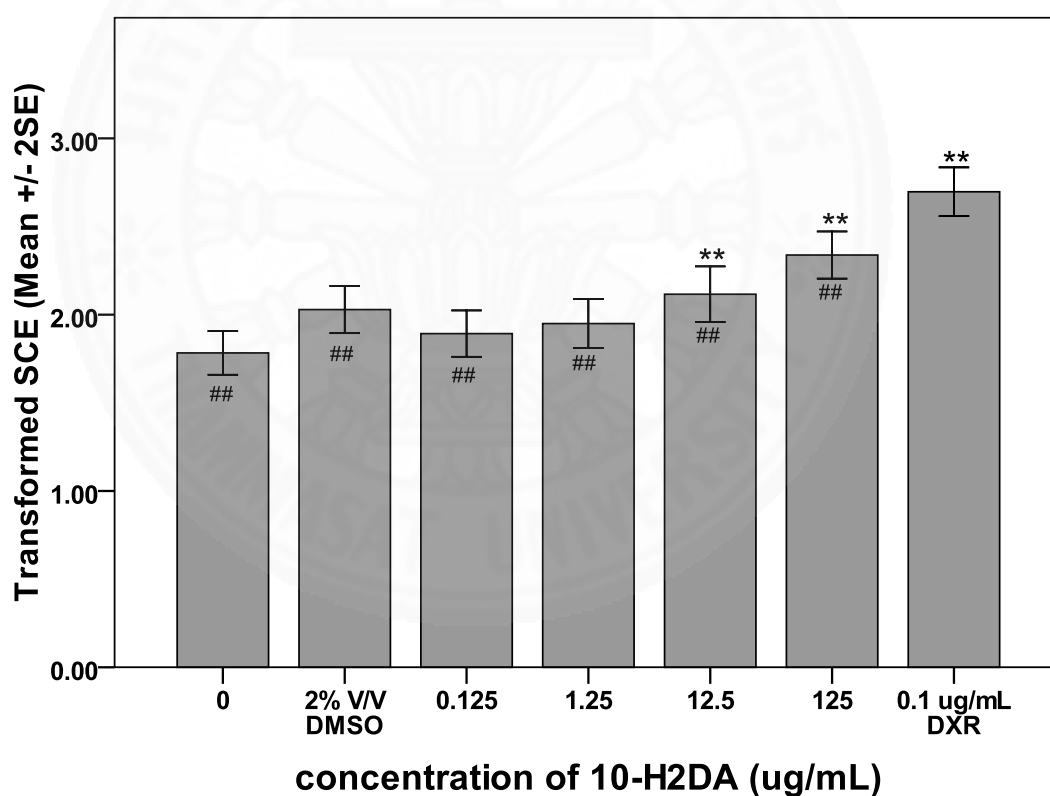
Figure 4.10 Transformed SCE induced by various concentrations of 10-H2DA treatments on human lymphocytes for 3 h

** p < 0.05 significantly different from the DXR-treated positive control

p < 0.05 significantly different from the RPMI-treated negative control

Table 4.4 M.I. and P.I. induced by various concentrations of 10-H2DA treatments on human lymphocytes (n = 3)

10-H2DA (µg/mL)	M.I. (mean ± SE)	P.I. (mean ± SE)
0	19.0 ± 2.0	2.7 ± 0.3
2% V/V DMSO	18.5 ± 0.7	2.4 ± 0.0
0.125	16.5 ± 2.1	1.9 ± 0.1
1.25	14.0 ± 7.0	1.8 ± 0.7
12.5	13.5 ± 0.7	2.0 ± 0.3
125	11.0 ± 1.4	1.4 ± 0.4
1,250	0	0
0.1 µg/mL DXR	12.0 ± 4.2	1.6 ± 0.4
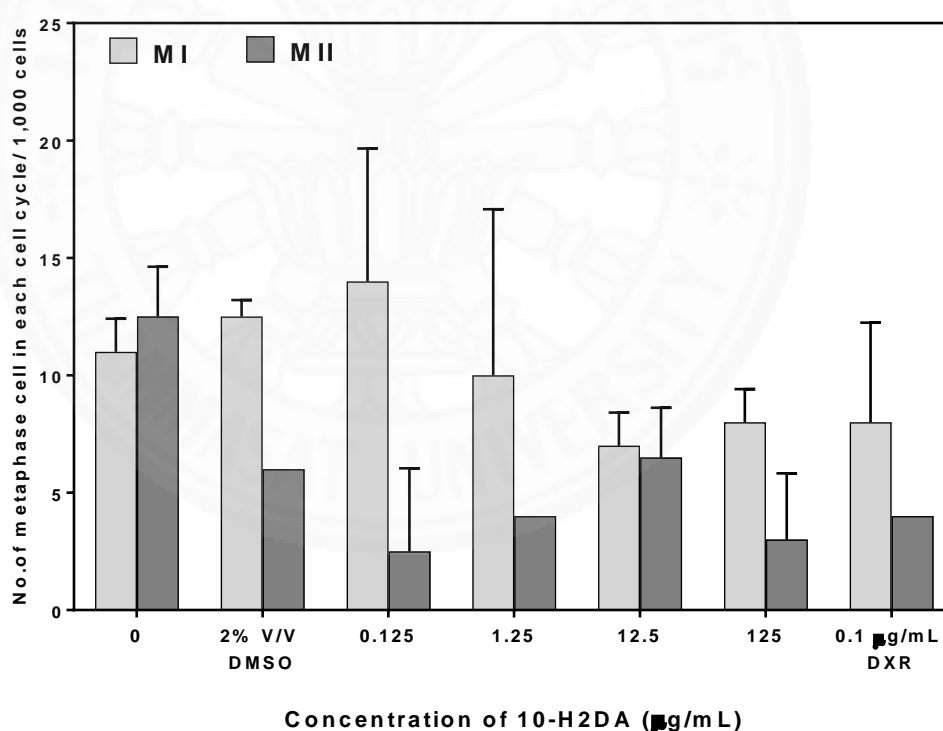
Figure 4.11 Effects on cell cycle progression induced by various concentrations of 10-H2DA treatments on human lymphocytes for 3 h (mean ± SE); MI and MII were the number of metaphase cells in the first and the second phase of the cell cycle, respectively (n = 3)

4.3.1.2 Antiproliferative effects of RJ treatments for 24 h by MTS assay

As shown in Figure 4.12, treatments of various concentrations of RJ (0.0005–5 mg/mL) for 24 h significantly decreased cell viability to 78–75% with a slight dose-dependent manner (p< 0.05), compared to the untreated medium control. DXR significantly decreased cell viability to 76%.
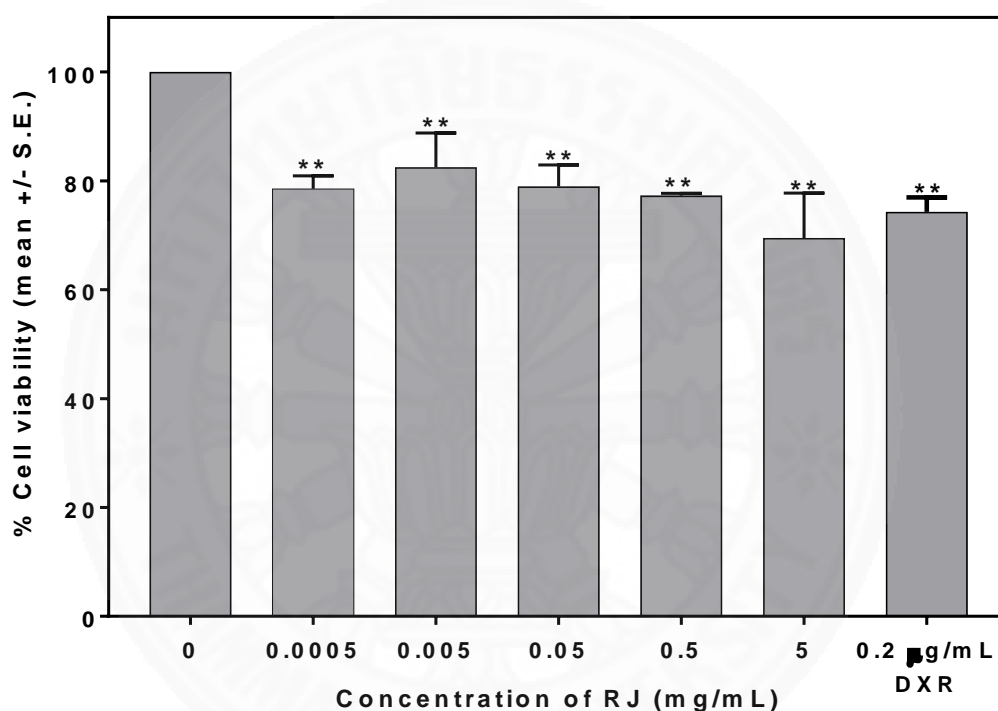
Figure 4.12 The relative cell viability in response to various concentrations of RJ treatments for 24 h on human lymphocytes (n = 3), [**]$P < 0.05$ significantly different from the RPMI-treated negative control

4.3.1.3 Analysis of pivotal gene expressions induced by RJ treatments for 24 h by Western blot analysis

(1) Analysis of cell cycle regulatory proteins: cyclin E1 and cyclin B1

There were bell-shaped curves for cyclin E1 and cyclin B1 responses to various doses of RJ treatments for 24 h (Figure 4.13). Cyclin E1 and cyclin B1 levels increased to an optimum at 0.05 mg/mL RJ treatment. Also, most of the treated cells had much higher cyclin E1 than cyclin B1 (Figure 4.14), suggesting that most of the treated cells progressed from G1 to S phases.
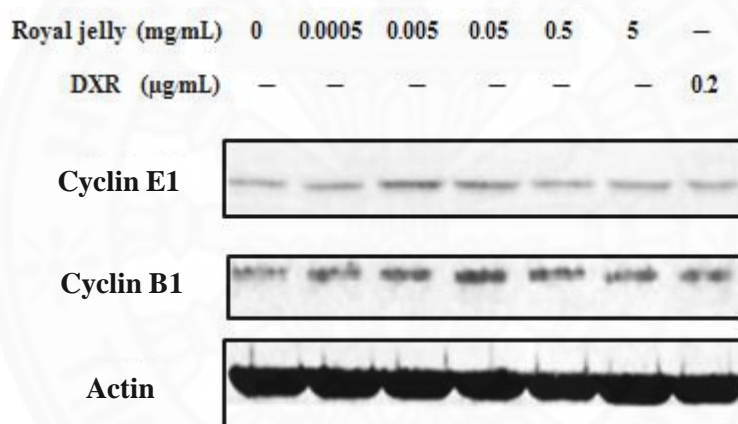
Figure 4.13 Representative Western blot analysis of cyclin E1 and cyclin B1 protein levels in response to various concentrations of RJ treatments on human lymphocytes for 24 h; 0.2 µg/mL DXR was used as a positive control

(a)
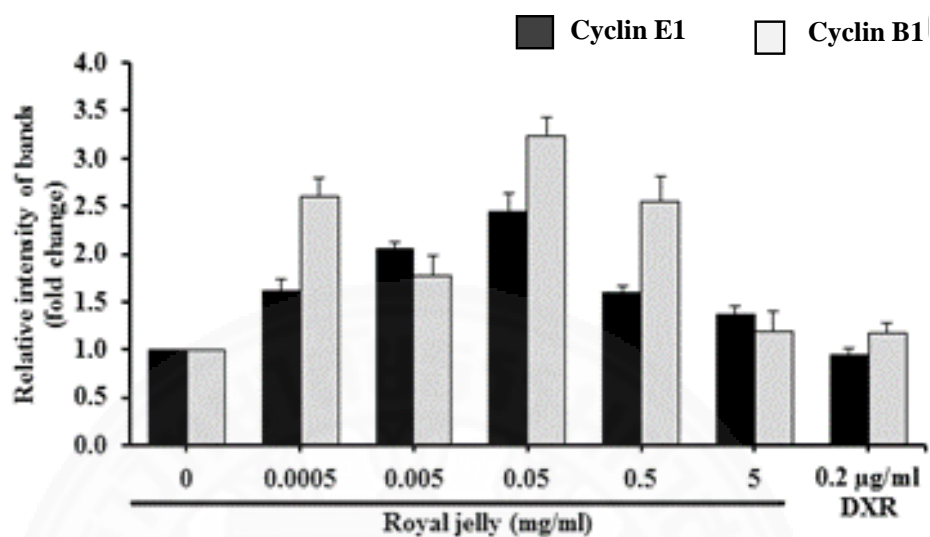
(b)
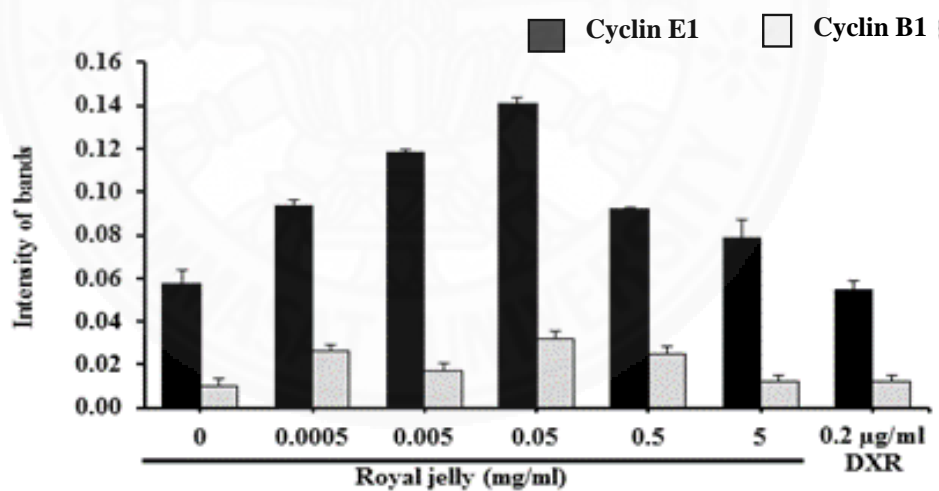
Figure 4.14 (a) Relative intensity of bands (fold change) and (b) Expression level of cyclin E1 and cyclin B1 (mean ± SE) in response to various concentrations of RJ treatments for 24 h on human lymphocytes (n = 3)

(2) Analysis of gene expression of h-TERT, c-MYC, BCL2, BAX, NRF2, and HO-1

As shown in Figure 4.15 and 4.16, there was a 2.3-fold increase of hTERT (optimum at 0.05 mg/mL RJ), followed by a slow decrease. The level of c-MYC protein tended to have a slight dose-dependent decrease (from 1.0-fold to 0.5-fold) with all doses from 0.0005 to 5 mg/mL. For BCL2 and BAX, 0.05 mg/mL RJ treatment increased BCL2 and BAX to maximum levels at 1.3-fold and 1.8-fold, respectively. There was a trend of dose-dependent increase in NRF2 (from 1.0-fold to 1.6-fold). However, the levels of HO-1 tended to decrease (from 1-fold to 0.4-fold) as the dose increased. In contrast, DXR treatment decreased all hTERT (0.9-fold), c-MYC (0.7-fold), BCL2 (0.9-fold), NRF2 (1.0-fold) and HO-1(0.6-fold), except increased BAX (1.4-fold).
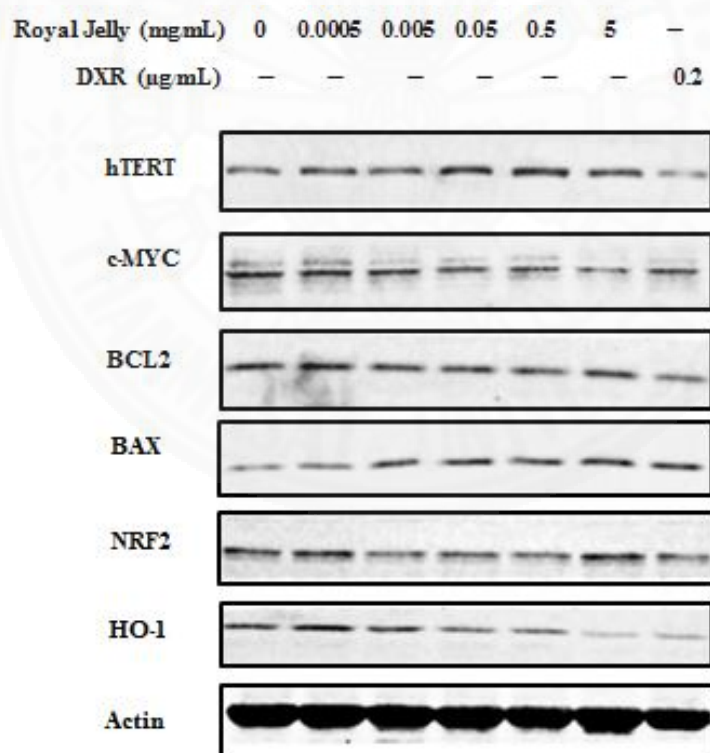
Figure 4.15 Representative Western blot analysis of hTERT, c-MYC, BCL2, BAX, NRF2 and HO-1 protein levels in response to various concentrations of RJ treatments on human lymphocytes for 24 h; 0.2 µg/mL DXR was used as a positive control

(a)
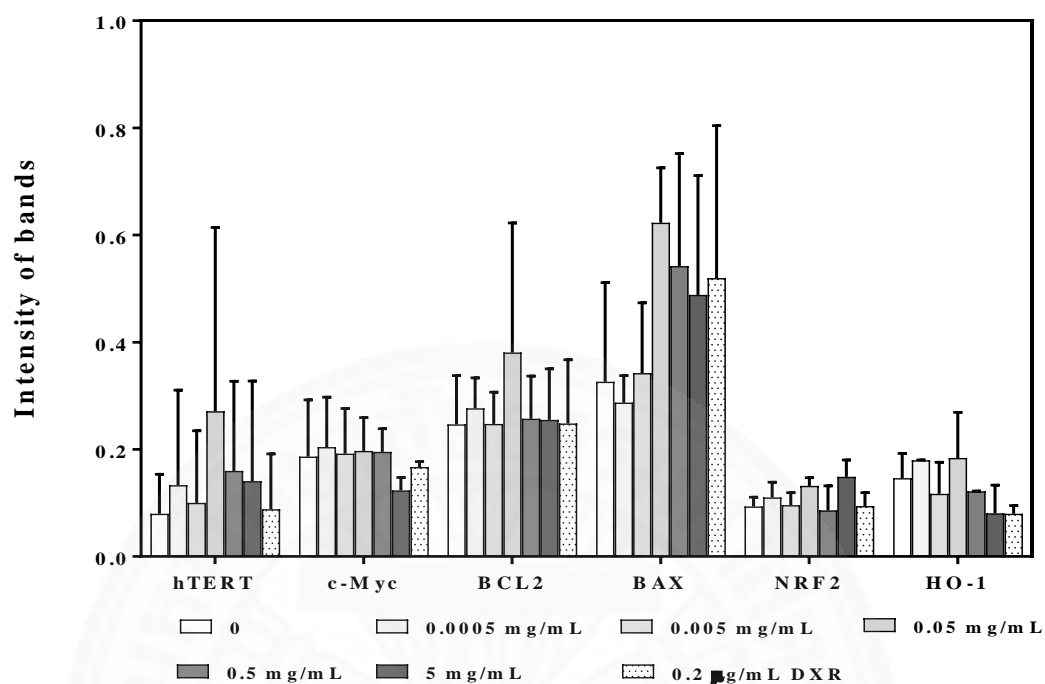
(b)
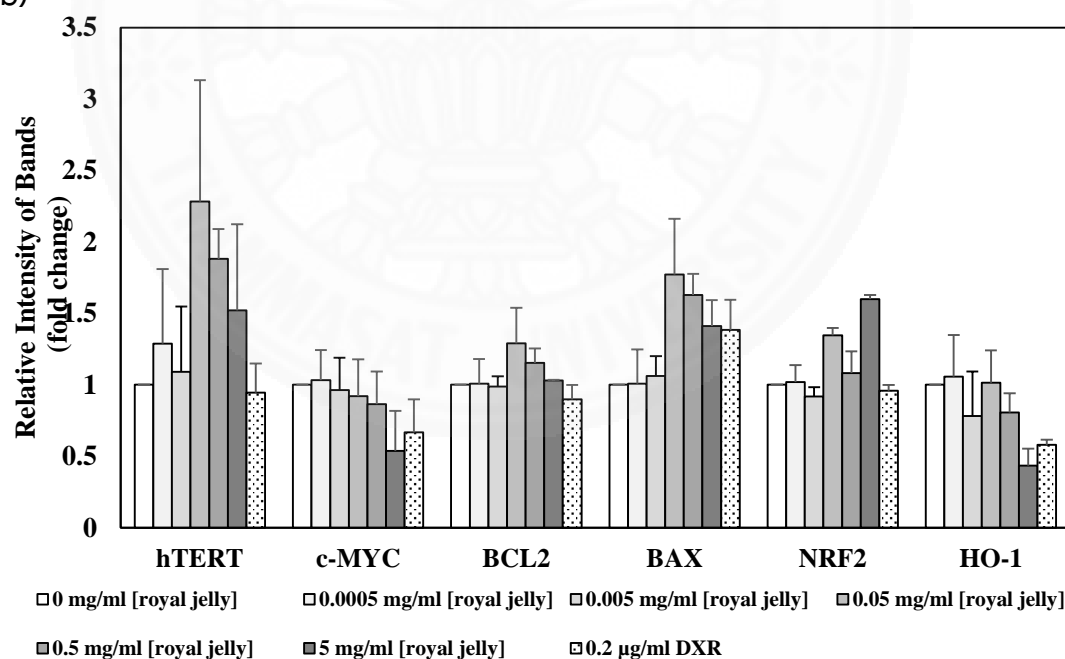
Figure 4.16 (a) Expression level of hTERT, c-MYC, BCL2, BAX, NRF2 and HO-1 in response to various concentrations of RJ treatments on human lymphocytes for 24 h (mean ± SE); 0.2 μg/mL DXR was used as a positive control (n=3) and (b) Relative intensity of bands (fold change)

To validate the overall effects of RJ on certain regulatory protein levels, we expressed h-TERT, c-MYC, BCL2, HO-1 and NRF2 levels in a relationship with BAX as follows: hTERT/BAX, C-MYC/BAX, BCL2/BAX, HO-1/BAX and NRF2/BAX (Figure 4.17). Such evaluation reflects health or weakness (death) in treated cells similar to BCL2/BAX, a rheostat that regulates life and death. Alternatively, BAX level was used as an internal control to compare different levels of regulatory proteins. As shown in Figure 4.17, the results demonstrated that there were dose-dependent decreases of C-MYC/BAX, BCL2/BAX, NRF2/BAX (only at 0.0005–0.5 mg/mL RJ) and HO-1/BAX ratios with a high correlation coefficient (r) equal to (-0.9) to (1) (Table 4.5). It indicated that the higher the concentration, the lower the ratios of cell proliferation, cell survival and antioxidative enzyme over cell death, or vice versa. For hTERT/BAX, all doses of RJ treatments increased hTERT/BAX without dose-dependency. It remained high at approximately 1.2-fold (range from 1.3- to 1.1- fold), proposing a longevity potential. The correlation coefficient of h-TERT/BAX was -0.37 (Table 2) suggesting its value was relatively stable. The exception was the NRF2/BAX ratio in which there was a dose-dependent decrease (1.0-fold to 0.7-fold decrease) at low doses of 0.0005–0.5 mg/mL RJ treatments, and then a sharp increase of 1.1- fold appeared at the highest dose of 5 mg/mL RJ.
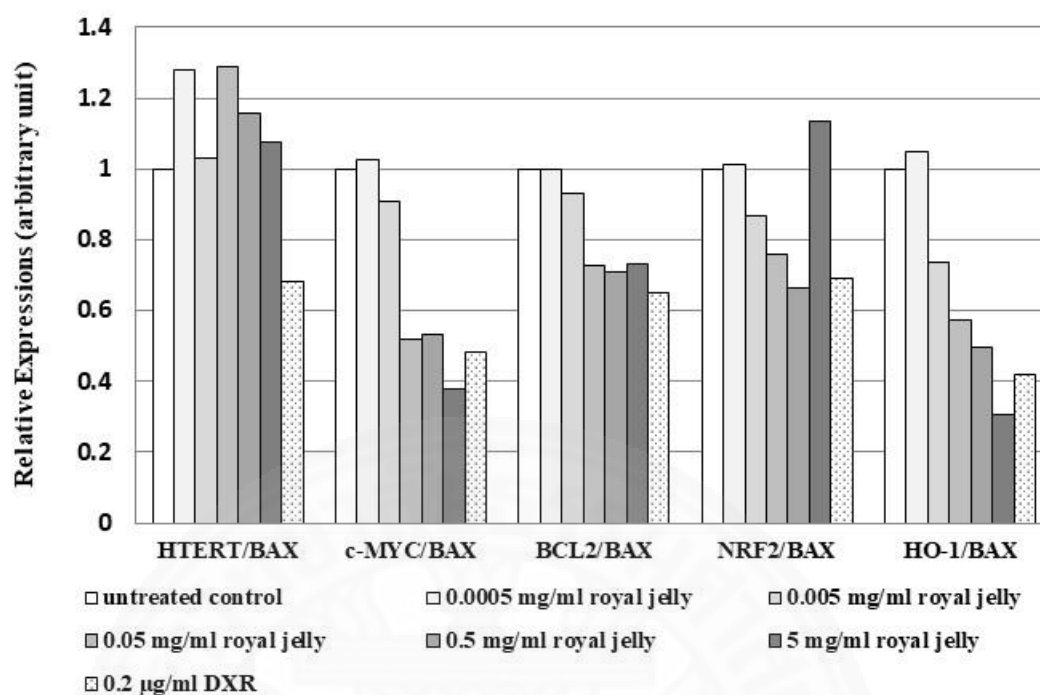
Figure 4.17 Representative the ratios of h-TERT/BAX, c-MYC/ BAX, BCL2/BAX, NRF2/BAX and HO1/BAX levels in response to various concentrations of RJ treatments on human lymphocytes for 24 h

Table 4.5 Correlation coefficients of the relative expressions of regulatory proteins over BAX in response to 0.0005-5 mg/mL RJ treatments on human lymphocytes

Relative expressions	Correlation coefficient (r)
hTERT/BAX	-0.37
c-MYC/BAX	-0.95
BCL2/BAX	-0.89
NRF2/BAX	- 1.0 (only at 0.0005-0.5 mg/mL RJ)
HO-1/BAX	-0.98

The results indicate that the lowest dose of 0.0005 mg/mL RJ had the highest beneficial effects by maintaining cell proliferation (c-MYC/BAX), cell survival, (BCL2/BAX), antioxidant enzyme level (HO-1/BAX), antioxidative response (NRF2/BAX) at approximately normal level, and enhanced telomerase level ratio (hTERT/BAX) by 1.3-fold. On the contrary, the highest dose of 5 mg/mL RJ caused more harm, though

maintaining the telomere length protection and enhancing antioxidative response (hTERT/BAX and NRF2/BAX = 1.1-fold). It decreased cell proliferation, cell survival and antioxidant enzyme level. The deleterious effects at the highest dose of RJ corresponded with its genotoxicity. In comparison with DXR, the toxicity induced by the highest dose of RJ still maintained hTERT/BAX and increased NRF2/BAX, which empowered cells to fight oxidative damage. On the contrary, DXR decreased all BCL2/BAX (-0.6-fold), C-MYC/BAX (-0.5-fold), HO-1/BAX (-0.4-fold), hTERT/BAX (-0.7-fold) and NRF2/BAX (-0.7-fold), suggesting its toxicity in promoting cell death, decreasing cell proliferation, decreasing antioxidative response and shortening telomere.

These results also revealed that cells undergoing active proliferation from G1/S phase (at 0.05 mg/mL RJ) activated hTERT, NRF2, BCL2 and also BAX levels. These data indicated that when cells were activated during G1/S cell cycle progression, more cells proliferated and at the same time, more cells entered apoptosis. Therefore, the gene expression levels of hTERT, c-MYC, NRF2, HO-1 and BCL2 alone may not provide informative data on cell status or cell quality. Those gene expression values should be corrected by formulating their ratios over BAX to validate the actual cellular status.

4.3.1.4 Analysis of glutathione peroxidase (GPx) activities on human lymphocytes treated with different concentrations of RJ

Treatments with RJ at 0.0005, 0.005, 0.05, 0.5 and 5 mg/mL as well as 0.2 µg/mL DXR treatment tended to slightly decrease GPx activities compared to the medium RPMI control, although no statistical significance was observed (Figure 4.18). The lowest dose, 0.0005 mg/mL RJ treatment maximally increased GPx activity to 5.8 units/µg though it was slightly lower that of the medium control (0.9-fold). The highest dose 5 mg/mL RJ as well as the 0.2 µg/mL DXR treatments induced the GPx activity to 5.1 units/µg.
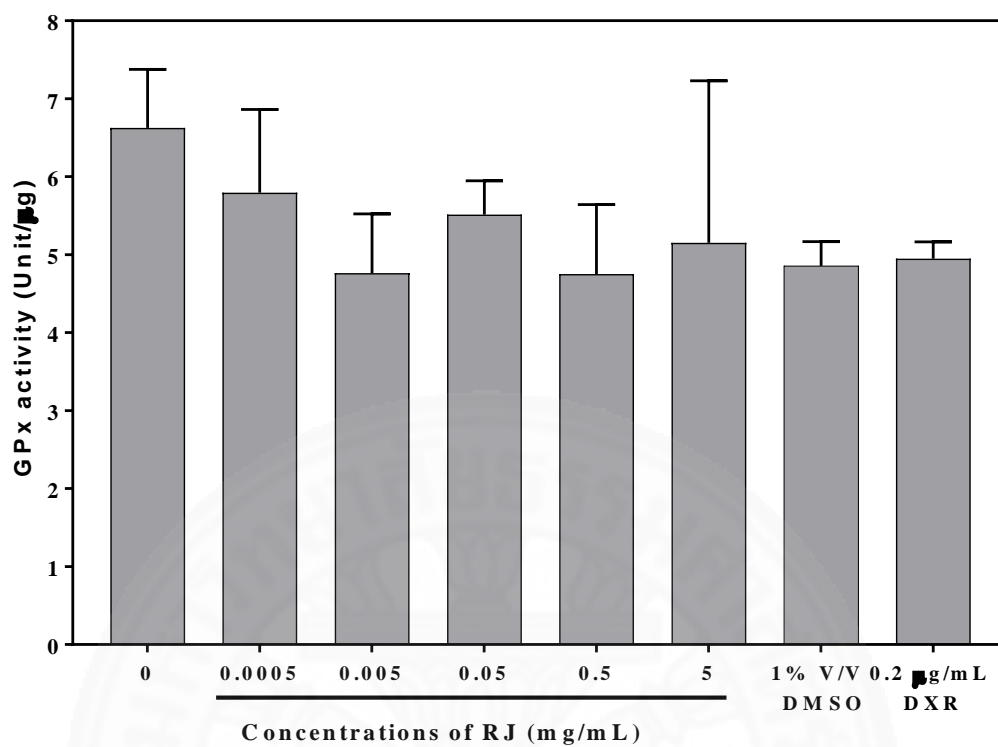
Figure 4.18 The effects on GPx activities of various concentrations of RJ treatments on human lymphocytes for 24 h (n=2)

4.3.2 Antigenotoxic studies on human lymphocytes by *in vitro* SCE assay

4.3.2.1 Antigenotoxic studies of RJ, DM, EE, and 10-H2DA pretreatments followed by DXR on human lymphocytes

(1) Antigenotoxic and anticytotoxic effects of RJ pretreatments

Pretreatments of RJ at concentrations of 0.0005 and 5 mg/mL followed by 0.1 µg/mL DXR significantly decreased SCE levels compared to DXR alone by a factor of 1.25 ($p<0.05$) (Figure 4.19). RJ pretreatments at other concentrations of 0.0005, 0.5, and 5 mg/mL also appeared to decrease the DXR-induced SCE level, without statistical significance. Pretreatment with 2%V/V DMSO, however, slightly increased DXR-induced SCE level by a factor of 1.5. Accordingly, RJ pretreatments at concentrations of 0.005 and 0.05 mg/mL significantly decreased DXR-induced SCE levels by a factor of 1.44 ($p<0.05$) when compared to the DMSO pretreatment control.

Figure 4-19 Transformed SCE induced by various concentrations of RJ pretreatments against DXR on human lymphocytes *in vitro* (n=3)

[**]$p<0.05$ significantly different from the negative control, RPMI

[##]$p<0.05$ significantly different from the positive control, DXR

Table 4.6 M.I. and P.I. induced by various concentrations of RJ pretreatments against DXR on human lymphocyte (n=3)

Conc. of RJ (mg/mL)	Conc.of DXR (µg/mL)	M.I. (mean±S.E.)	P.I. (mean±S.E.)
0	0	19.5±2.5	3.7±0.2
2% V/V DMSO	0	19.5±0.5	3.1±0.4
0.0005	0.1	22.5±3.5	4.2±1.4
0.005	0.1	22.0±6.0	3.7±1.4
0.05	0.1	21.0±10.0	3.6±2.0
0.5	0.1	20.0±5.0	3.5±1.0
5	0.1	17.0±1.0	2.8±0.4
2%V/V DMSO	0.1	15.0±0.0	1.8±0.2
0	0.1	19.5±2.5	2.8±0.2

RJ pretreatments at concentrations of 0.0005, 0.005, 0.05 and 0.5 mg/mL but not at 5 mg/mL tended to stimulate cell proliferation more efficiently than those of the DXR alone and DMSO pretreatments as shown by higher levels of M.I. and P.I (Table 4.6). Further analysis of the effect of RJ pretreatments on each phase of the cell cycle (Figure 4.20), demonstrated that all RJ pretreatments enhanced cell cycle progression (higher MII than MI cells), while DXR treatment alone slightly delayed cell cycle (less MII than MI cells). The 2% DMSO pretreatment, however, noticeably delayed cell cycle.
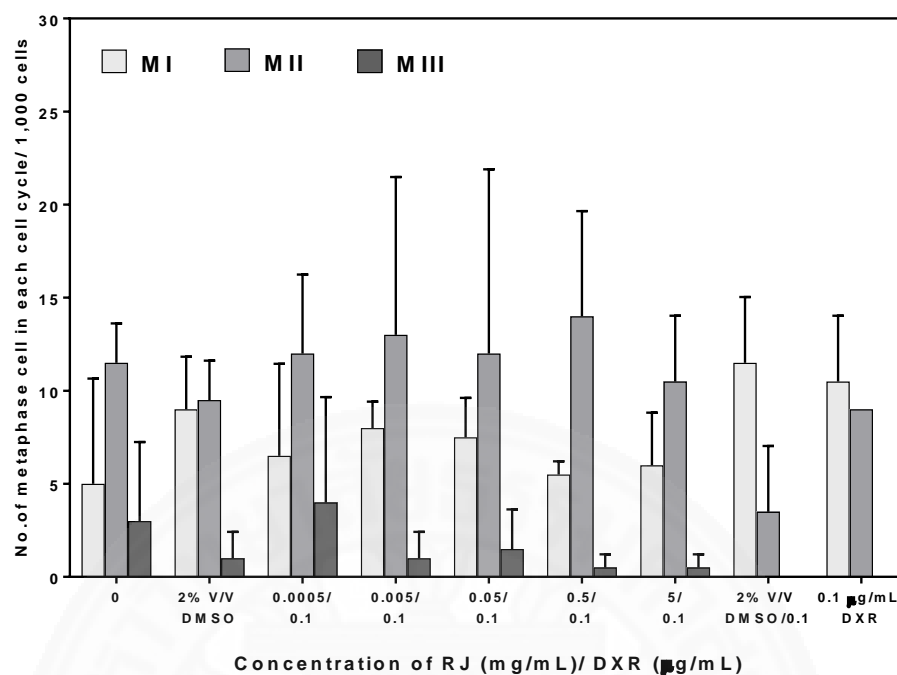
Figure 4-20 Cell cycle progression induced by RJ pretreatments against DXR on human lymphocytes; MI, MII and MIII: the number of metaphase cells in the first cell cycle, second cell cycle, and third cell cycle, respectively

(2) Antigenotoxic and anticytotoxic effects of DM pretreatments

As shown in Figure 4.21, DXR-treated cells significantly increased SCE level by 2.2-fold above that of the negative RPMI control (p<0.05). The SCE levels of all DM pretreatments (0.0125, 0.125, 1.25, 12.5 and 125 mg/mL) were not significantly different from that of the DXR-treated cells alone. The 2%V/V DMSO pretreatment tended to increase SCE level compared to DXR-treated cells but such increase was not statistically significant.

In addition, there was no significant difference of M.I. nor P.I. induced by DM pretreatments compared to the DXR treatment alone (Table 4-7). Further analysis of the effect of DM pretreatments on each phase of the cell cycle demonstrated that DM pretreatments at the lowest dose (0.0125 mg/mL) and at the highest dose (125 mg/mL) tended to increase cell cycle progression (higher MII and MIII) when compared to DXR treatment alone (Figure 4-22).
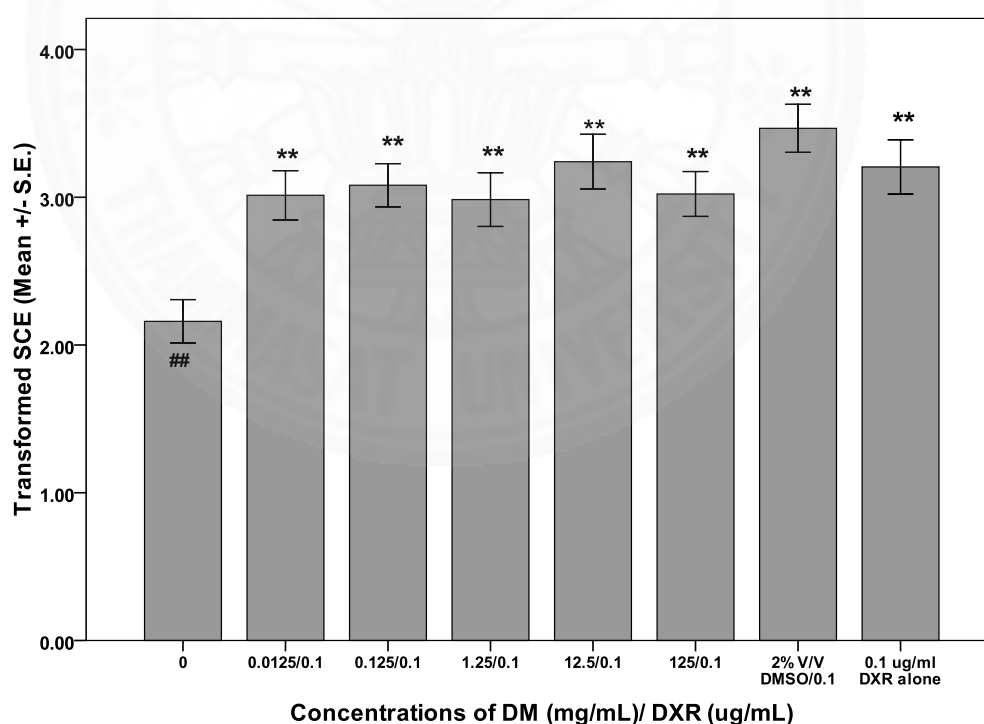
Figure 4.21 Transformed SCE induced by various concentrations of DM pretreatments against DXR on human lymphocytes *in vitro* (n=3)

[**]p<0.05 significantly different from the negative control, RPMI

[##]p<0.05 significantly different from the positive control, DXR

Table 4.7 M.I.and P.I. induced by various concentrations of DM pretreatments against DXR on human lymphocytes (n=3)

Conc. of DM (mg/mL)	Conc. of DXR (µg/mL)	M.I. (mean ± S.E.)	P.I. (mean ± S.E.)
0	0	19.5 ± 3.5	3.7 ± 2.8
0.0125	0.1	17.0 ± 2.8	2.9 ± 4.2
0.125	0.1	25.5 ± 4.9	3.6 ± 7.0
1.25	0.1	22.0 ± 2.8	3.2 ± 4.2
12.5	0.1	18.0 ± 1.4	2.5 ± 1.4
125	0.1	19.5 ± 0.7	3.1 ± 0.7
0	0.1	19.5 ± 3.5	2.9 ± 3.5
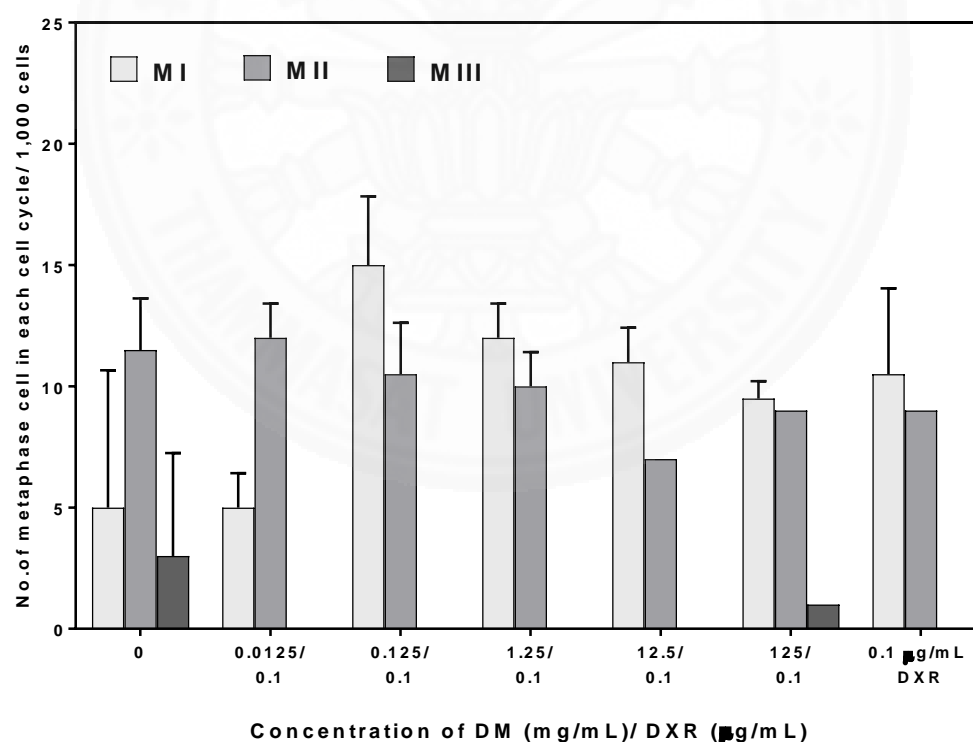
Figure4.22 Cell cycle progression induced by DM pretreatments against DXR on human lymphocytes; MI, MII and MIII: the number of metaphase cells in the first cell cycle, second cell cycle, and third cell cycle, respectively

(3)   Antigenotoxic   and   anticytotoxic   effects   of   EE pretreatments

As shown in Figure 4.23, DXR-treated cells significantly increased SCE level by 2.2-fold above that of the negative RPMI control (p<0.05). There were no significant difference between SCE levels induced by all EE (0.00025,0.0025, 0.025, 0.25, and 2.5 mg/mL) pretreatments compared to that induced by DXR treatment alone.

In addition, there was no significant difference of M.I. nor P.I. induced by EE pretreatments compared to the DXR treatment alone (Table 4.8), Further analysis on cell cycle progression demonstrated that EE pretreatments at higher doses (0.025 and 0.25 mg/mL) enhanced cell cycle progression as shown by higher number of MII and MIII cells compared to that of DXR treatment alone. (Figure 4.24).
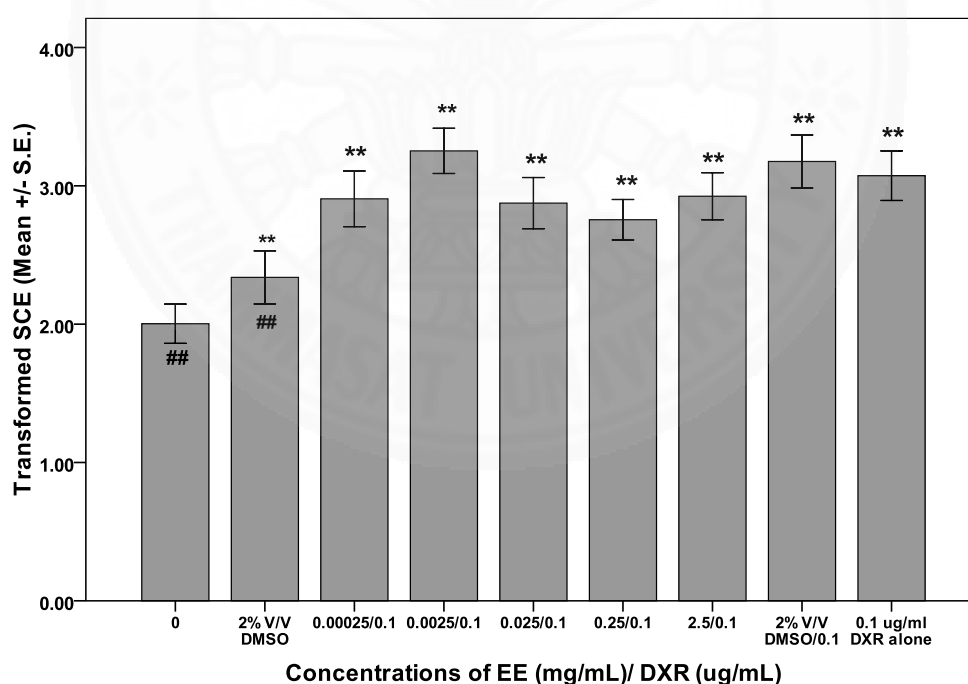
Figure 4.23 Transformed SCE induced by various concentrations of EE pretreatments against DXR on human lymphocytes *in vitro* (n=3)

[**]p<0.05 significantly different from the negative control, RPMI

[##]p<0.05 significantly different from the positive control, DXR

Table 4.8 M.I. and P.I. induced by various concentrations of EE pretreatments against DXR on human lymphocytes (n=3).

Conc. of EE (mg/mL)	Conc.of DXR (µg/mL)	M.I. (mean ± S.E.)	P.I. (mean± S.E.)
0	0	19.5 ± 3.5	3.7 ± 2.8
2% V/V DMSO	0	19.5 ± 0.7	3.1 ± 5.6
0.00025	0.1	20.0 ± 1.4	2.6 ± 2.1
0.0025	0.1	19.0 ± 1.4	2.6 ± 2.1
0.025	0.1	18.5 ± 3.5	2.9 ± 4.9
0.25	0.1	21.0 ± 2.8	3.4 ± 4.2
2.5	0.1	12.5 ± 2.1	2.1 ± 3.5
2%V/V DMSO	0.1	15.0 ± 0.0	1.9 ± 5.6
0	0.1	19.5 ± 3.5	2.9 ± 3.5
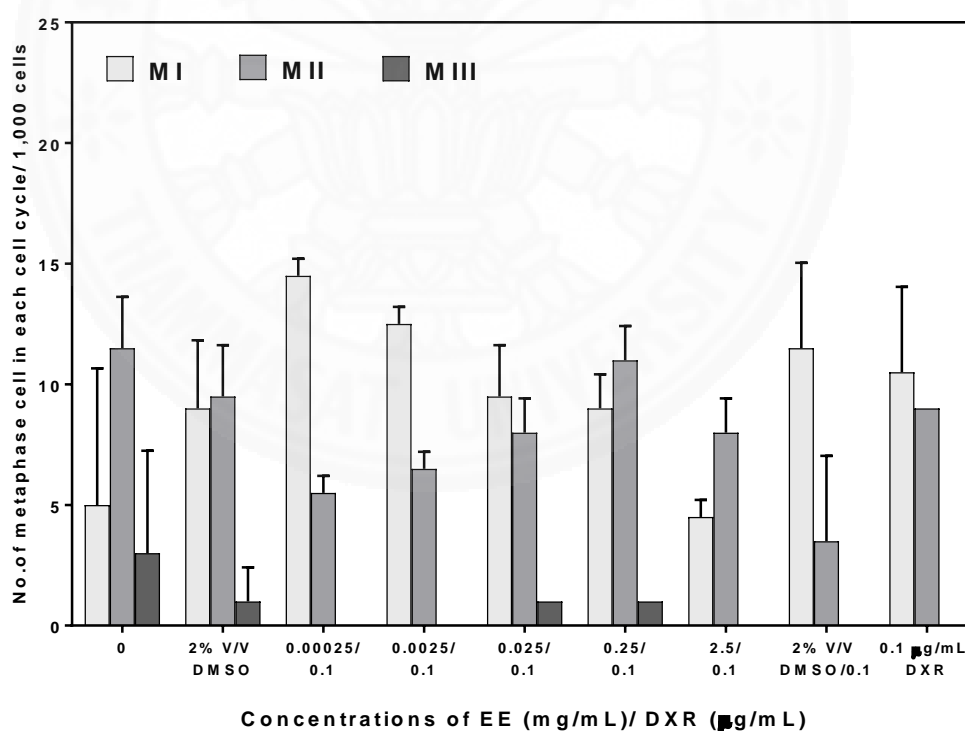
Figure 4.24 Cell cycle progression induced by EE pretreatments against DXR on human lymphocytes; MI, MII and MIII: the number of metaphase cells in the first cell cycle, second cell cycle, and third cell cycle, respectively

(4) Antigenotoxic and anticytotoxic effects of 10-H2DA pretreatments

As shown in Figure 4.25, DXR-treated cells significantly increased SCE level by 2.2-fold above that of the negative RPMI control ($p < 0.05$). There was no significant difference between SCE levels induced by all 10-H2DA pretreatments compared to DXR treatment alone. In addition, there was no significant difference of M.I. and P.I. induced by 10-H2DA pretreatments (Table 4.9). Further analysis of the effect of 10-H2DA pretreatments on each phase of the cell cycle (Figure 4.26), demonstrated that 10-H2DA pretreatments at higher doses (1.25, 12.5 and 125 µg/mL) tended to enhance cell cycle progression (higher MII/MIII than MI cells) compared to that of DXR-treatment alone. The 2% DMSO pretreatment noticeably delayed cell cycle.
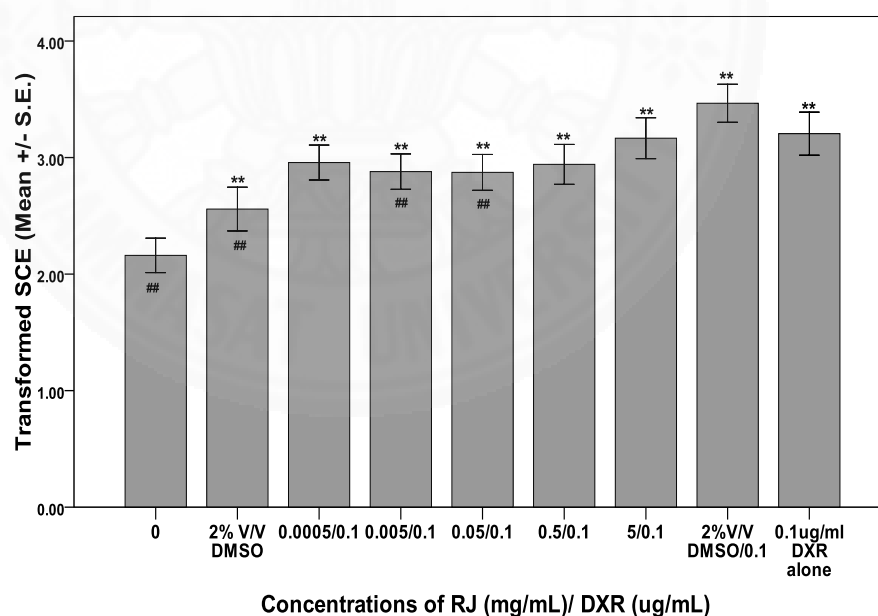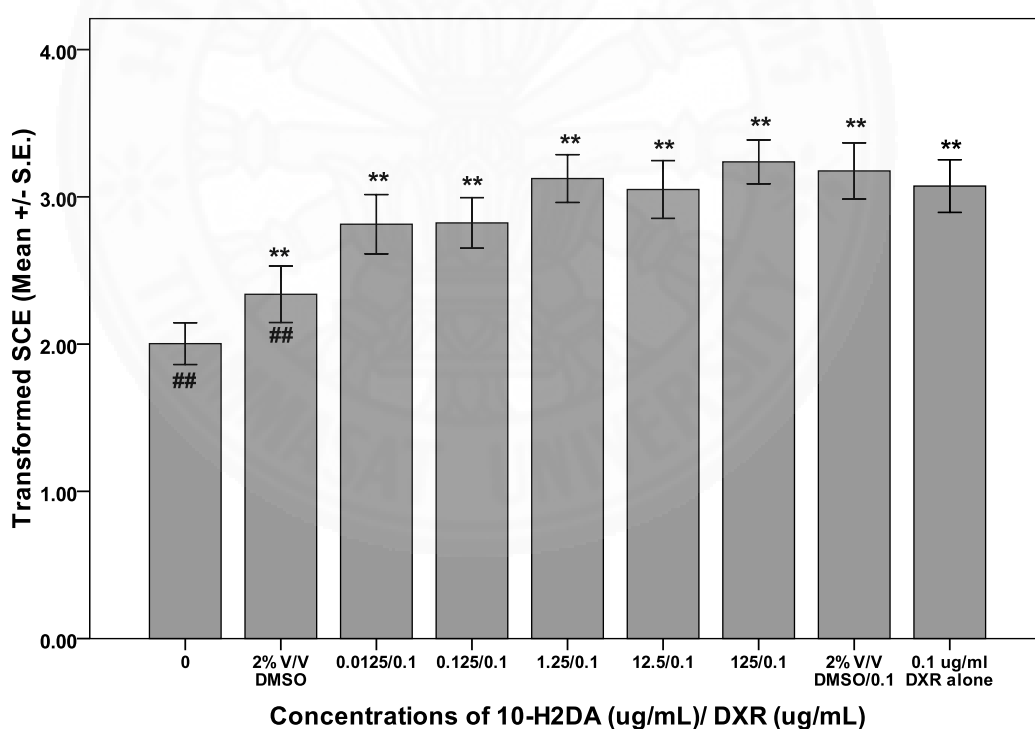

Figure 4.25 Transformed SCE induced by various concentrations of 10-H2DA pretreatments against DXR on human lymphocytes *in vitro* (n=3)

[**]p<0.05 significantly different from the negative control, RPMI

[##]p<0.05 significantly different from the positive control, DXR

Table 4.9 M.I. and P.I. induced by various concentrations of 10-H2DA pretreatments against DXR on human lymphocytes (n=3)

Conc.of 10-H2DA (μg/mL)	Conc.of DXR (μg/mL)	M.I. (mean ± S.E.)	P.I. (mean ± S.E.)
0	0	19.5 ± 3.5	3.7 ± 2.8
2% V/V DMSO	0	19.5 ± 0.7	3.1 ± 5.6
0.0125	0.1	18.5 ± 0.7	2.8 ± 1.4
0.125	0.1	19.0 ± 1.4	2.9 ± 2.1
1.25	0.1	14.0 ± 1.4	2.6 ± 1.4
12.5	0.1	16.0 ± 1.4	2.8 ± 2.1
125	0.1	17.5 ± 3.5	3.1 ± 5.6
2%V/V DMSO	0.1	15.0 ± 0.0	1.9 ± 5.6
0	0.1	19.5 ± 3.5	2.9 ± 3.5
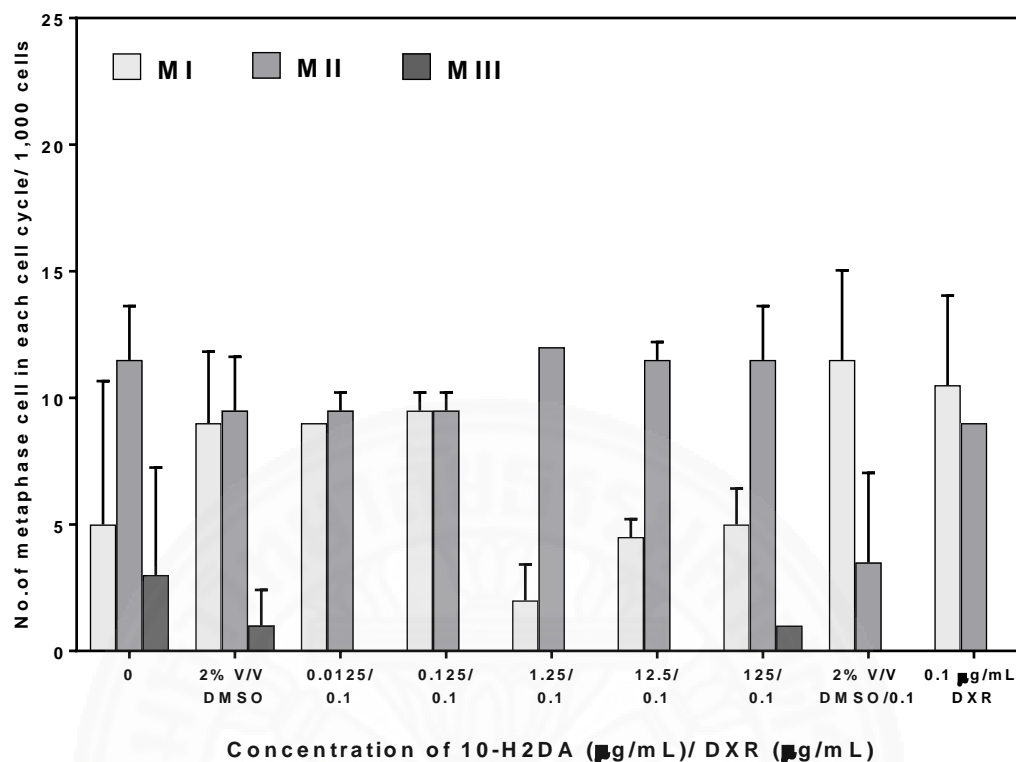
Figure 4.26 Cell cycle progression induced by 10-H2DA pretreatments against DXR on human lymphocytes; MI, MII, and MIII: the number of metaphase cells in the first cell cycle, second cell cycle, and third cell cycle, respectively

4.3.2.2 Antiproliferative studies of RJ co-treatments with DXR for 24 h on human lymphocytes detected by MTS tetrazolium assay

As shown in Figure 4.27, DXR treatment alone decreased cell viability by 50% compared to the negative, RPMI control. There was no significant difference between cell viabilities induced by all RJ co-treatments compared to that induced by DXR treatment alone. RJ co-treatments at only 0.0005 and 5 mg/mL, however, slightly increased cell viability by approximately 10% compared to that of DXR alone.
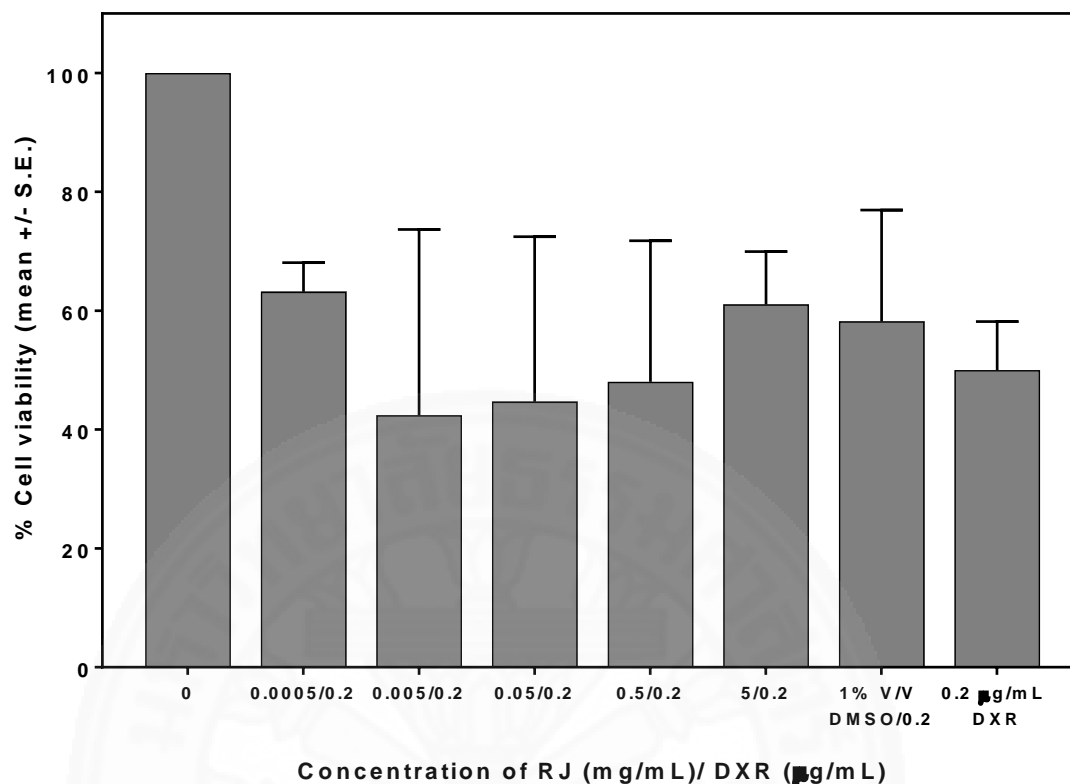
Figure 4.27 Relative cell viabilities in response to various concentrations of RJ co-treatments with DXR for 24 h on human lymphocytes (n = 3)

4.3.2.3 Analysis of pivotal gene expressions induced by RJ co-treatments with DXR for 24 h by Western blot analysis

(1) Analysis of cell cycle regulatory proteins: cyclin E1 and cyclin B1 induced by RJ co-treatments

As shown in Figure 4.28, RPMI medium-treated human lymphocytes had similar cyclin E1 and cyclin B1 levels (both have 0.03-fold compared to actin). On the other hand, DXR treatment decreased the levels of cyclin E1 by 0.9-fold while markedly decreasing cyclin B1 by 0.3-fold. Compared to the DXR treatment, RJ co-treatments at 0.005 and 0.05 mg/mL profoundly enhanced cyclin E1 at approximately 1.3-fold and 1.5-fold, while decreasing cyclin B1 0.7-fold and 0.3-fold, respectively. Results suggest that 0.005 and 0.05 mg/mL RJ co-treatments activated cell proliferation and progression from G1 to S phase. RJ co-treatment at the highest dose (5 mg/mL) maintained cyclin E1 (1-fold) but decreased cyclin B1 (0.6-fold). On the contrary, 1% V/V DMSO co-treatment maintained cyclin E1 but markedly increased cyclin B1 (3.4-fold).

(a)

Royal jelly (mg/mL)	0	0.0005	0.005	0.05	0.5	5	—	—
DMSO (% V/V)	—	0.0001	0.001	0.01	0.1	1	—	1
DXR (µg/mL)	—	0.2	0.2	0.2	0.2	0.2	0.2	0.2
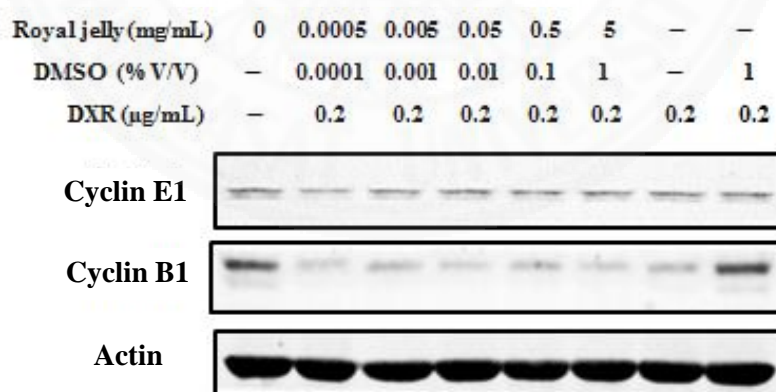
(b)
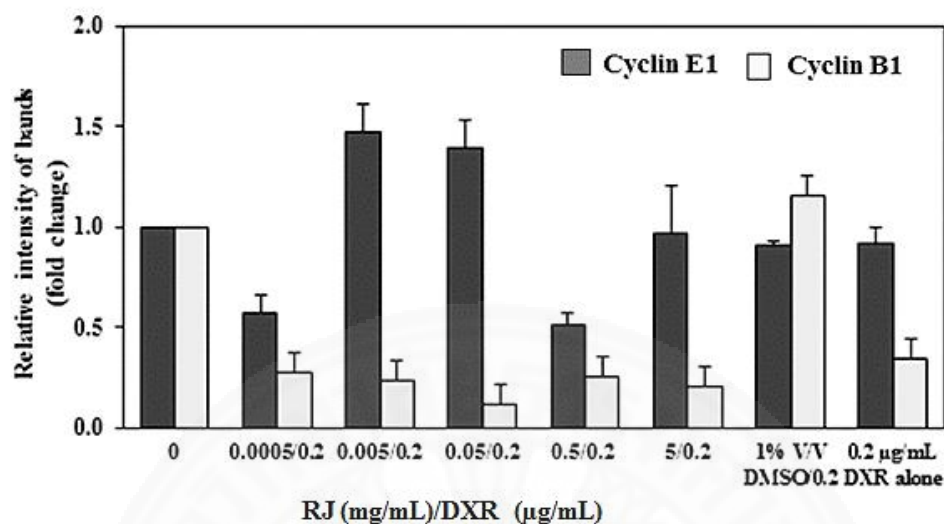
Figure 4.28 (a) Representative Western blot analysis and (b) relative intensity of cyclin E1 and cyclin B1 in response to various concentrations of RJ co-treatments with DXR for 24 h on human lymphocytes, compared to RPMI medium control (n=3)

(2) Analysis of h-TERT, c-MYC, BCL2, BAX, NRF2, and HO-1 levels induced by RJ co-treatments with DXR on human lymphocytes

Compared to those of RPMI control (Figure 4.29a, b), DXR treatment alone increased the levels of c-MYC (1.4-fold) and h-TERT (1.2-fold), maintained the levels of NRF2, and decreased the levels of BAX (0.9-fold), BCL2 (0.8-fold) and HO-1 (0.6-fold). Results suggest that DXR treatment induced more cell death than cell survival and used up antioxidative enzyme, HO-1. However, cells still maintained telomere length and kept proliferating. DMSO co-treatment markedly decreased HO-1 (0.2-fold), h-TERT (0.7-fold), and C-MYC (0.9-fold), maintained BCL2, BAX, and slightly increased NRF2 (1.1-fold). This result indicates that DMSO possibly enhanced DXR-induced oxidative damage and used up antioxidative enzyme HO-1, reduced longevity while slightly activating antioxidative response, NRF2.

RJ co-treatments at all doses increased hTERT (1.3-1.7-folds), BCL2 (1.2-2.1-folds) (except at the lowest dose) and BAX (1.4-1.8- folds) (except at the

highest dose), compared to those of DXR treatment alone. They had an overall dose-dependent increase trend of NRF2 (0.8- to 1.3-folds) but had a dose-dependent decrease of c- MYC (1.6- to 1.1-folds) and HO-1 (0.6- to 0.3-folds). Both levels of BCL2, a survival regulatory protein, and BAX, a death regulatory protein, increased when cyclin E1 level increased. It possibly indicated that during the active cell cycle status (increased cyclin E), there were induction of both cell survival and cell death. Therefore, analysis of health status of the treated cells using those individual protein expression levels may not properly represent cellular health status. Interpretations of the protein expression levels formulated as ratios over cell death such as BCL2/BAX, NRF2/BAX, h-TERT/BAX, c-MYC/BAX and HO-1/BAX are possibly more meaningful in understanding updated cellular status similar to the use of BCL2/BAX, which strongly represents life or death.

.

(a)

Royal jelly (mg/mL)	0	0.0005	0.005	0.05	0.5	5	—	—
DMSO (% V/V)	—	0.0001	0.001	0.01	0.1	1	—	1
DXR (µg/mL)	—	0.2	0.2	0.2	0.2	0.2	0.2	0.2
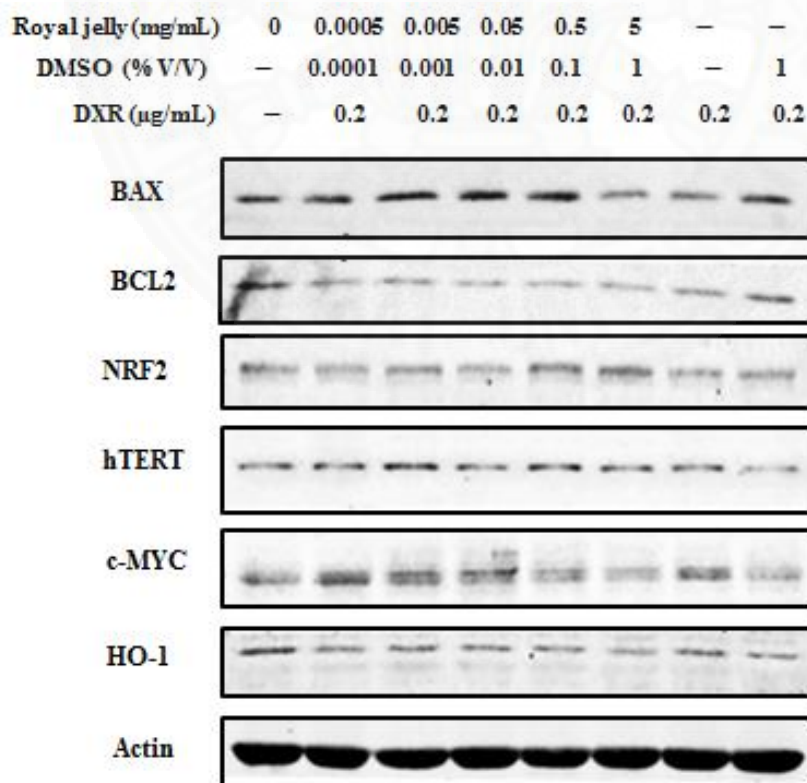
(b)
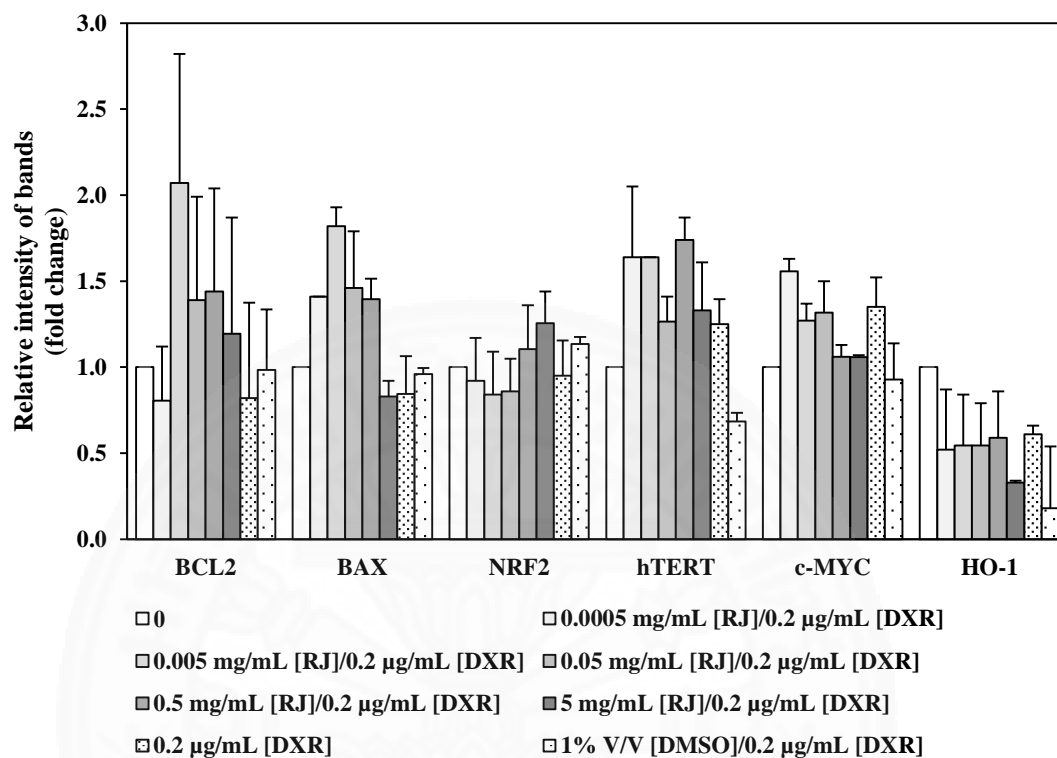
Figure 4.29 (a) Representative Western blot analysis and (b) relative gene expression levels of BCL2, BAX, NRF2, hTERT, c-MYC, and HO-1 in response to various concentrations of RJ co-treatments with DXR on human lymphocytes for 24 h (mean±S.E.); DXR alone was used as a positive control (n=3)

In comparison with RPMI control (Figure 30a, b), DXR treatment increased the ratios of c-MYC/BAX (1.6-fold), hTERT/BAX (1.5- fold), NRF2/BAX (1.1-fold); maintained the ratios of BCL2/BAX (1-fold); and decreased the ratio of HO-1/BAX (0.7-fold). Compared to DXR treatment (Figure 5b), RJ co-treatment at the highest dose of 5 mg/mL maximally increased the ratios of BCL/BAX (1.5-fold), NRF2/BAX (1.3-fold) and hTERT/BAX (1.1- fold), while decreasing c-MYC/BAX (0.8-fold) and HO-1/BAX (0.58-fold). On the contrary, RJ co-treatments at lower concentrations (0.0005-0.5 mg/mL) tended to decrease all these ratios. RJ co-treatment at the lowest dose (0.0005 mg/mL) decreased all BCL2/BAX (0.6-fold), NRF2/BAX (0.6-fold), hTERT/BAX (0.8-fold), c-MYC/BAX (0.7-fold), and HO1/BAX (0.5-fold). These data demonstrated that RJ co-treatment at the highest dose enhanced cell survival, antioxidative response, and maintenance of telomere over cell death and therefore induced health protection against DXR. On the contrary, RJ co-treatments at the lower doses especially at 0.0005 mg/mL diminished cell survival, antioxidative response, longevity, cell proliferation and antioxidative enzyme HO-1, demonstrating its intensifying DXR toxicity. Therefore, beneficial or harmful effects of RJ co-treatments depend on its dosage. DMSO co-treatment decreased HO-1/BAX (0.3-fold), hTERT/BAX (0.5-fold), c-MYC/BAX (0.6- fold) and slightly increased BCL2/BAX and NRF2/BAX (1.05- fold). The DMSO solvent possibly had little additional effect on reduction of HO-1/BAX, hTERT/BAX, and c-MYC/BAX but did not show any major effects on RJ activity.

(a)

Legend:
- □ 0
- □ 0.0005 mg/mL [RJ]/0.2 μg/mL [DXR]
- □ 0.005 mg/mL [RJ]/0.2 μg/mL [DXR]
- ▨ 0.05 mg/mL [RJ]/0.2 μg/mL [DXR]
- ▨ 0.5 mg/mL [RJ]/0.2 μg/mL [DXR]
- ■ 5 mg/mL [RJ]/0.2 μg/mL [DXR]
- ▨ 0.2 μg/mL DXR
- ▨ 1% V/V [DMSO]/0.2 μg/mL [DXR]
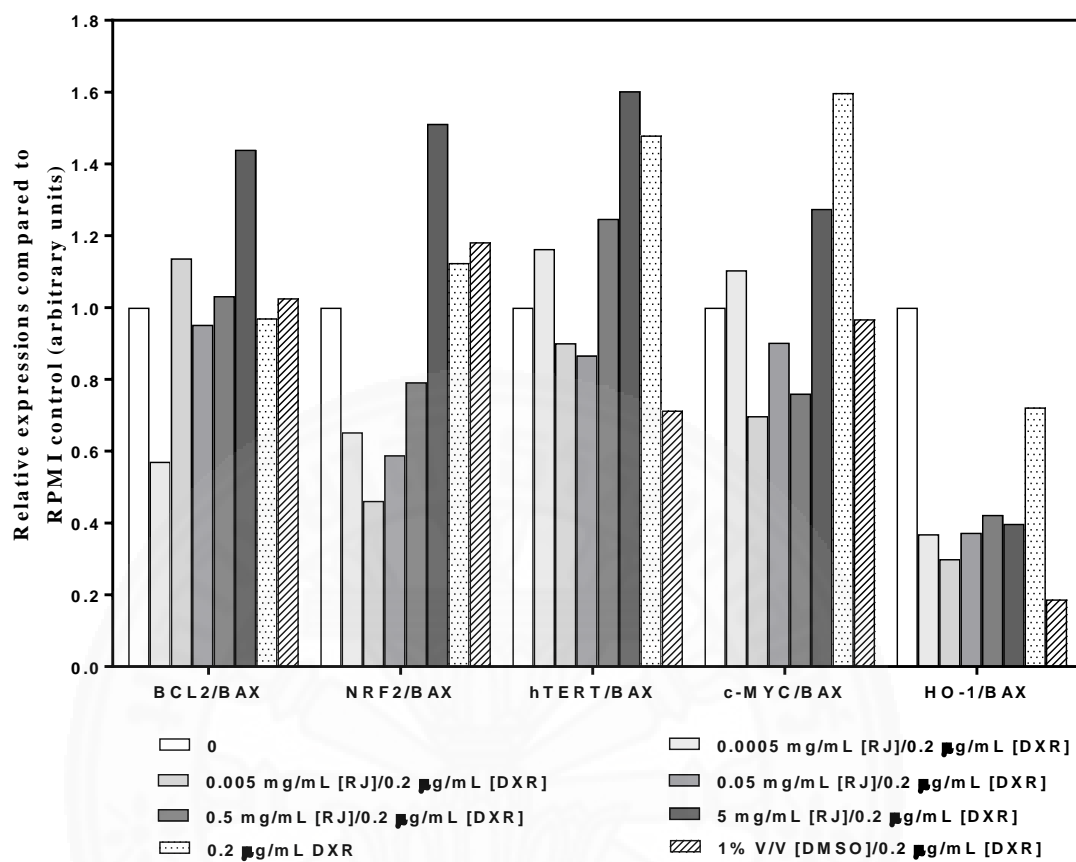
(b)
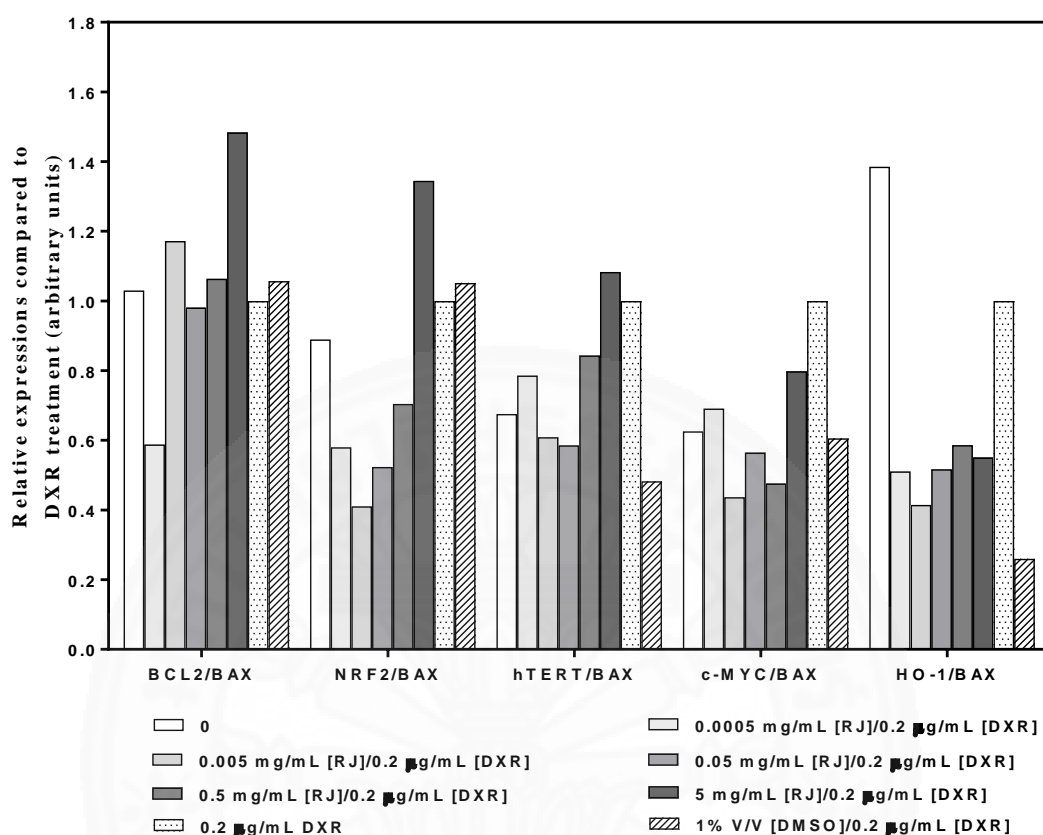
Figure 4.30 (a) Relative gene expressions of the ratios: BCL2/BAX, NRF2/BAX, h-TERT/BAX, c-MYC/BAX, and HO1/BAX, compared to RPMI control, and (b) Relative gene expressions of those ratios compared to DXR treatment, in response to various concentrations of RJ co-treatments with DXR for 24 h on human lymphocytes

4.3.2.4 Analysis of glutathione peroxidase (GPx) acitivities on human lymphocytes treated with different concentrations of RJ co-treatments with DXR for 24 h on human lymphocytes

DXR treatment alone increased GPx activity (1.4-fold), compared to RPMI medium control. No dose-dependent response was observed from RJ co-treatments. However, co-treatments with RJ at 0.005 and 5 mg/mL tended to increase GPx activities (1.1-1.2-fold) compared to the DXR treatment alone, although, no statistical significance was observed. These increased GPx activities corresponded to results from the induction of NRF2 level in response to RJ co-treatments (Figure 4.31).
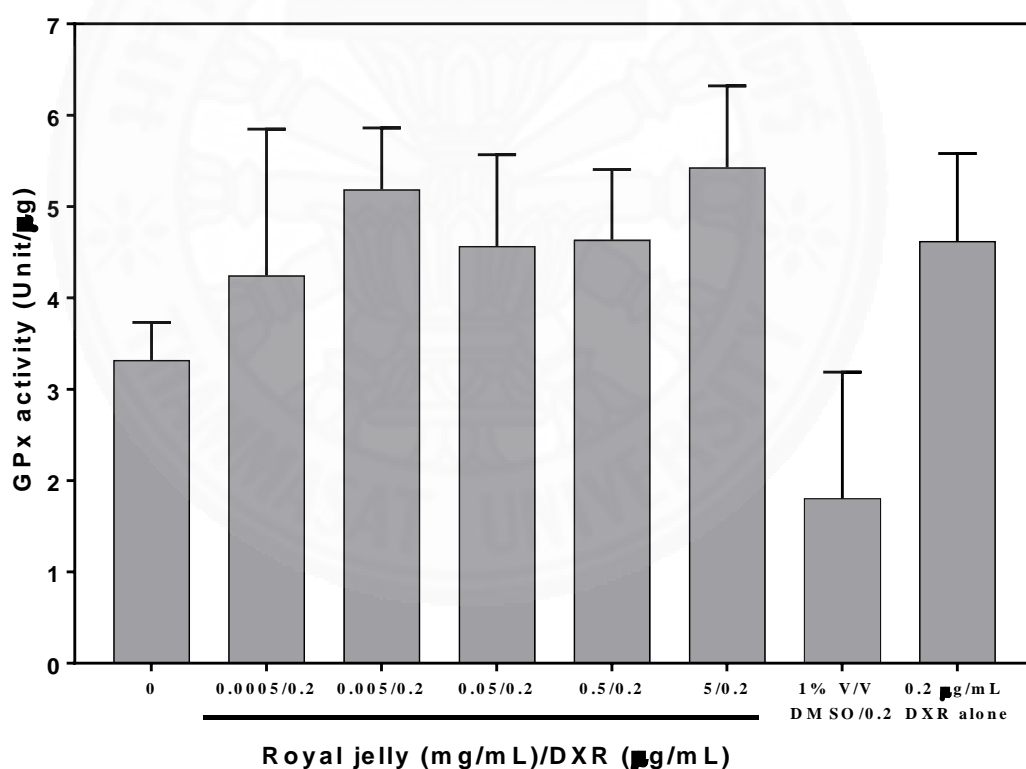
Figure 4.31 Effects of various concentrations of RJ co-treatments with DXR for 24 h on GPx activity on human lymphocytes (n=2)

4.4 Effects of 10-H2DA treatment alone and co-treatments with DXR on MCF-7 human breast cancer cell line

4.4.1 Effect of 10-H2DA treatments alone for 24 h

4.4.1.1 Antiproliferative effects of 10-H2DA treatments on MCF-7 cells detected by the MTS tetrazolium assay

Treatments of 10-H2DA at 0.0125, 0.125, 1.25, 12.5, and 125 µg/mL for 24 h significantly decreased cell viability in a dose-dependent manner (94.5, 87.6, 78.3, 62.5, and 37.6% respectively), compared to that of MEM medium control (Figure 4.32). The DXR treatment (1 µM=0.54 µg/mL), a positive control, decreased cell viability to 52%. The 50% inhibition concentration (IC50) of 10-H2DA treatments against MCF-7 cells was 13.9 µg/mL.

(a)
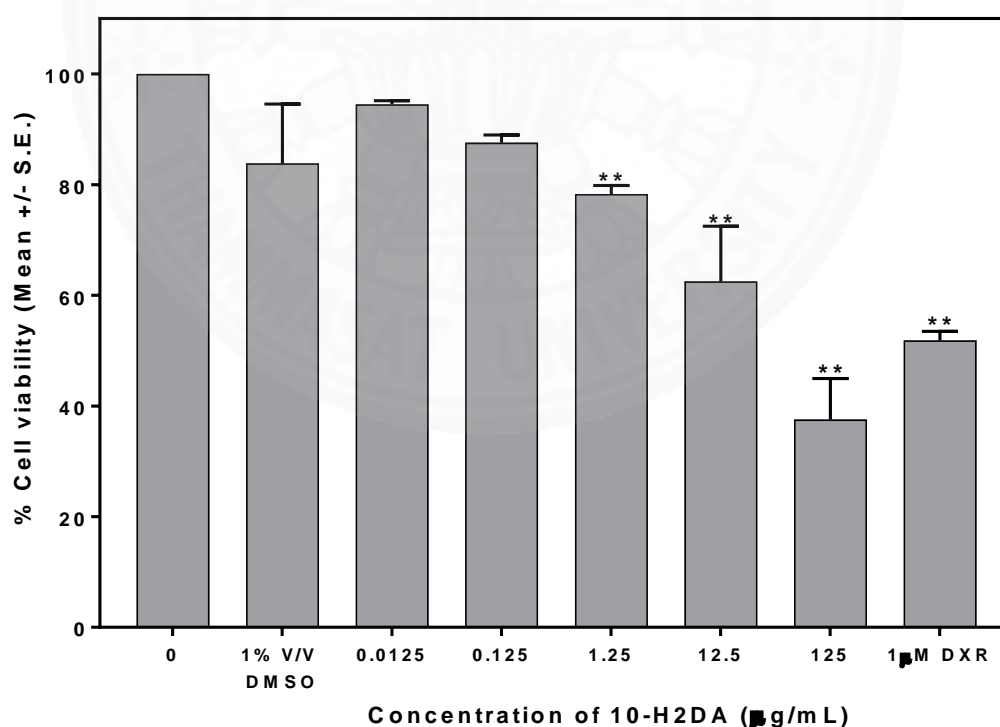
Figure 4.32 The percentages of cell viability in response to various concentrations of 10-H2DA treatments for 24 h on MCF-7 breast cancer cells (n = 3) **p < 0.05 significantly different from the MEM-treated negative control

4.4.1.2 Determination of GI50, TGI and LC50 of aged 10-H2DA treatments on MCF-7 cells

In order to determine cytotoxicity of 10-H2DA in terms of GI50, TGI and LC50, methodology to study cell viability or cell survival required detection of cell density at time zero. 10-H2DA (aged 2 years old) was used to determine GI50, TGI50, and LC50 values of 10-H2DA treatments. As shown in Figure 4.33a and 4.33b, of aged 10-H2DA (1.25, 12.5, 125, and 250 µg/mL) treatments were 20.1, 130.9, and 192.3 µg/mL, respectively.

We also studied antiproliferative effects of aged 10-H2DA using regular protocol in which cell viability is detected without subtraction of cell density at day 0. It was shown that aged 10-H2DA treatments (1.25, 12.5, 50, 125, and 250 µg/mL) decreased MCF-7 cell viability to 82.8, 77.5, 76.5, 53.7, and 3.8%, respectively when compared to MEM medium control (Figure 4.33c). The IC50 of aged 10-H2DA was 20 µg/mL which was higher than fresh 10-H2DA in 4.4.1.1 (IC50 was 13.9 µg/mL). The DXR significantly decreased cell viability to 52%.

(a)
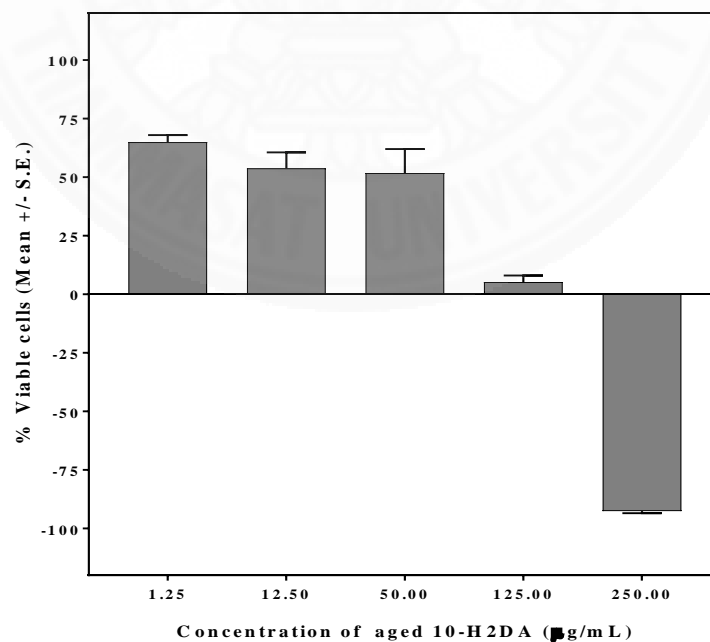
(b)
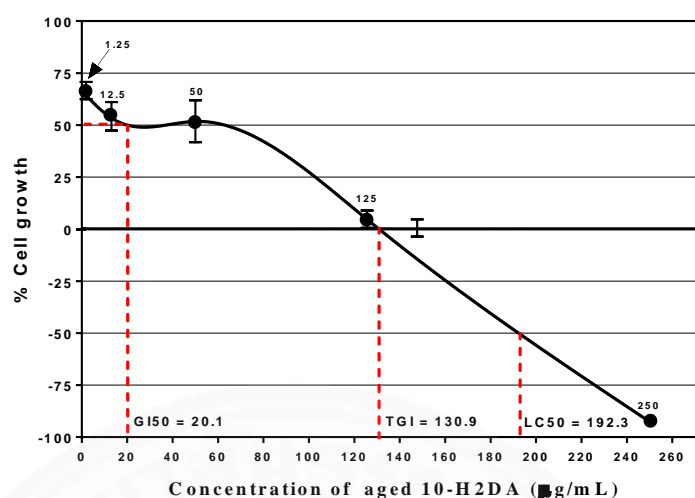
(c)
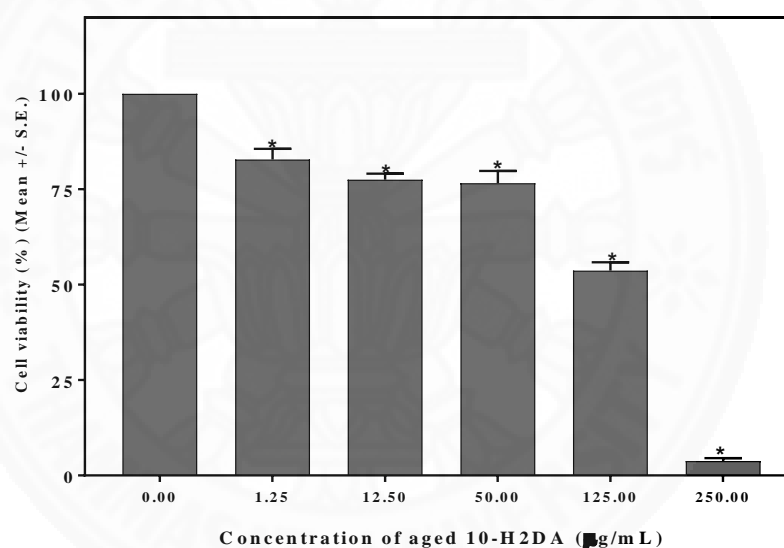
Figure 4.33 (a) The percentages of cell viability in response to various concentrations of aged 10-H2DA treatments for 24 h on MCF-7 cells (n = 3). **P < 0.05 significantly different from the MEM-treated negative control, 24 h culture, (b) The cytotoxic activity of aged 10-H2DA treatments against MCF-7 cells demonstrated that growth percent of 100 corresponds to growth seen in untreated cells. Growth percent of 50 corresponds to 50% growth (50% inhibition). Growth percent of 0 indicates no growth (TGI: total growth inhibition). Growth percent of -50 indicates lethality in 50% of the starting cells (LC50), (c) The percentages of cell viability in response to various concentrations of aged 10-H2DA treatments for 24 h on MCF-7 cells (n = 3), compared to zero time initial density

Treatment of 250 µg/mL aged 10-H2DA was cytotoxic since few viable cells were detected. Effects of aged 10-H2DA treatments on cell morphology as shown in (Figure 4.34) corresponded well with results from the MTS tetrazolium assay showing that treatments at higher doses of aged 10-H2DA increased cell toxicity (more unattached and round cells).
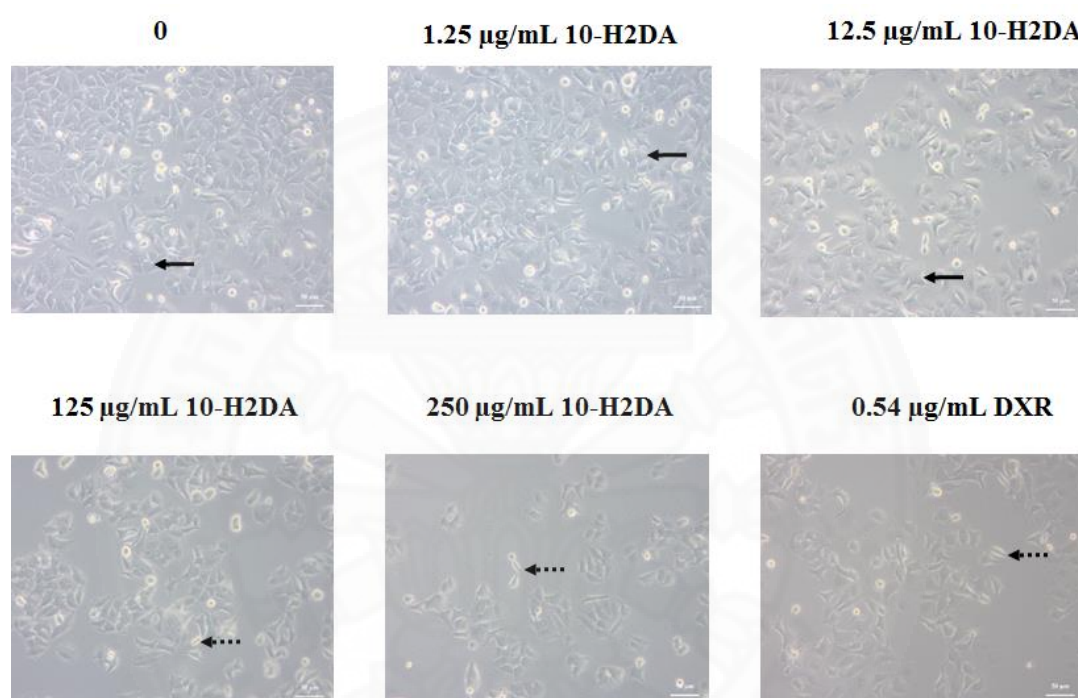
Figure 4.34 Effects on cell morphology induced by various concentrations of 10-H2DA compared to MEM medium (0) and 0.54 µg/mL DXR

→   normal cells: attached elongated shape

--▶   damaged cells: unattached rounded shape

4.4.1.3 Analysis of pivotal gene expressions induced by 10-H2DA treatment for 24 h on MCF-7 cells by Western blot analysis

          (1) Analysis of cell cycle regulatory proteins: cyclin D1, CDK4, cyclin E1, and cyclin B1 induced by 10-H2DA treatments

          As shown in Figure 4.35a and 4.35b, the medium control treatment had higher levels of cyclin D1, CDK4, and cyclin B1 but not cyclin E1, suggesting that more control cells progressed from G0 to G1 phase than from G2 to M phase, and the least control cells progressed from G1 to early S phase. DXR treatments, however, increased cyclin E1 (2-fold) but decreased cyclin D1 (0.5-fold), CDK4 (0.8-fold), and cyclin B1 (0.4-fold) levels compared to MEM treatment (Figure 4-35c). These observations suggest that the DXR treatment greatly decreased G2/M progression, slightly decreased G0/G1 progression, but highly increased G1/S phase progression, as compared to the MEM control. For 10-H2DA treatments, there were dose-dependent decreases of cyclin B1, cyclin D1, and CDK4 with correlation coefficient (r) equal to −0.9, -0.8 and -0.8 respectively (Table 4.10) whereas cyclin E1 levels were relatively stable (r= -0.07). The highest dose of 10-H2DA treatment (125 µg/mL) extensively decreased cyclin D1 (0.2-fold) and CDK4 (0.2-fold), moderately decreased cyclin B1 (0.5-fold), while slightly increasing cyclin E (1.1-fold) levels. The data suggest that 125 µg/mL 10-H2DA treatment induced more cell arrest in G0/G1 phase while DXR treatment induced more cell arrest in G2 phase.

(a)
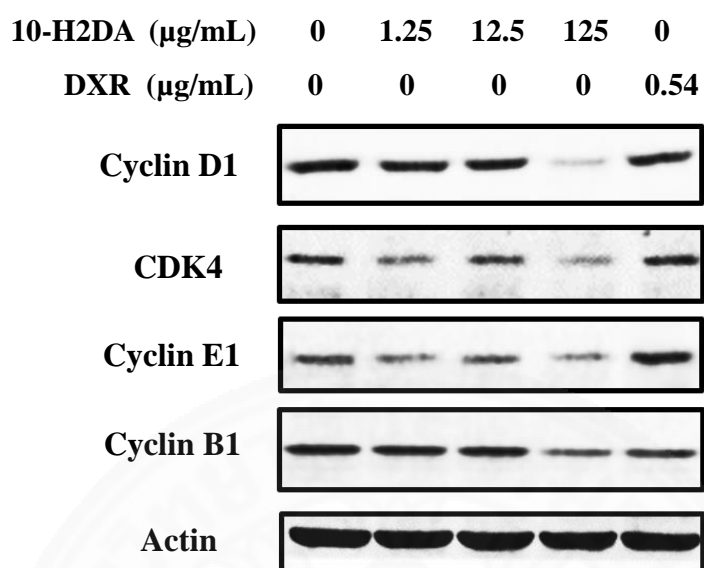
(b)
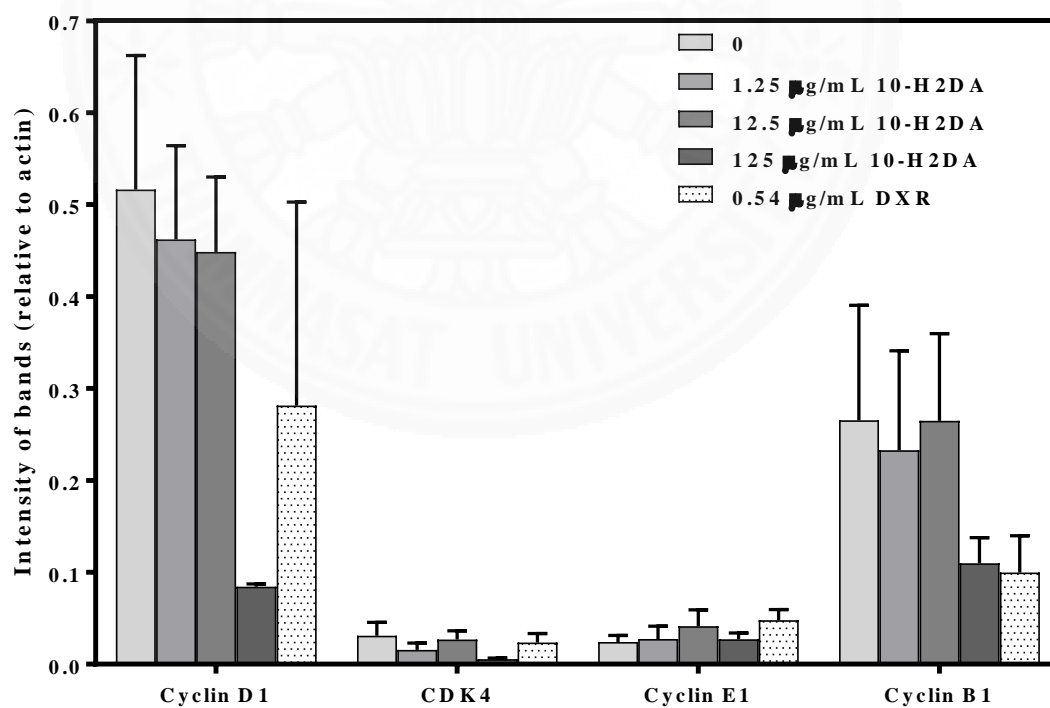
(c)
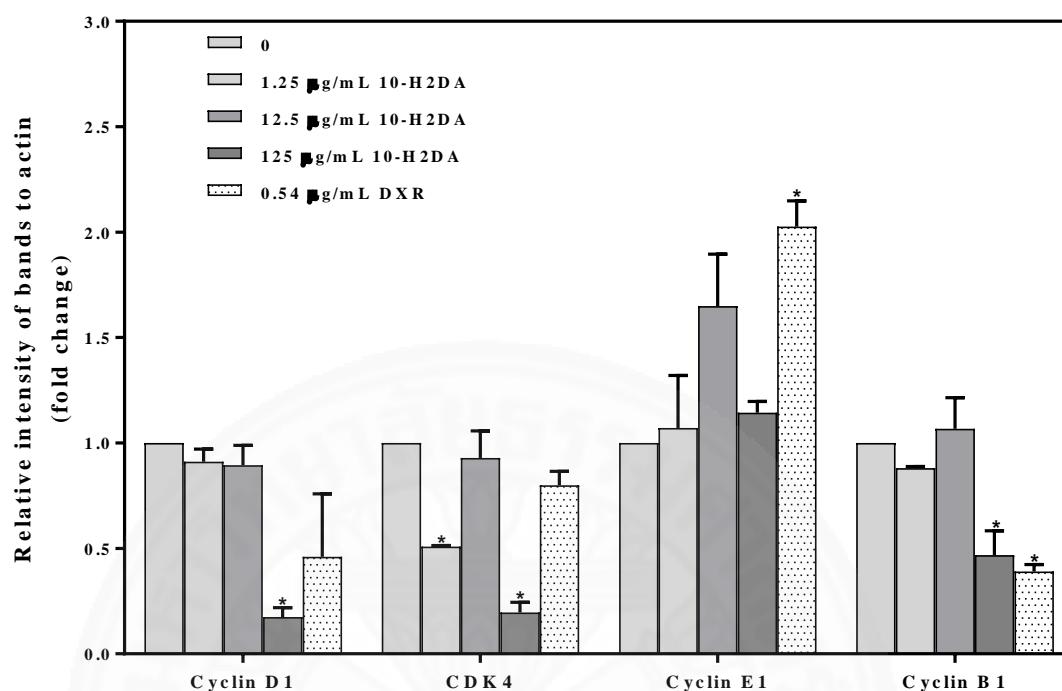
Figure 4.35 (a) Representative Western blot analysis, (b) Relative intensity of bands (fold change) and (c) Relative expression level of cyclin D1, cyclin E1 and cyclin B1 (mean ± SE) in response to various concentrations of 10-H2DA treatments for 24 h on MCF-7 cells (n = 3)

Table 4.10: Correlation coefficients of the relative expressions of cyclins and CDK4 in response to 1.25-125 µg/mL 10-H2DA treatments on MCF-7 cells

Relative regulatory gene expressions	Cyclin B1	Cyclin D1	CDK4	Cyclin E1
Correlation coefficient (r):	-0.9	-0.8	-0.8	-0.07

(2) Analysis of pivotal gene expressions: hTERT, c-MYC, BCL2, BAX,, NRF2, HO-1 induced by 10-H2DA treatments on MCF-7 cells

As shown in Figure 4.36a and 4.36b, and Table 4.11, 10-H2DA treatments (1.25-125 µg/mL) had a dose-dependent decrease in c-MYC (0.8 to 0.2-fold), h-TERT (0.8 to 0.7-fold), BCL2 (0.8 to 0.5-fold), BAX (1.1 to 0.8 fold) and BCL2/BAX ratio (0.7 to 0.6-fold) with correlation coefficient (r) equal to - 0.96, -0.67, -0.81, -0.67, and -0.72 respectively (Table 4.11). The p53 values were relatively stable (r = 0.09). On the contrary, there were dose-dependent increases in HO-1 (1.4 to 29.7-fold) (r =1.0) and NRF2 (0.8 to 3.1) (r =1.0). The data suggest that 125 µg/mL 10-H2DA treatment strongly inhibited cancer cell growth through the reduction of c-MYC, h-TERT, and BCL2/ BAX resulting in declining cell proliferation and lifespan while increasing cell apoptosis. However, it was able to induce antioxidative potential through induction of NRF2 and HO-1 suggesting that cells were protected from oxidative damage. The DXR positive control treatment increased p53 (18.9-fold), HO-1 (2.9-fold), and BAX (1.6-fold), while decreased hTERT (0.2-fold), c-MYC (0.3-fold), BCL2 (0.5-fold), NRF2 (0.6-fold) and BCL2/BAX ratio (0. 3-fold), as compared to those of MEM controls (Figure 4.36c). Therefore, DXR potentially inhibited cancer cell growth through reduction of c-MYC, hTERT, NRF2 levels and BCL2/BAX ratio while increasing p53 which induced cell apoptosis.

(a)

| 10-H2DA (µg/mL) | 0 | 1.25 | 12.5 | 125 | 0 |
| DXR (µg/mL) | 0 | 0 | 0 | 0 | 0.54 |

HO-1

NRF2

c-MYC

hTERT

p53

BAX

BCL2

Actin
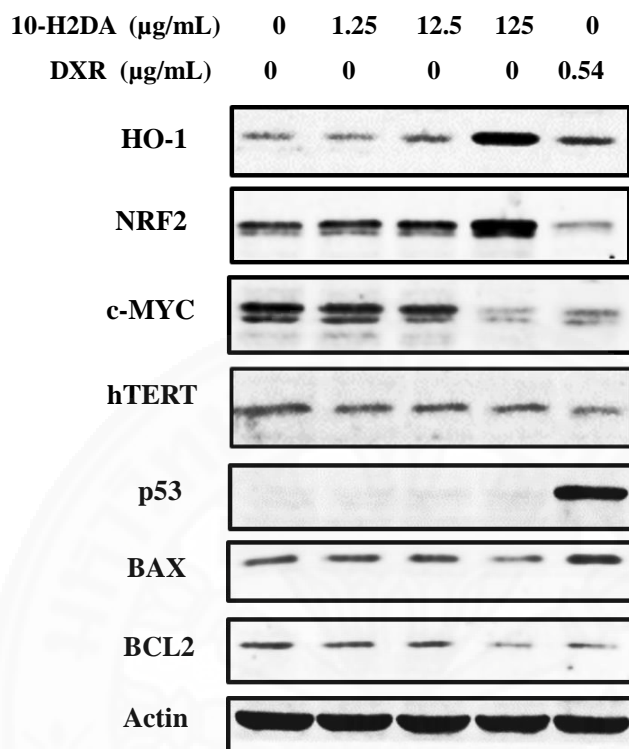
(b)
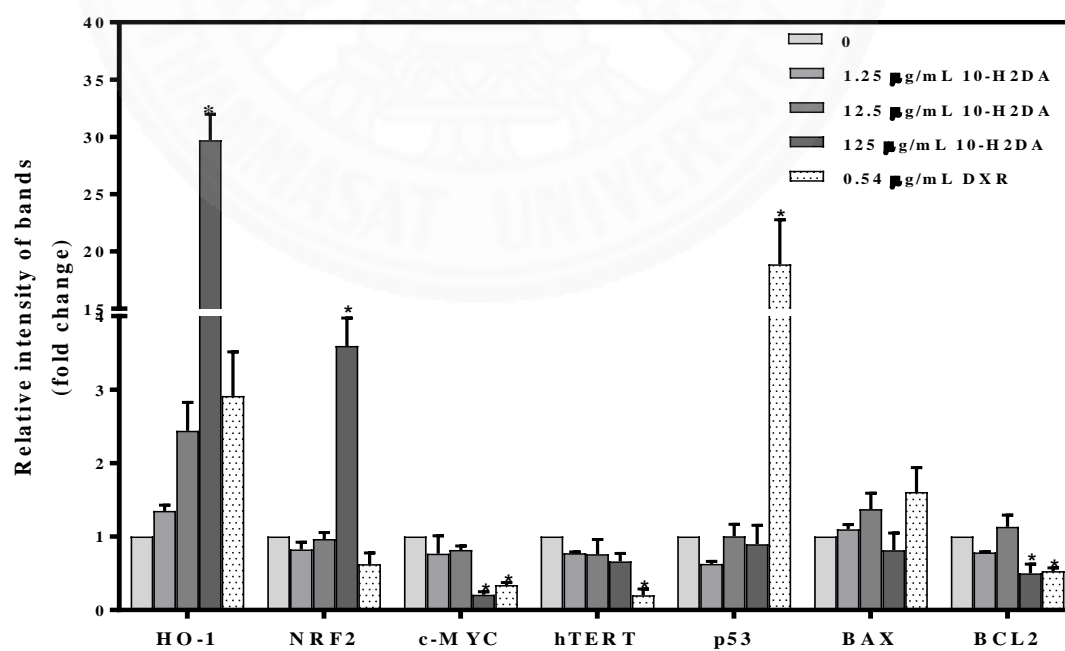
(c)
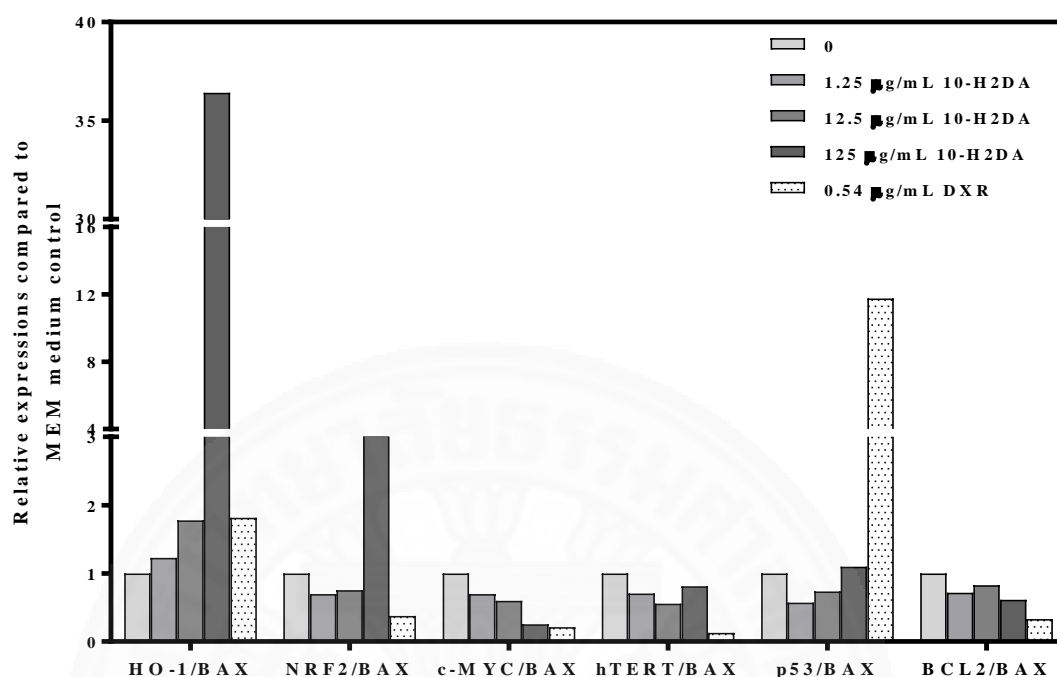
Figure 4.36 (a) Representative Western blot analysis and (b) Relative gene expression levels of HO-1, NRF2, C-MYC, hTERT, p53, BAX, and BCL2 in response to various concentrations of 10-H2DA treatments on MCF-7 human breast cancer cells for 24 h (mean ± SE); 0.54 µg/mL DXR was used as a positive control (n = 3), *p<0.05 significant difference from the MEM medium negative control

Table 4.11 Correlation coefficients of the relative expressions of regulatory proteins in response to 1.25-125 µg/mL 10-H2DA treatments on MCF-7 cells

Gene expressions	Correlation coefficient (r)
c-MYC	-0.96
BCL2	-0.81
h-TERT	-0.67
BAX	-0.67
p53	0.09
NRF2	0.99
HO-1	1
BCL2/BAX	-0.7

4.4.1.4 Cell cycle distribution analysis of 10H2DA treatments on MCF-7 cells by flow cytometry

As shown in Figure 4.37a and 4.37b, treatments with 10-H2DA at 1.25-250 µg/mL induced a dose-dependent increase in the percentage of cells in the sub G1 (0.6-to 2.4-fold) and G0/G1 phase (1.1-to 1.2-fold) but a dose-dependent decrease in the S phase (0.9-to 0.8-fold) and the G2/M phases (1.1- to 0.9-fold), compared to MEM control. For 0.54 µg/mL DXR control, there was a decrease in S phase (0.6-fold), stability in G0/G1 phase (1.0-fold) while there was an increase in G2/M phase (1.2-fold) and sub G1(1.1-fold). The data confirm that there was a greater accumulation of 10-H2DA treated cells in the sub G1 and the G0/G1 phases, but DXR-treated cells were more evident in the G2/M phase.

(a)
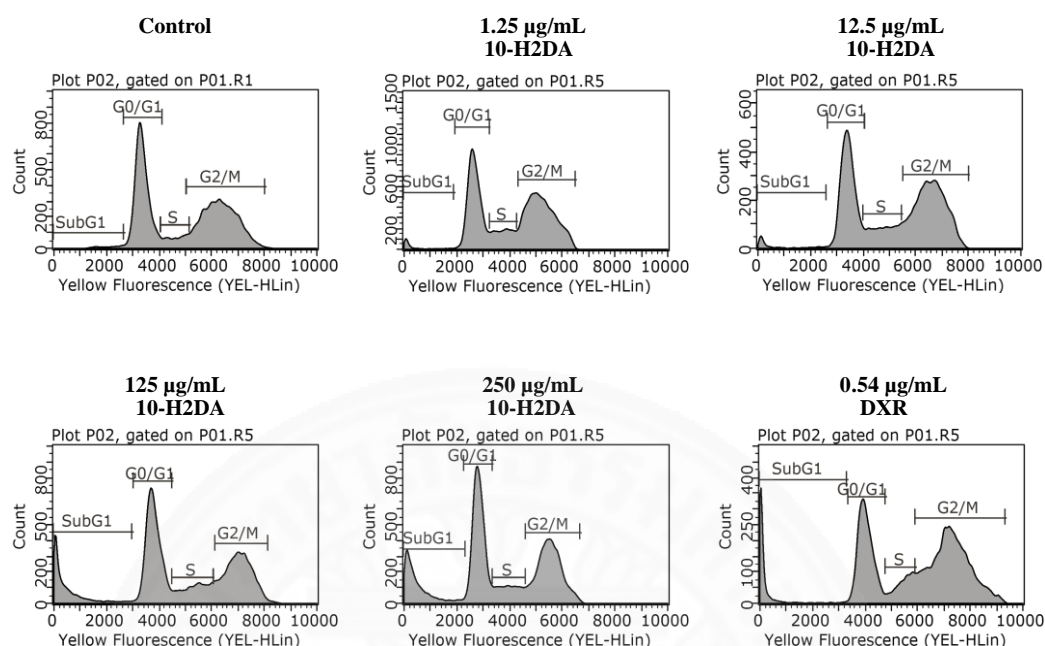
(b)
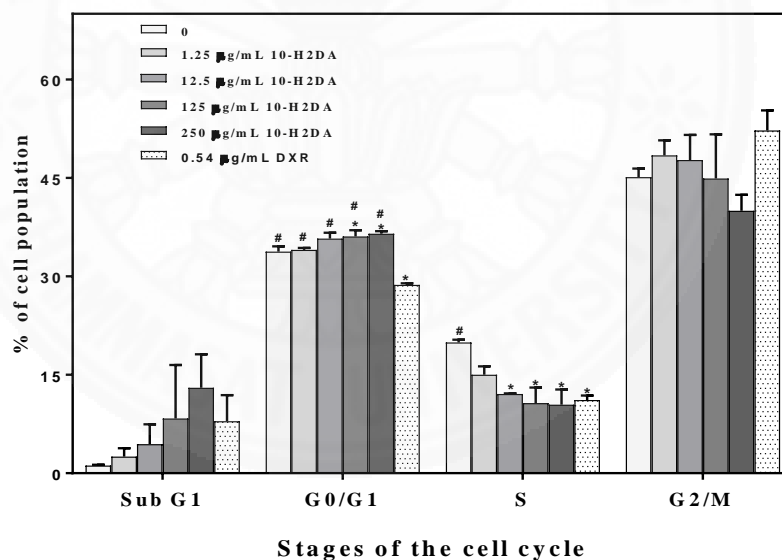
Figure 4.37 (a) Cell cycle analysis of MCF-7 cells exposed to various concentrations of 10-H2DA for 24 h by flow cytometer. MEM medium and DXR were used as negative and positive controls, respectively. (b) The percentage of cell population in each phase of the cell cycle after exposure to various concentrations of 10-H2DA, MEM medium and DXR (mean± S.E.), *$p<0.05$ significant difference from MEM medium control #$p<0.05$ significant difference from 0.54 µg/mL DXR, a positive control

4.4.1.5 Apoptosis analysis of 10-H2DA treatments against MCF-7 cells by flow cytometry

As shown in Figure 4.38a and 4.38b, 10-H2DA treatments (1.25, 12.5, 125, and 250 µg/mL) slightly decreased the percentages of live cells (1.09 to 1.04-fold) but markedly increased the percentages of early apoptosis (2.0 to 5.2-fold), late apoptosis (1.0 to 1.2-fold) and decreased necrosis (0.4 to 0.5-fold) in a dose-dependent manner. The highest dose of 250 µg/mL 10-H2DA increased early apoptosis to 5.2-fold indicating higher cell damage. The DXR treatment increased the percentage of early apoptosis to 2.3-fold and late apoptosis to 1.2-fold. The data confirms that 10-H2DA (125 and 250 µg/mL) induced cell death through apoptosis.

(a)
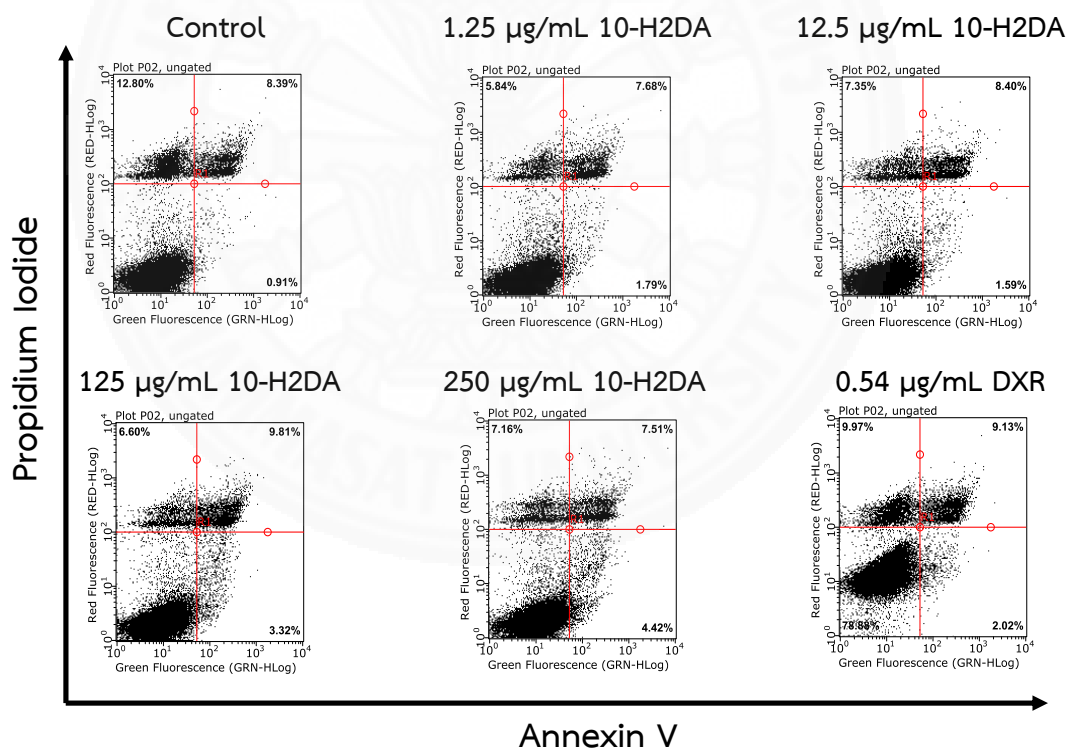
(b)
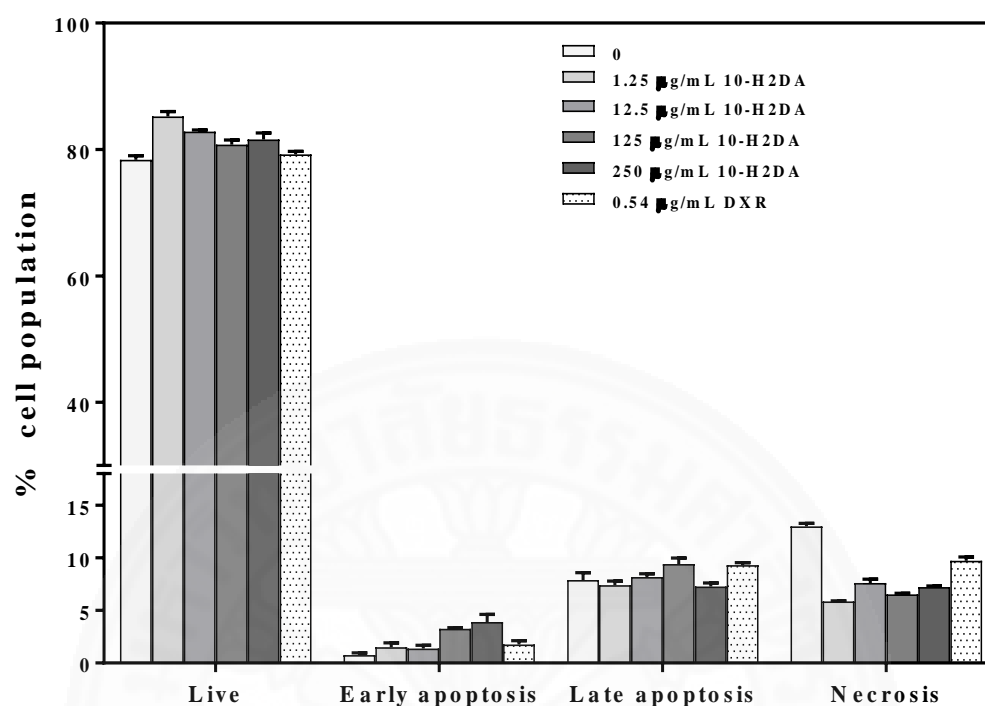
Figure 4.38 (a) Representative apoptosis analysis of 10-H2DA-treated MCF-7 breast cancer cells with MEM medium negative control and DXR positive control by flow cytometry, and (b) The percentage of live, early apoptosis, late apoptosis and necrosis cells in response to 10-H2DA treatments compared to controls

4.4.1.6 Morphological analysis of 10-H2DA and DXR treatments on MCF-7 cells detected by Hoecst33258/propidium iodide double fluorescence staining

As shown in Figure 4-39, compared between MEM medium control, 125 µg/mL 10-H2DA, and 0.54 µg/mL DXR treatments, 10-H2DA treatment showed a higher number of dead cells with apoptotic nuclei and the MEM medium control showed few dead cells with some apoptotic nuclei. The 0.54 µg/mL DXR treatment demonstrated a higher number of dead cells with irregular apoptotic nuclei. The data confirm previous results that 10-H2DA treatments induced cell apoptosis.
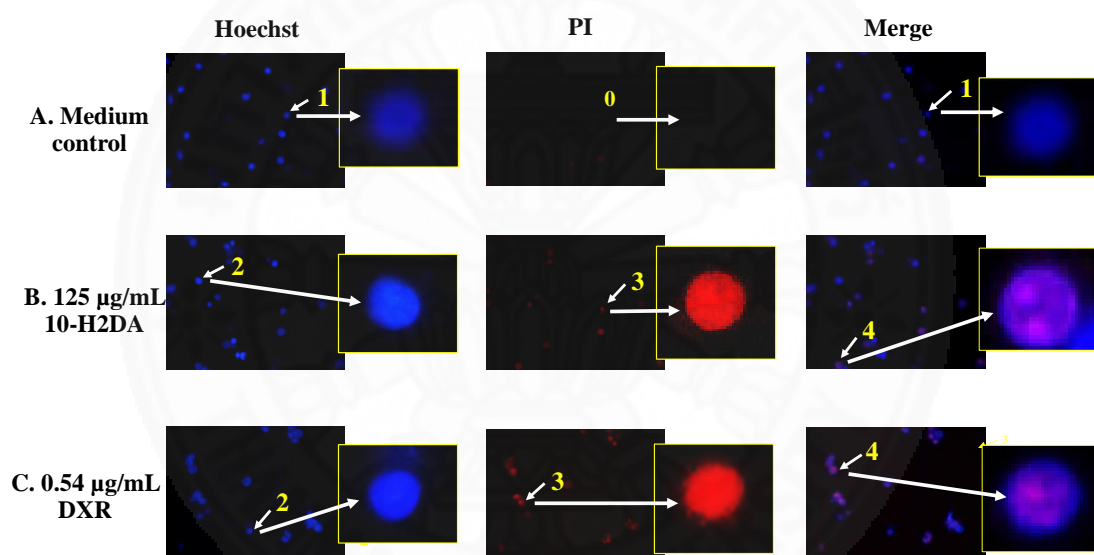
Figure 4.39 Representative photos of Hoechst 33258 and propidium iodide double staining on treated MCF-7 cells (A) MEM medium control, (B) 125 µg/mL 10-H2DA, (C) 0.54 µg/mL DXR; Arrows indicated (0) no dead cell (1) viable cells with normal nuclei, (2) live cells with apoptotic nuclei, (3) dead cells and (4) dead cells with apoptotic nuclei

4.4.2 Effect of 10-H2DA co-treatments with DXR on MCF-7 cells

4.4.2.1 Antiproliferative effects of 10-H2DA co-treatments with DXR detected by MTS tetrazolium assay

As shown in Figure 4.40, co-treatments of 10-H2DA at higher concentrations of 0.125, 1.25, 12.5, and 125 µg/mL with 0.54 µg/mL DXR for 24 h significantly decreased MCF-7 cell viability in a dose-dependent manner to 73.1%, 70.7%, 50.8%, and 27.9%, respectively, compared to MEM medium control. 0.54 µg/mL DXR treatment alone significantly decreased cell viability to 58.1% (p<0.05).
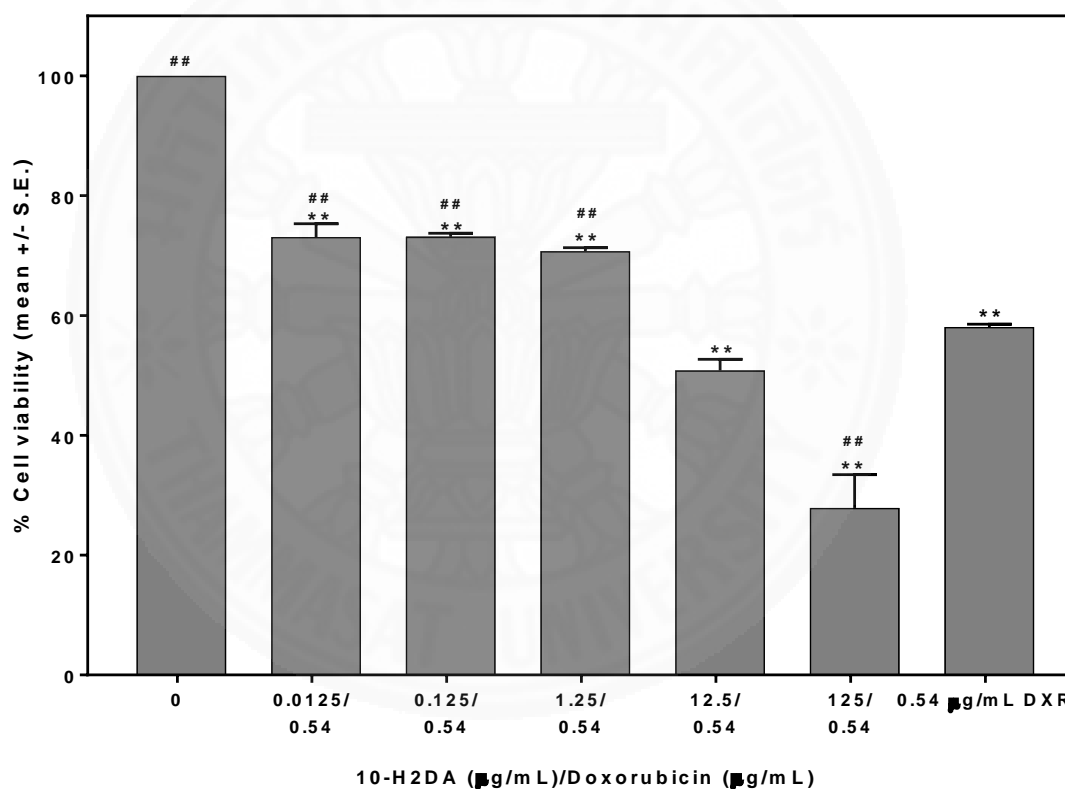
Figure 4-40 The relative cell viability in response to various concentrations of 10-H2DA co-treatment with DXR for 24 h on MCF-7 cells (n = 3)

**P < 0.05 significantly different from the MEM-treated negative control

##P < 0.05 significantly different from the DXR-treated positive control

To investigate morphological changes, MCF-7 cells were co-treated with 10-H2DA (1.25, 12.5 and 125 µg/mL) and 0.54 µg/mL DXR for 24 h. Treated cells were observed under microscopy for changing in number, volume and shape. As shown in Figure 4-41, 10-H2DA co-treatments with DXR increased the number of dead cells (unattached and round shape) in a dose-dependent manner, compared to MEM medium control. A large number of dead cells were observed at 12.5 µg/mL 10-H2DA co-treatment and reached the highest at 125 µg/mL 10-H2DA co-treatment. The DXR treatment alone revealed a higher number of dead cells than all 10-H2DA co-treatments.
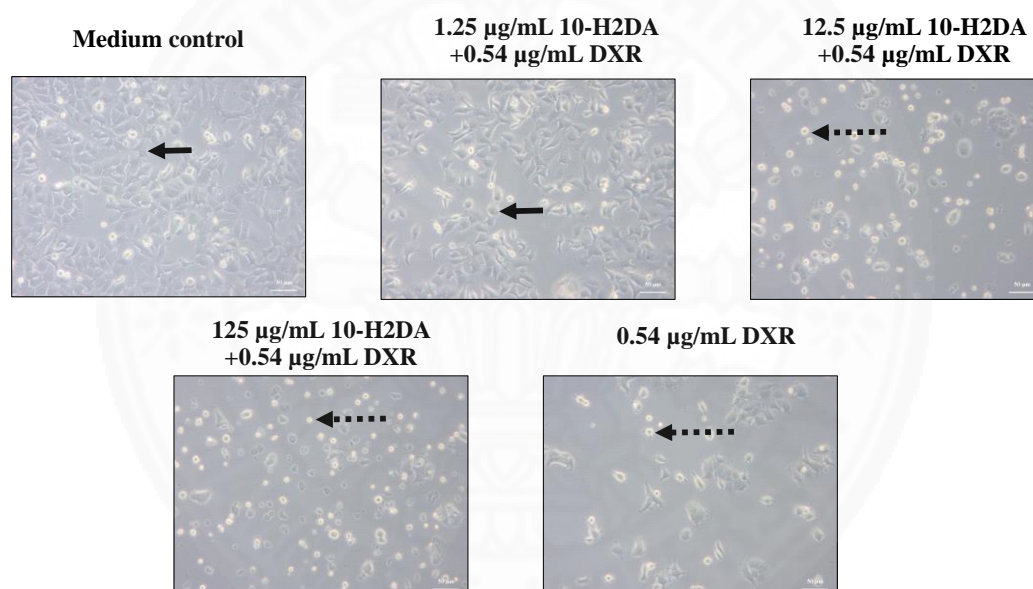
Figure 4.41 Effects on cell morphology induced by MEM medium control (0), 1.25, 12.5 and 125 µg/mL 10-H2DA co-treatments with 0.54 µg/mL DXR, and DXR treatment alone

→ normal cells: attached elongated shape

---▶ damaged cells: unattached rounded shape

4.4.2.2 Analysis of pivotal gene expressions induced by 10-H2DA co-treatments with DXR for 24 h against MCF-7 cells by Western blot

(1) Analysis of cell cycle regulatory proteins: cyclin D1, CDK4, cyclin E1, and cyclin B1 induced by 10-H2DA co-treatments

As shown in Figure 4.42a and 4.42b, MEM medium control-treated cells highly increased in cyclin D1 level, followed by cyclin B1 and cyclin E1 levels, respectively. The data suggested that cells actively progressed from G0 to G1 phases, less from G2 to M phase and the least from G1 to early S phase. The DXR treatment alone moderately decreased the levels of cyclin B1 (0.4-fold), slightly decreased CDK4 (0.8-fold), slightly increased cyclin D1 (1.2-fold) and highly increased cyclin E1 (2.5 fold), compared to the medium control (Figure 4.42c). Compared to the DXR treatment alone (Figure 4.42d), 10-H2DA co-treatments (1.25-125 µg/mL) decreased the levels of CDK4 (0.9-to 0.3-fold), cyclin D1 (0.8-to 0.4-fold), but increased the level of cyclin B1 (1.2 to 3.9-fold) in a dose-dependent manner. Besides, 10-H2DA co-treatment showed variable dose-dependent in cyclin E1. It increased cyclin E1 level (1.5-fold) at the lowest dose (1.25 µg/mL) and then decreased to 1.1- and 0.8-fold when treated with higher doses of 12.5 and 125 µg/mL 10-H2DA. The data suggested that the DXR treatment alone induced cell cycle arrest in G2/M phase and increased cells in G1/S phase. The highest dose 10-H2DA co-treatment (125 µg/mL) increased cell cycle arrest at G0/G1 and G1/S, while the lower dose co-treatments enhanced G1/S cell cycle progression.

(a)

| 10-H2DA (µg/mL) | 0 | 1.25 | 12.5 | 125 | 0 |
| DXR (µg/mL) | 0 | 0.54 | 0.54 | 0.54 | 0.54 |
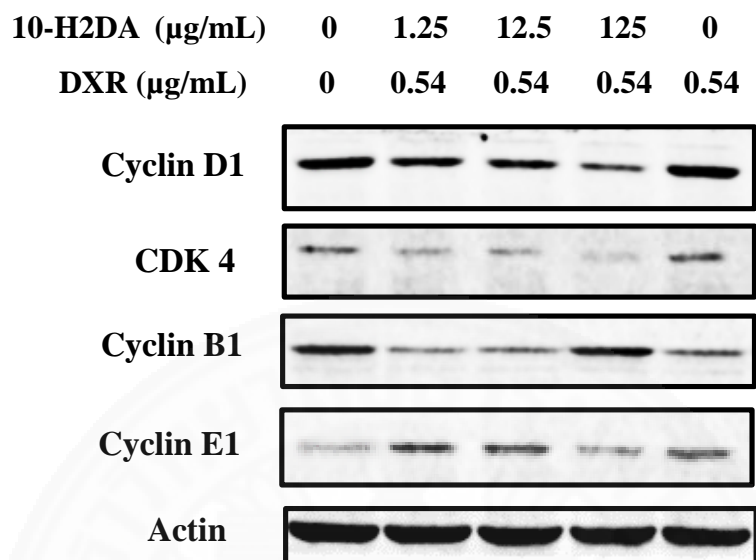
(b)
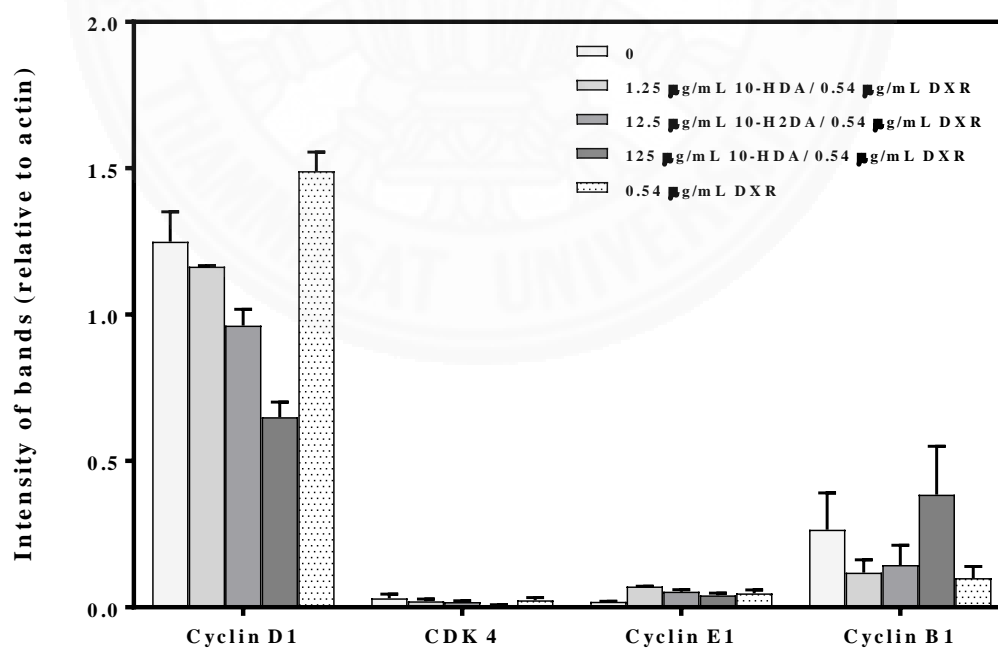
(c)
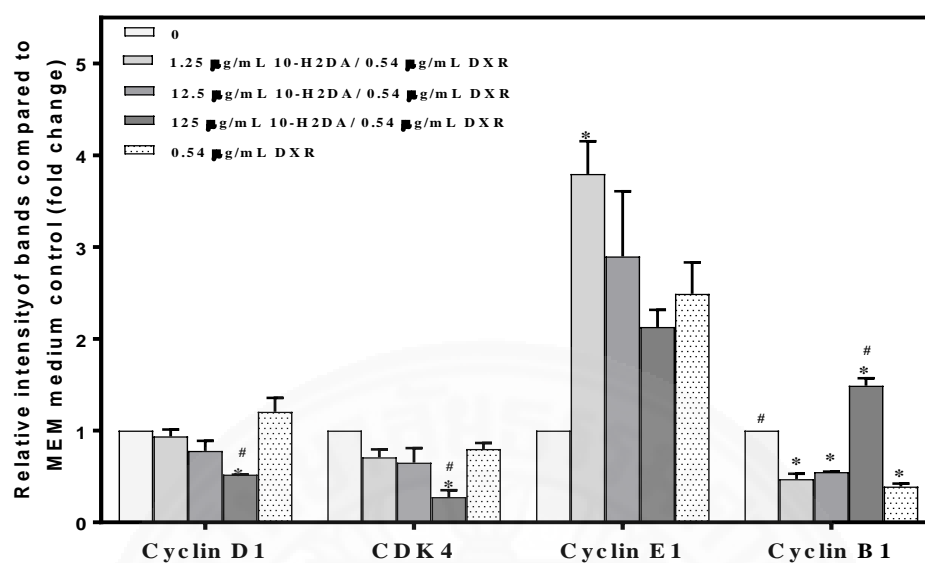
(d)
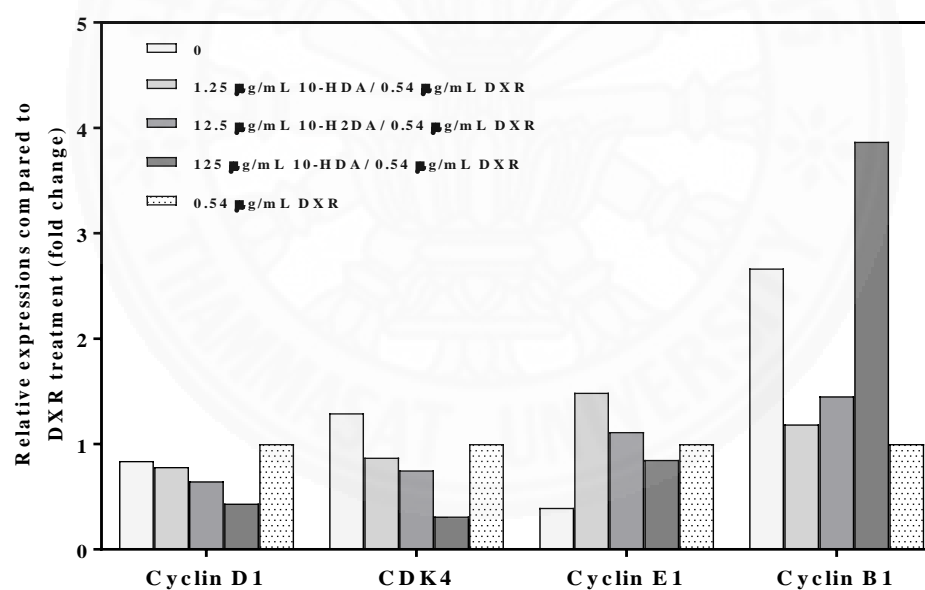
Figure 4.42 (a) Representative Western blot analysis of various concentrations 10-H2DA co-treatments with DXR for 24 h against MCF-7 cells (n = 3) (b) Intensity of bands (relative to actin) of cyclin D1, CDK4, cyclin E1, and cyclin B1 (mean ± SE) (c) Relative intensity of bands (fold change), compared to MEM medium control (d) Relative intensity of bands (fold change), compared to DXR-treated cells; $^*p < 0.05$ significantly different from the MEM medium control, $^\#p < 0.05$ significantly different from the DXR

(2) Analysis of pivotal gene expressions: hTERT, c-MYC, BCL2, BAX,, NRF2, HO-1 induced by 10-H2DA co-treatments

As shown in Figure 4-43a and 4.43b, DXR treatment alone decreased the expression level of c-MYC (0.3-fold), hTERT (0.3-fold), NRF2 (0.6-fold), BCL2 (0.6-fold) whereas it increased BAX (1.7-fold), HO-1 (2.8-fold), and extensively increased p53 (20.2-fold), compared to MEM medium control. Compared to DXR treatments alone, the highest dose of 10-H2DA (125 µg/mL) co-treatment maximally decreased the level of c-MYC (0.4-fold), BCL2 (0.6-fold), but maximally increased the levels of BAX (1.3-fold), NRF2 (2.4-fold), and HO-1 (3.7-fold). It slightly increased p53 (1.4-fold) and hTERT (2.3-fold). The lowest dose of 10-H2DA (1.25 µg/mL) co-treatment, however, just slightly decreased c-MYC (0.8-fold), BCL2 (0.8-fold), BAX (0.6-fold), NRF2 (0.8-fold), but increased hTERT (2.7-fold), p53 (1.9-fold), HO-1 (1.1-fold).

Analysis of the gene expression levels indicated that DXR treatment alone strongly inhibited cancer cell growth through reduction of the oncoprotein, c-MYC, inhibited longevity through a reduction of h-TERT, inhibited cell survival through a reduction of BCL2, and inhibited antioxidative response through NRF2 reduction. However, it increased antioxidative enzyme, HO-1 possibly involving rapid response against free radical damage induced by DXR itself. DXR increased p53 in response to DNA damage, leading to increase cell apoptosis. Compared to DXR treatment alone, the highest dose of 10-H2DA co-treatment effectively decreased the levels of c-MYC and BCL2 while increased the levels of BAX, hTERT, p53, NRF2, and HO-1. The lowest dose of 10-H2DA co-treatment increased all levels of c-MYC, BCL2, BAX, h-TERT, p53, NRF2 and HO-1.

To clarify the effectiveness of treatments against cell death, we use the gene expression ratios over BAX as we described and reported earlier (99) similar to BCL2/BAX, a rheostat that regulates life and death. BAX is used as an internal control to compare different level of regulatory proteins. As shown in Figure 4.44, the highest dose of 10-H2DA co-treatment maximally decreased C-MYC/BAX (0.3-fold), p53/BAX, (1.1-fold), BCL2/BAX (0.5-fold), hTERT/BAX (1.8-fold), but increased NRF2/BAX (1.9-fold) and HO-1/BAX (3.0-fold), compared to DXR treatment alone. The data suggested that the highest dose of 10-H2DA co-treatment effectively potentiated the

inhibition of cell proliferation induced by DXR alone, through reduction of c-MYC/BAX (reduction of cell proliferation) and BCL2/BAX (increased cell apoptosis), and induction of p53/BAX ratios (increased DNA damage response e.g. induced apoptosis). However, the highest dose of 10-H2DA co-treatment increased the hTERT/BAX (longevity), NRF2/BAX (antioxidative response), and HO-1/BAX (antioxidative enzyme) suggested that this highest dose co-treatment also provided some protective effects on the cells than the DXR treatment alone. The lowest dose of 10-H2DA co-treatment, however, increased c-MYC/BAX (1.3-fold), BCL2/BAX (1.3-fold), p53/BAX (3.1-fold), hTERT/BAX (4.3-fold), NRF2/NBAX (1.3-fold), and HO-1/BAX (1.8-fold). The data indicated that the lowest dose of 10 H2DA co-treatment decreased the effectiveness of antiproliferative effect of DXR treatment alone. It enhanced cancer cell proliferation (increased cMYC/BAX), cancer cell survival (increased BCL2/BAX), longevitiy (increased hTERT/BAX), DNA damage response (p53/BAX), and antioxidative response (increased NRF2/BAX, HO-1/BAX).

(a)
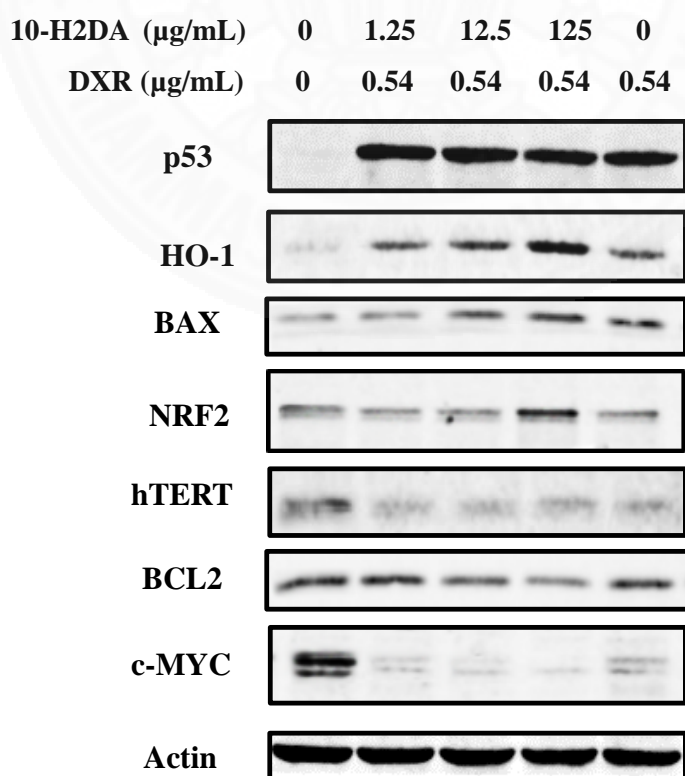
(b)
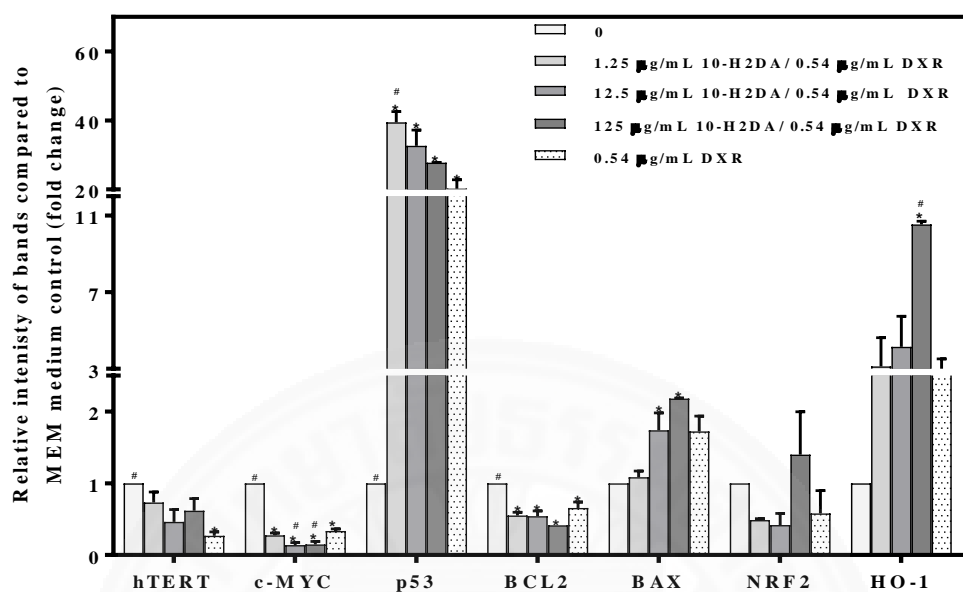
(c)
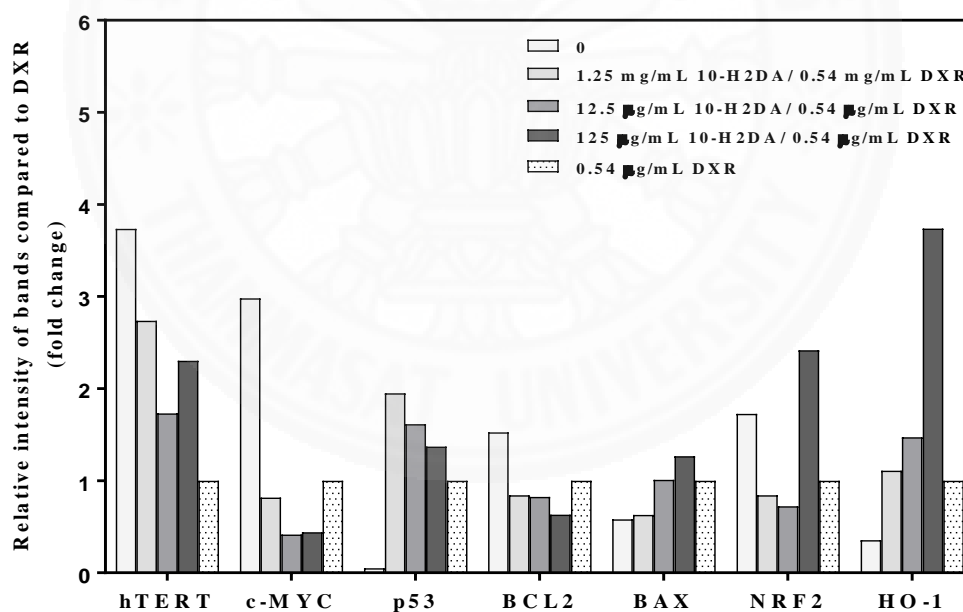
Figure 4.43 (a) Representative Western blot analysis. (b) Relative gene expression levels of h-TERT, c-MYC, p53, BCL2, BAX, NRF2, and HO-1 in response to various concentrations of 10-H2DA co-treatments with DXR for 24 h on MCF-7 cells, compared to medium control (mean ± SE) (n = 3). (c) Relative gene expression, compared to DXR; *p<0.05 significant difference from the MEM control; #p<0.05 significant difference from the DXR positive control
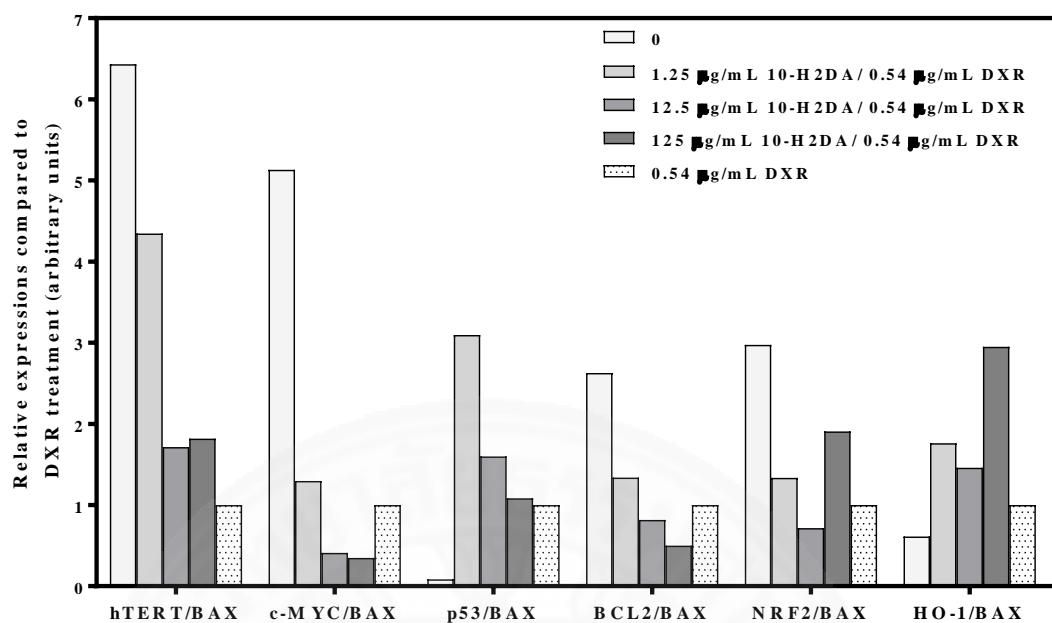
Figure 4-44 Representative diagram of the ratios of hTERT/BAX, C-MYC/BAX, p53/BAX, BCL2/BAX, NRF2/BAX, and HO-1/BAX levels in response to various concentrations of 10-H2DA co-treatments with DXR for 24 h in MCF-7 cells, compared to the DXR treatment alone (mean ± SE) (n = 3)

4.4.2.3 Analysis of cell cycle distribution induced by 10-H2DA co-treatments with DXR by flow cytometry

As shown in Figure 4.45a and 4.45b, the percentages of DXR-treated cells increased in G2/M phase (1.3-fold) but decreased in sub G1 (0.8-fold), G0/G1 (0.8-fold), and S phases (0.8-fold), compared to MEM medium control. It supported the finding in 4.4.1.4 that DXR-treated cells inhibited cyclin B1 levels, leading to cell cycle arrest and cells accumulated in G2/M phase. Compared to DXR-treatment alone, co-treatments of 10-H2DA (1.25, 12.5 and 125 µg/mL) induced a trend of dose-dependent increase in sub G1 (Figure 4.45c). The highest dose of 10-H2DA co-treatment extensively increased the percentage of cells in sub G1 (2.2-fold) but decreased in G0/G1 (0.8-fold), S (0.7-fold) and G2/M (0.7-fold) phases. The lowest dose of 10-H2DA co-treatments, however, decreased the percentage of cells in sub G1 (0.3-fold), slightly increased in G2/M (1.2-fold) and G0/G1 (1.1-fold) and relatively unchanged in S phase (1.0-fold). The data suggested that only the highest dose of 10-H2DA co-treatment but not the lowest dose effectively induced cell apoptosis (highly increased in sub G1 cells).

(a)
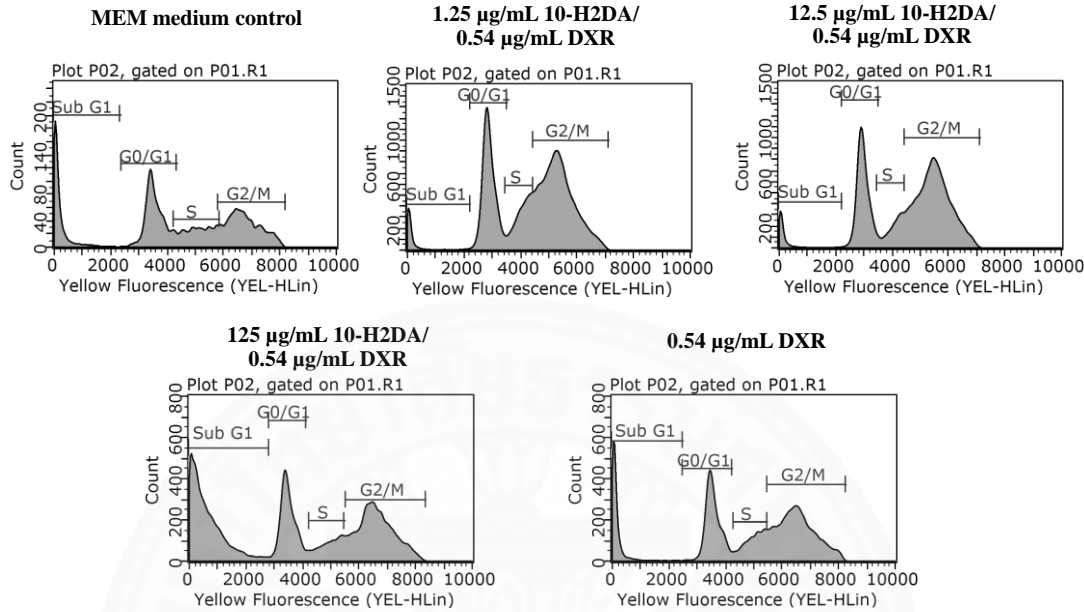
(b)
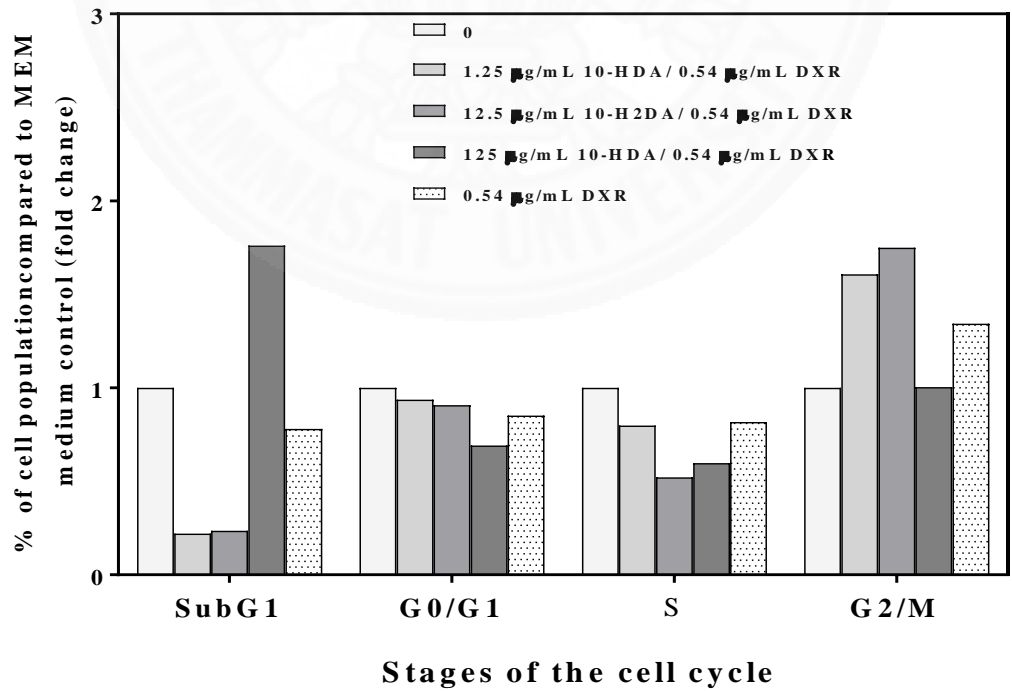
(c)
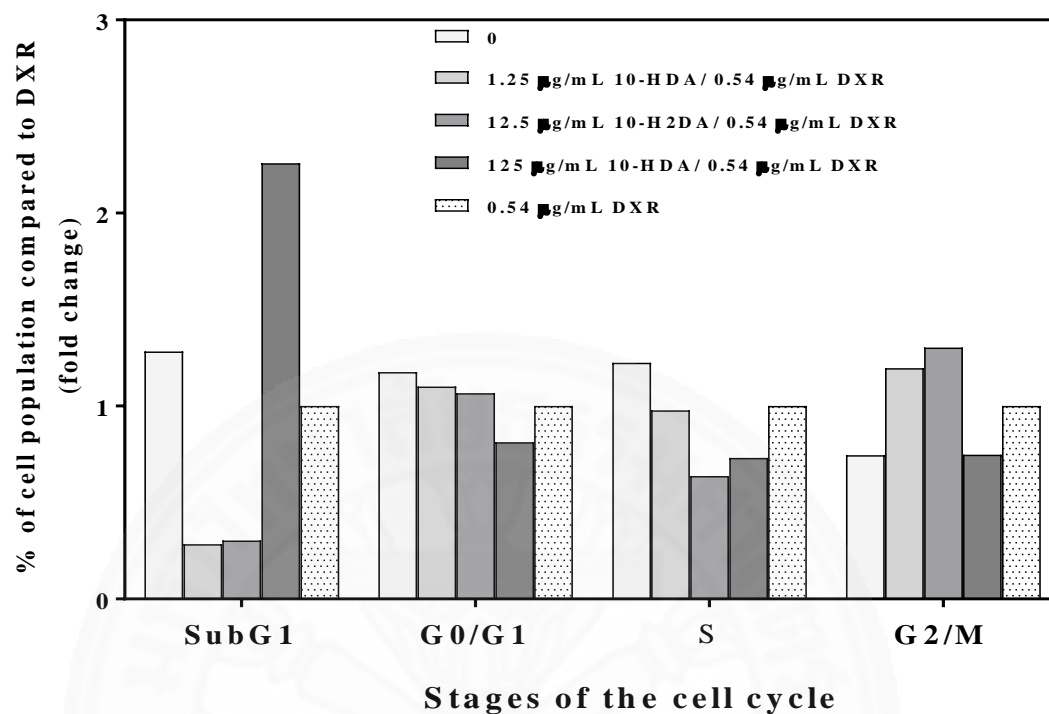
Figure 4.45 (a) Cell cycle analysis of MCF-7 cells exposed to various concentrations of 10-H2DA co-treatments with DXR for 24 h by flow cytometer. MEM medium and DXR were used as negative and positive controls, respectively. The percentage of cell population in each phase of the cell cycle after exposure to MEM medium, 10-H2DA co-treatments and DXR alone, compared to MEM medium (b) and compared to DXR treatment alone (c)

4.4.2.4 Analysis of cell apoptosis induced by 10-H2DA co-treatments with DXR detected by flow cytometry using annexin V and propidium iodide double staining

As shown in Figure 4.46a and 4.46b, the DXR treatment alone increased the percentages of early apoptosis (2.4-fold), late apoptosis (1.2-fold) while slightly decreasing cell necrosis (0.8-fold), compared to MEM medium control. Compared to DXR treatment alone, 125 µg/mL 10-H2DA co-treatment maximally enhanced apoptosis (increased early apoptosis 2.1-fold and late apoptosis 1.2-fold) and increased necrosis (1.2-fold). 1.25 µg/mL 10-H2DA treatment also maximally enhanced late apoptosis (1.5-fold) but slightly decreased, early apoptosis (0.7-fold) and increased necrosis (1.2-fold). The data suggested that the 10-H2DA co-treatments enhanced DXR-induced cell death through apoptosis and necrosis.

(a)
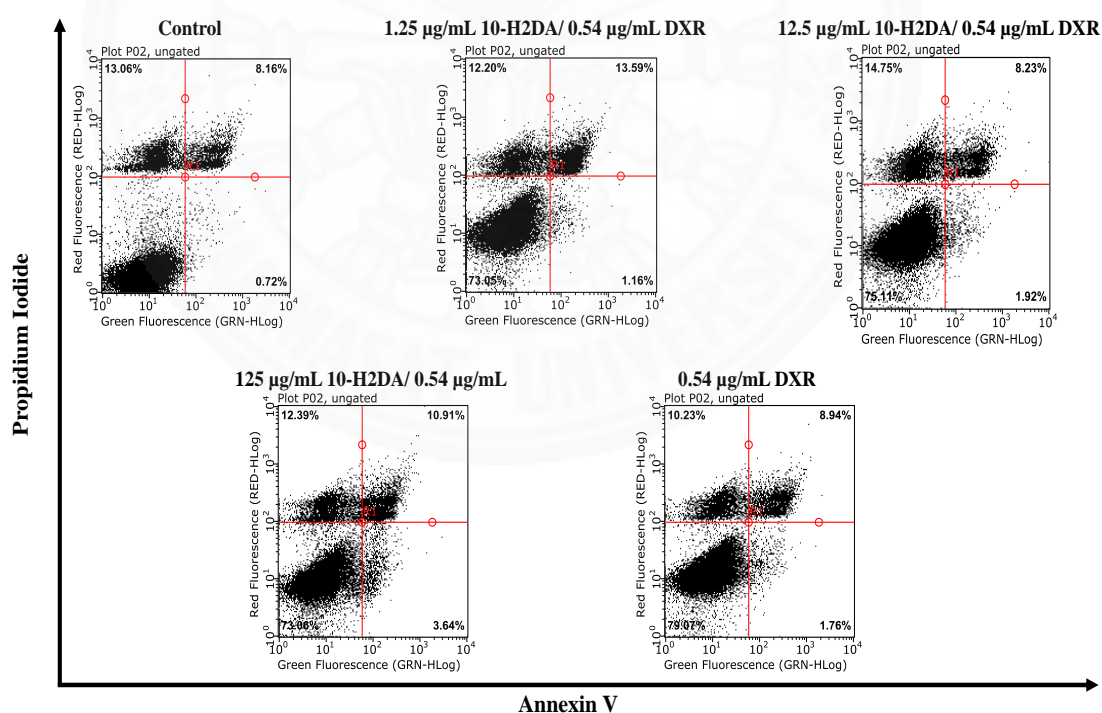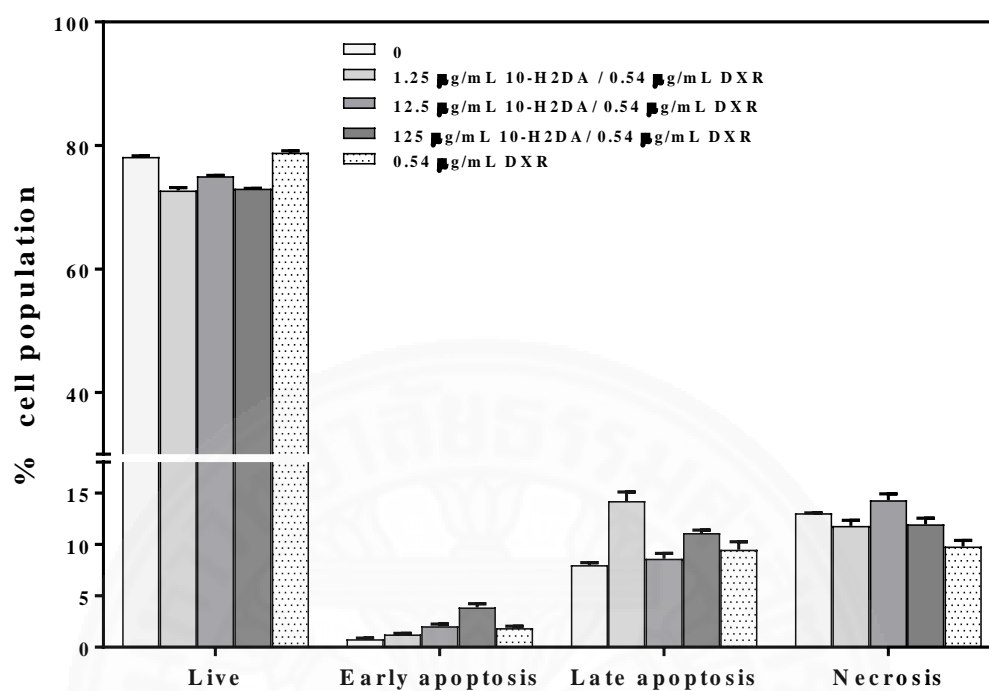
Figure 4-46 (a) Representative apoptosis diagram of MCF-7 cells exposed to various concentrations of 10-H2DA co-treatments with DXR for 24 h detected by flow cytometer. MEM medium and DXR were used as negative and positive controls, respectively, **(b)** The percentages of live, early apoptosis, late apoptosis and necrosis cells in response to the treated cells compared to MEM medium control (mean± S.E.) (n=3)

4.4.2.5 Analysis of morphological changes induced by 10-H2DA co-treatments with DXR detected by Hoechst 33258 and propidium iodide double staining under fluorescence microscope

As shown in Figure 4.47, using Hoechst 33258 and propidium iodide double staining, the 125 µg/mL 10-H2DA co-treatment showed a higher number of dead cells with apoptotic nuclei than those of the MEM medium control. The 0.54 µg/mL DXR treatment demonstrated a higher number of dead cells with apoptotic nuclei. The data confirm previous results that the highest dose of 10-H2DA co-treatments induced cell death through apoptosis.
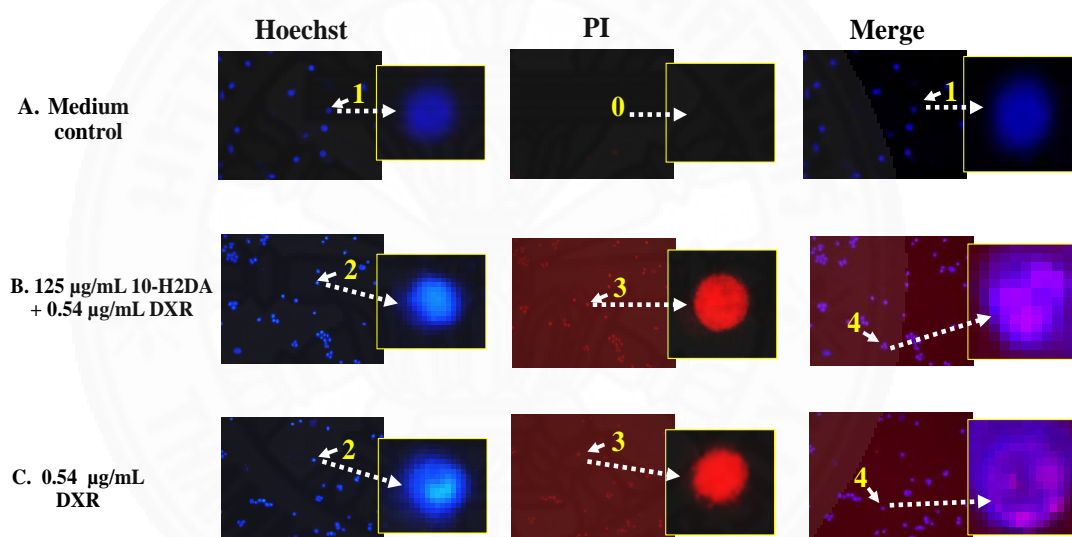
Figure 4.47 Representative photos of Hoechst 33258 and propidium iodide double staining of treated MCF-7 cells. (A) medium control, (B) 125 µg/mL 10-H2DA co-treatment with 0.54 µg/mL DXR, (C) 0.54 µg/mL DXR treatment alone; Arrows indicated (0) no dead cell; (1) live cells with normal nuclei; (2) cells with apoptotic nuclei; (3) dead cells and (4) dead cells with apoptotic nuclei

CHAPTER 5
DISCUSSION AND CONCLUSION

5.1. Chemical composition and antioxidant properties of RJ from northern Thailand

Our results indicated that the chemical compositions of our frozen RJ samples from Chiang Mai, northern Thailand were composed of approximately 65% moisture, 2.5% lipid, 2.2% protein, 32% carbohydrate 0.2% fiber and no ash (w/w) with pH 4.0. 10-H2DA content was 0.82% w/w. The current samples had lower nutrient contents, especially proteins, lipids, and carbohydrates, compared to that of our previous report in which fresh RJ with pH 3.5, 67.4% moisture, 12.1% carbohydrate, 4% lipid, 12% proteins and 1% ash was used (97).

The compositions of RJ from Romania and Bulgaria also reported higher protein contents of 13% and 15.5% w/w, respectively, and both had pH 3.9 (98). As we reported earlier, there was a seasonal variation that influence mainly the carbohydrate and lipid content and slightly changes in protein and moisture contents but no alteration in ash content or pH value (97). The carbohydrate content was the highest in the rainy season whereas the lipid content was the highest in the hot season.

Total phenolic acid from our RJ samples was 1.8 ± 0.5 mg gallic acid /g RJ. This quantity of phenolic compounds was similar to those reported by Liu et al., 2008 (1.3- 2.2 mg/g RJ) (100) but less than 21.2 mg/g RJ reported by Nagai and Inoue, 2004 (101). Total flavonoid was 0.9±0.08 mg Rutin equivalent/g RJ. The antioxidant activity of RJ was 17.9±1.9 µM Trolox equivalent. Compared to bee pollen also from Chiang Mai, northern Thailand reported earlier (102), phenolic and flavonoid contents in bee pollen were much higher than those in RJ (9.3-fold and 13.8-fold, respectively).

5.2 Effects of RJ alone on human lymphocytes

Our present study determined levels of genotoxic activity and mechanisms of action of RJ at various doses on human lymphocytes *in vitro*. It demonstrated that RJ treatments at 0.0005–5 mg/ml for 3 h did not induce cytotoxicity on human lymphocytes, however, a high dose of 5 mg/ml induced genotoxicity (1.4-fold). There was no statistical significance on the P.I. of the treated cells and the control, but there was a trend of increased cell cycle progression from MI to MII with the increasing doses of RJ. By the SCE assay, our data indicate that RJ ≤ 0.5 mg/ml was quite safe with no genotoxic nor cytotoxic damage to human cells *in vitro*. From the assumption that an Asian individual weighs 60 Kg and the body is mostly made up of water, we assume that 1 ml *in vitro* equals to 1 gm of tissue for conversion of *in vitro* to human doses. Thus, consumption of less than 30 g RJ for a 60 kg man should be considered safe. However, intake of RJ is prohibited for those with allergies since it may induce anaphylaxis and death.

Western blot analysis demonstrated that RJ had both beneficial and harmful effects, depending on the doses. The lowest dose of 0.0005 mg/ml RJ had the highest beneficial effects by maintaining cell proliferation (c-MYC/BAX), cell survival (BCL2/BAX), antioxidant enzyme level (HO-1/BAX), and antioxidative response (NRF2/BAX) at approximately normal level, and enhanced telomerase level ratio (hTERT/BAX) by 1.3-fold. Our data suggest that RJ treatment at a low dose of 0.0005 mg/ml provided maximum benefits to human cells especially protecting telomere and prolonged lifespan.

Our *in vitro* mechanistic study of RJ also supports previous *in vivo* studies. Inoue et al., 2012, reported that dietary RJ reduced oxidative damage: 8-hydroxydeoxyguanine (8-OHdG) in mice and extended survival time (103). Our study provided new insight molecular mechanisms, showing the antioxidative power of RJ through modifying NRF2 and HO-1 levels. In another report, intake of freeze-dry RJ by *Drosophila melanogaster* decreased their developmental time to adulthood, extended lifespan and increased female fecundity (104). Our data revealed that RJ induced an increase in hTERT and hTERT/BAX levels, possibly preventing cellular

senescence, and extending lifespan. Previous studies already reported that hTERT proteins detected in normal human lymphocytes correlated with telomerase activity (105). In addition, telomerase-expressing normal human clones extended normal lifespan but not telomerase negative clones (106). This molecular study supported previous reports of RJ benefits. Inoue et al., 2013 and Detienne et al., 2014 demonstrated that RJ prolonged the lifespan of mice (103) and extended lifespan of *Caenorhabditis elegans* (107). 57 KD protein isolated from RJ stimulated rat hepatocyte proliferation and promoted antiapoptosis (108). Our study additionally revealed that RJ-induced longevity possibly mediates through h-TERT/BAX activation. Valiollahpoor et al., 2015 demonstrated that RJ improved blastocyst formation with increasing BCL2/BAX in sheep oocytes (109).

On the contrary, the highest dose of 5 mg/ml RJ caused more harm, though maintaining the telomere length protection and enhanced antioxidative response (hTERT/BAX and NRF2/BAX = 1.1-fold). It decreased cell proliferation, cell survival and antioxidant enzyme level. The deleterious effects at the highest dose of RJ corresponded with its genotoxicity (1.4 fold increase in SCE level compared to RPMI control). Few studies have reported on RJ toxicity. El- Aidy et al., 2015 noted that RJ induced lung inflammation in mouse conalbumin-induced asthma model (110).

5.3 Effects of RJ in combination with DXR on human lymphocytes

Therefore, our study verified that a specific dose of RJ protected human cells from DXR-induced toxicity. Its protective mechanisms possibly mediate through an increase of BCL2/BAX ratio for cell survival, increase in hTERT/BAX for enhancing longevity, and increase in NRF2/BAX for amplifying antioxidative response. Nevertheless, its protective effects remain dose-dependent. The improper dosage of RJ can enhance toxicity. Results from this mechanistic study are in agreement with previous reports, demonstrating that the antioxidant activity of RJ protected testis from diabetes-induced impairment (111) and cisplatin-induced oxidative damage in rats (112). In addition, RJ protected rats from paclitaxel-induced cardiotoxicity as shown by reduction of creatine kinase (CK-BM), and pathological injuries (113). Therefore, RJ might protect against DXR-induced cardiotoxicity, which is a common side effect of DXR as well.

Our study clarified the genoprotective effects of RJ against DXR on human lymphocytes *in vitro*. However, the improper dosage of RJ can enhance toxicity. Usage of RJ needs careful consideration.

5.4 Effects of 10-H2DA treatments on MCF-7 breast cancer cell line

Our present study revealed novel molecular mechanisms of antiproliferative effects from 10-H2DA treatments against MCF-7 breast cancer cells. Specifically, the data demonstrated that 10-H2DA (1.25, 12.5 and 125 μg/mL) treatments inhibited MCF-7 cancer cell proliferation in a dose-dependent manner. Treatment with 125 μg/mL 10-H2DA effectively decreased cancer cell viability to 36.4%. The underlying mechanisms involved reduction of pivotal protein expression levels of C-MYC, cyclin D1, CDK4, cyclin B1, h-TERT, and also BCL2/BAX ratio, resulting in an inhibition of cell proliferation, cell cycle arrest (mostly at G0/G1), shortened lifespan, and induction of cell apoptosis.

Our results provide mechanistic understanding of previous studies which demonstrated that 10-H2DA had antitumor activities against transplantable leukemia, the ascites form of Ehrlich carcinoma and the TA3 mammary carcinoma in AKR mice (18). In addition, antitumor activities of RJ against tumor transplantable mice were highly effective against Ehrlich and Sarcoma 180 solid tumors and less effective against Ehrlich and Sarcoma-180 ascites tumors but not effective against slow growing tumors such as advance leukemia (114). In addition, 10-H2DA also showed anti-inflammatory activities. It inhibited lipopolysaccharide (LPS)-induced IkB-zeta and interleukin 6 (IL-6) production on LPS-induced cytokine production in murine macrophage cell line, RAW264 cells. It inhibited LPS- and interferon beta (IFN-β)- induced nitric oxide (NO) production through inhibiting nuclear factor-kB (NF-kB) activation (115). Taking into account of *in vivo* animal studies and our *in vitro* molecular studies, 10-H2DA has a potential as a candidate for anti-inflammation and anticancer.

Nevertheless, our data indicated that 10-H2DA treatments stimulated antioxidative response by high induction of HO-1 and NRF2 levels. These anti-oxidative activities protected microenvironment against oxidative damage. Frohlich et al., 2008 reported that the loss of NRF2 increased oxidative stress and DNA damage in the initiation of prostate tumorigenesis (116). Therefore, cancer cells under protected environment with inhibition of oncogene c-MYC and induction of cell cycle delay may selectively regain normal cell growth by decreasing tumor cell invasion and

metastastis. Correspondingly, Gharaee-Kermani, et al., (2016) reported that resveratrol, induced phenoconversion of myofibroblast to lung and prostate fibroblast (117). Melling, et al., (2018) used miRNA-145 reverted cancer-associate fibroblast towards a normal fibroblast phenotype (28). Induction of NRf2 and HO-1, therefore, might provide protective microenvironment having benefits not only for protecting neighboring normal cells from oxidative damage but also for leading irregular uncontrolled growth of cancer cells towards controlled normal growth. Our study also revealed that RJ substantially enhances NRF2 and HO-1 on human lymphocytes (99). Pretreatments of RJ protected DXR-induced genotoxicity on human lymphocytes with highly induction of NRF2 and HO-1 as well (118). Alternatively, increased antioxidative response, NRF2 and HO-1 could also cause harm by promoting cancer cell survival and resistance. Indeed, it has been reported that overexpression of NRF2 has selective advantage for cancer cells survival (119, 120).

5.5 Effects of 10-H2DA co-treatments with DXR on MCF-7 breast cancer cell line

Our present study demonstrated that co-treatments of 125 µg/mL 10-H2DA potentiated DXR-increased antiproliferation against MCF-7 breast cancer cells by 62.4%, compared to DXR treatment alone. It increased cell apoptosis (decreased BCL2/BAX: 0.5-fold and increased p53/BAX: 1.1-fold), decreased cell proliferation (decreased c-MYC/BAX: 0.3-fold), increased cell cycle arrest at G0/G1 (decreased cyclin D1: 0.4-fold and CDK4: 0.3-fold), compared to DXR alone. In addition, it increased antioxidative response (increased NRF2/BAX: 1.9-fold and HO-1/BAX: 3.0-fold) and increased lifespan (increased hTERT/BAX: 1.8-fold). These values also concur with increasing in percentages of cells in sub G1 (increased cell apoptosis). Therefore, the highest dose of 10-H2DA co-treatment inhibited cancer cell growth effectively through inhibition of oncoprotein transcription factor (c-MYC), induction of cell cycle arrest (decreased cyclin D1 and CDK4), and induction of cell apoptosis (decreased BCL2/BAX). However, the effectiveness of antiproliferation strictly depends on the dose. The lowest dose of 10-H2DA co-treatments tended to enhance cancer cell proliferation more effectively than DXR treatment alone did. It increased BCL2/BAX (1.3-fold), c-

MYC/BAX (1.3-fold), h-TERT/BAX (4.3-fold), although it increased p53/BAX (3.1-fold), NRF2/BAX (1.3-fold), and HO-1/BAX (1.8-fold). It increased cell cycle progression from G1 to S phase (increased cyclin E1: 1.5 fold) and G2 to M phase (increased cyclin B1: 1.2 fold), however it still slightly increased cell cycle arrest at G0/G1 (decreased cyclin D1 (0.8-fold and CDK4 (0.9-fold). Cells had less apoptosis (less cells in sub G1 (0.3-fold)).

Previous studies have reported various pharmacological activities of 10-H2DA. It decreased triglyceride, cholesterol, low density lipoprotein (LDL) and increased high density lipoprotein (HDL) in hyperlipoidemic rats (121). It promoted collagen production by human skin fibroblasts cell line in the presence of ascorbic acid-2-O-alpha-glucoside (AA-2G) (122), promoted neurogenesis by neural stem/progenitor cells *in vitro* (123) and extended lifespan of the nematode *Caenorhabditis elegans* (20). Importantly, it inhibited VEGF-induced angiogenesis on human umbilical vein endothelial cells (21) and inhibited LPS-induced inflammatory response through inhibition of IL6, TNFα, NO, COX-2, IL-10, JNK in RAW264.7 macrophage cell line, which substantiated anticancer properties (13). Viewing these advantages of 10-H2DA, combination of 10-H2DA with DXR have beneficial effect for chemotherapy. From the present study, 10-H2DA co-treatment at the highest dose markedly inhibited cancer cell proliferation with less side effects on neighboring cells compared to DXR treatment alone. It modulated all dominant regulators, c-MYC, p53, hTERT, cyclins and CDK leading cell to apoptosis. It increased antioxidative power to the cells and protected cells from aggressive deterioration. The number of dead cells caused by apoptosis was higher than that caused by necrosis, which which probably agrees with less side effect toxicity. Frohlich et al., 2008 reported that the loss of NRF2 initiates oxidative stress and DNA damage, and leads to prostate tumorigenesis (116). Therefore, increased NRF2 and HO-1, antioxidative responses provide unharm microenvironment and possibly reduce cancer cell proliferation. However, activation of these antioxidative power could increase self-protection of cancer cells leading to cancer resistance to chemotherapy. Yang et al., 2015 reported that NRF2-mediated ATP binding cassette transporter G2 (ABCG2) was over expression in lung adenocarcinoma SP cells involving in multidrug resistance (124). It is, therefore, careful

monitoring is required if 10-H2DA co-treatment is used for a long-term. Usage for a period of time and dosage control are needed for effective treatment and limited the resistance.

In conclusion, our study provides insight molecular evidence on antiproliferative activities of 10-H2DA co-treatment with DXR against MCF-7 breast cancer cell line. At specific doses, 10-H2DA in combination with DXR sharply inhibited c-MYC/BAX, BCL2/BAX, cyclin D1 and CDK4 and activated p53/BAX leading to inhibition of cancer cell growth, inducing cell cycle arrest and apoptosis. Concurrently, its ability in promoting antioxidative response possibly allowed cells to undergo in controlled and regular manner and less aggresiveness. However, caution of induction of cancer cell resistance is needed. Further *in vitro* and *in vivo* studies are needed to verify proper administration of 10-H2DA in chemotherapy.

In conclusion, our study evaluate the effectiveness of RJ and 10-H2DA for chemoprevention on human lymphocytes and chemotherapy on MCF-7 breast cancer cells. On human lymphocytes, RJ at proper dose which is not genotoxic, enhanced normal cell growth, longevity and antioxidative response. It protected human lymphocytes from DXR-induced DNA damage by inducing of cell cycle arrest, and cell apoptosis by increasing antioxidative response and longevity through cyclin D1, BCL2/BAX, NRF2/BAX and h-TERT/BAX. This study reveals the effectiveness of RJ as a potential chemopreventive compound in promoting cell growth, protecting human lymphocyte cells from oxidative damage and promoting longevity. In addition, this study demonstrated the effectiveness of 10-H2DA at proper dose as a potential chemotherapeutic compound in inhibiting MCF-7 cell growth and enhancing cell apoptosis and cell cycle arrest. Combination with DXR potentiates the effectiveness of cytotoxic effects against cancer cells. However, both RJ and 10-H2DA at proper doses increase antioxidative power by induction of NRF2. This provides protection from oxidative damage for both normal cells and cancer cells therefore it might lead to cancer cell resistance although protecting normal cells. At last, careful selection of the dose and monitoring of the usage of these compounds are important for the effectiveness. Further *in vitro* and *in vivo* study are needed to assure the usefulness of RJ and its products.

REFERENCES

1.   Bray F, Ren JS, Masuyer E, Ferlay J. Global estimates of cancer prevalence for 27 sites in the adult population in 2008. International journal of cancer. 2013;132(5):1133-45.

2.   Ferlay J SI, Ervik M, Dikshit R, Eser S, Mathers C, Rebelo M, Parkin DM, Forman D, Bray, F. GLOBOCAN 2012 v1.0, Cancer Incidence and Mortality Worldwide: IARC CancerBase No. 11 [Internet]. Lyon, France: International Agency for Research on Cancer. 2013.

3.   Hanahan D, Weinberg RA. Hallmarks of cancer: the next generation. Cell. 2011;144(5):646-74.

4.   Thorn CF, Oshiro C, Marsh S, Hernandez-Boussard T, McLeod H, Klein TE, et al. Doxorubicin pathways: pharmacodynamics and adverse effects. Pharmacogenetics and genomics. 2011;21(7):440-6.

5.   Octavia Y, Tocchetti CG, Gabrielson KL, Janssens S, Crijns HJ, Moens AL. Doxorubicin-induced cardiomyopathy: From molecular mechanisms to therapeutic strategies. Journal of molecular and cellular cardiology. 2012;52(6):1213-25.

6.   Villani F, Comazzi R, Lacaita G, Guindani A, Genitoni V, Volonterio A, et al. Possible enhancement of the cardiotoxicity of doxorubicin when combined with mitomycin C. Medical oncology and tumor pharmacotherapy. 1985;2(2):93-7.

7.   Kushi LH, Doyle C, McCullough M, Rock CL, Demark-Wahnefried W, Bandera EV, et al. American cancer society guidelines on nutrition and physical activity for cancer prevention: reducing the risk of cancer with healthy food choices and physical activity. CA: a cancer journal for clinicians. 2012;62(1):30-67.

8.   Hao F, Kumar S, Yadav N, Chandra D. Neem components as potential agents for cancer prevention and treatment. Biochimica et biophysica acta. 2014;1846(1):247-57.

9.   Alzohairy MA. Therapeutics Role of *Azadirachta indica* (Neem) and their active constituents in diseases prevention and treatment. Evidence-based complementary and alternative medicine : eCAM. 2016;2016:7382506.

10.   Aggarwal BB, Bhardwaj A, Aggarwal RS, Seeram NP, Shishodia S, Takada Y. Role of resveratrol in prevention and therapy of cancer: preclinical and clinical studies. Anticancer research. 2004;24(5a):2783-840.

11.   Cal C, Garban H, Jazirehi A, Yeh C, Mizutani Y, Bonavida B. Resveratrol and cancer: chemoprevention, apoptosis, and chemo-immunosensitizing activities. Current medicinal chemistry anti-cancer agents 2003;3(2):77-93.

12.   Lee YJ, Lee YJ, Im JH, Won SY, Kim YB, Cho MK, et al. Synergistic anti-cancer effects of resveratrol and chemotherapeutic agent clofarabine against human malignant mesothelioma MSTO-211H cells. Food and chemical toxicology. 2013;52:61-8.

13.   Chen Y F, Wang K, Zhang Y Z, Zheng Y F, Hu F L. *In vitro* anti-inflammatory effects of three fatty acids from royal jelly. Mediators of inflammation. 2016;2016:11.

14.   Nagai T, Inoue R, Suzuki N, Nagashima T. Antioxidant properties of enzymatic hydrolysates from royal jelly. Journal of medicinal food. 2006;9(3):363-7.

15.   Kamakura M, Mitani N, Fukuda T, Fukushima M. Antifatigue effect of fresh royal jelly in mice. Journal of nutritional science and vitaminology (Tokyo). 2001;47(6):394-401.

16.   Hattori N, Ohta S, Sakamoto T, Mishima S, Furukawa S. Royal jelly facilitates restoration of the cognitive ability in trimethyltin-intoxicated mice. Evidence-based complementary and alternative medicine : eCAM. 2011;2011:165968.

17.   Narita Y, Nomura J, Ohta S, Inoh Y, Suzuki KM, Araki Y, et al. Royal jelly stimulates bone formation: physiologic and nutrigenomic studies with mice and cell lines. Bioscience, biotechnology, and biochemistry. 2006;70(10):2508-14.

18.   Townsend GF, Morgan JF, Tolnai S, Hazlett B, Morton HJ, Shuel RW. Studies on the *in vitro* antitumor activity of fatty acids. I. 10-Hydroxy-2-decenoic acid from royal jelly. Cancer research. 1960;20:503-10.

19.   Yang XY, Yang DS, Wei Z, Wang JM, Li CY, Hui Y, et al. 10-Hydroxy-2-decenoic acid from royal jelly: a potential medicine for RA. Journal of ethnopharmacology. 2010;128(2):314-21.

20.   Honda Y, Fujita Y, Maruyama H, Araki Y, Ichihara K, Sato A, et al. Lifespan-extending effects of royal jelly and its related substances on the nematode *Caenorhabditis elegans*. Plos one. 2011;6(8):e23527.

21.   Izuta H, Chikaraishi Y, Shimazawa M, Mishima S, Hara H. 10-Hydroxy-2-decenoic Acid, a major fatty acid from Royal jelly, inhibits VEGF-induced angiogenesis in human umbilical vein endothelial cells. Evidence-based complementary and alternative medicine : eCAM. 2009;6(4):489-94.

22.   Katayama M, Aoki M, Kawana S. Case of anaphylaxis caused by ingestion of royal jelly. The journal of dermatology. 2008;35(4):222-4.

23.   Roger A, Rubira N, Nogueiras C, Guspi R, Baltasar M, Cadahia A. Anaphylaxis caused by royal jelly. Allergologia et immunopathologia. 1995;23(3):133-5.

24.   Lee NJ, Fermo JD. Warfarin and royal jelly interaction. Pharmacotherapy. 2006;26(4):583-6.

25.   Antinelli J-F, Zeggane S, Davico R, Rognone C, Faucon J-P, Lizzani L. Evaluation of (E)-10-hydroxydec-2-enoic acid as a freshness parameter for royal jelly. Food Chemistry. 2003;80(1):85-9.

26.   Lialiaris TS. Sister Chromatid Exchange. In: Hughes SM, editor. Brenner's Encyclopedia of Genetics (Second Edition). San Diego: Academic Press; 2013. 454-7.

27.   Kotepui M, Chupeerach C. Age distribution of breast cancer from a Thailand population-based cancer registry. Asian pacific journal of cancer prevention. 2013;14(6):3815-7.

28.   Melling GE, Flannery SE, Abidin SA, Clemmens H, Prajapati P, Hinsley EE, et al. A miRNA-145/TGF-beta1 negative feedback loop regulates the cancer-associated fibroblast phenotype. Carcinogenesis. 2018, 39(6):798-807.

29.   Varoni EM, Lo Faro AF, Sharifi-Rad J, Iriti M. Anticancer molecular mechanisms of resveratrol. Frontiers in nutrition. 2016;3:8.

30.   Arora N, Bansal MP, Koul A. *Azadirachta indica* exerts chemopreventive action against murine skin cancer: studies on histopathological, ultrastructural changes and modulation of NF-kappaB, AP-1, and STAT1. Oncology research. 2011;19(5):179-91.

31.   Babykutty S, S PP, J NR, Kumar MA, Nair MS, Srinivas P, et al. Nimbolide retards tumor cell migration, invasion, and angiogenesis by downregulating MMP-2/9

expression via inhibiting ERK1/2 and reducing DNA-binding activity of NF-kappaB in colon cancer cells. Molecular carcinogenesis. 2012;51(6):475-90.

32. Johnson JJ, Bailey HH, Mukhtar H. Green tea polyphenols for prostate cancer chemoprevention: a translational perspective. Phytomedicine: international journal of phytotherapy and phytopharmacology. 2010;17(1):3-13.

33. Teiten M-H, Gaascht F, Eifes S, Dicato M, Diederich M. Chemopreventive potential of curcumin in prostate cancer. Genes & Nutrition. 2010;5(1):61-74.

34. Vermeulen K, Van Bockstaele DR, Berneman ZN. The cell cycle: a review of regulation, deregulation and therapeutic targets in cancer. Cell proliferation. 2003;36(3):131-49.

35. Meyer N, Penn LZ. Reflecting on 25 years with MYC. Nature reviews cancer. 2008;8(12):976-90.

36. Kelly K, Cochran BH, Stiles CD, Leder P. Cell-specific regulation of the c-myc gene by lymphocyte mitogens and platelet-derived growth factor. Cell. 1983;35(3 Pt 2):603-10.

37. Felsher DW. MYC inactivation elicits oncogene addiction through both tumor cell-intrinsic and host-dependent mechanisms. Genes & cancer. 2010;1(6):597-604.

38. Stocker R, Perrella MA. Heme oxygenase-1: a novel drug target for atherosclerotic diseases? Circulation. 2006;114(20):2178-89.

39. Wang J, Xie LY, Allan S, Beach D, Hannon GJ. Myc activates telomerase. Genes & development. 1998;12(12):1769-74.

40. el-Deiry WS, Tokino T, Velculescu VE, Levy DB, Parsons R, Trent JM, et al. WAF1, a potential mediator of p53 tumor suppression. Cell. 1993;75(4):817-25.

41. Vogelstein B, Kinzler KW. p53 function and dysfunction. Cell. 1992;70(4):523-6.

42. Han SS, Chung ST, Robertson DA, Ranjan D, Bondada S. Curcumin causes the growth arrest and apoptosis of B cell lymphoma by downregulation of egr-1, c-myc, bcl-XL, NF-kappa B, and p53. Clinical immunology. 1999;93(2):152-61.

43. Huang C, Ma WY, Goranson A, Dong Z. Resveratrol suppresses cell transformation and induces apoptosis through a p53-dependent pathway. Carcinogenesis. 1999;20(2):237-42.

44.   Hong C, Kim HA, Firestone GL, Bjeldanes LF. 3,3'-Diindolylmethane (DIM) induces a G(1) cell cycle arrest in human breast cancer cells that is accompanied by Sp1-mediated activation of p21(WAF1/CIP1) expression. Carcinogenesis. 2002;23(8):1297-305.

45.   Balmer MT, Katz RD, Liao S, Goodwine JS, Gal S. Doxorubicin and 5-fluorouracil induced accumulation and transcriptional activity of p53 are independent of the phosphorylation at serine 15 in MCF-7 breast cancer cells. Cancer biology & therapy. 2014;15(8):1000-12.

46.   Cohen SB, Graham ME, Lovrecz GO, Bache N, Robinson PJ, Reddel RR. Protein composition of catalytically active human telomerase from immortal cells. Science (New York, NY). 2007;315(5820):1850-3.

47.   Cong Y-S, Wright WE, Shay JW. Human telomerase and its regulation. Microbiology and molecular biology reviews. 2002;66(3):407-25.

48.   Campisi J, Kim SH, Lim CS, Rubio M. Cellular senescence, cancer and aging: the telomere connection. Experimental gerontology. 2001;36(10):1619-37.

49.   Zvereva MI, Shcherbakova DM, Dontsova OA. Telomerase: structure, functions, and activity regulation. Biochemistry Biokhimiia. 2010;75(13):1563-83.

50.   Poole JC, Andrews LG, Tollefsbol TO. Activity, function, and gene regulation of the catalytic subunit of telomerase (hTERT). Gene. 2001;269(1-2):1-12.

51.   Sharma GG, Gupta A, Wang H, Scherthan H, Dhar S, Gandhi V, et al. hTERT associates with human telomeres and enhances genomic stability and DNA repair. Oncogene. 2003;22(1):131-46.

52.   Zhang P, Chan SL, Fu W, Mendoza M, Mattson MP. TERT suppresses apoptotis at a premitochondrial step by a mechanism requiring reverse transcriptase activity and 14-3-3 protein-binding ability. The FASEB journal. 2003;17(6):767-9.

53.   Xi L, Chen G, Zhou J, Xu G, Wang S, Wu P, et al. Inhibition of telomerase enhances apoptosis induced by sodium butyrate via mitochondrial pathway. Apoptosis : an international journal on programmed cell death. 2006;11(5):789-98.

54.   Wesbuer S, Lanvers-Kaminsky C, Duran-Seuberth I, Bölling T, Schäfer K-L, Braun Y, et al. Association of telomerase activity with radio-and chemosensitivity of neuroblastomas. Radiation oncology. 2010;5(1):66.

55.   Zhang X, Mar V, Zhou W, Harrington L, Robinson MO. Telomere shortening and apoptosis in telomerase-inhibited human tumor cells. Genes & Development. 1999;13(18):2388-99.

56.   Hahn WC, Stewart SA, Brooks MW, York SG, Eaton E, Kurachi A, et al. Inhibition of telomerase limits the growth of human cancer cells. Nature medicine. 1999;5(10):1164-70.

57.   Makin G, Hickman JA. Apoptosis and cancer chemotherapy. Cell and tissue research. 2000;301(1):143-52.

58.   Elmore S. Apoptosis: a review of programmed cell death. Toxicologic pathology. 2007;35(4):495-516.

59.   Wong RSY. Apoptosis in cancer: from pathogenesis to treatment. Journal of experimental & clinical cancer research: CR. 2011;30(1):87.

60.   Jayakiran M. Apoptosis-biochemistry: A mini review. Journal of clinical & experimental pathology. 2015;05(01).

61.   Amma Owusu-Ansah SHC, Agne Petrosiute, John J. Letterio, Alex Yee-Chen Huang. Triterpenoid inducers of Nrf2 signaling as potential therapeutic agents in sickle cell disease: a review. Frontiers in medicine. 2015;9(1):46-56.

62.   Valko M, Leibfritz D, Moncol J, Cronin MT, Mazur M, Telser J. Free radicals and antioxidants in normal physiological functions and human disease. The international journal of biochemistry & cell biology. 2007;39(1):44-84.

63.   Hail N, Jr., Cortes M, Drake EN, Spallholz JE. Cancer chemoprevention: a radical perspective. Free radical biology medicine. 2008;45(2):97-110.

64.   Marel AK, Lizard G, Izard JC, Latruffe N, Delmas D. Inhibitory effects of trans-resveratrol analogs molecules on the proliferation and the cell cycle progression of human colon tumoral cells. Molecular nutrition & food research. 2008;52(5):538-48.

65.   Ma Q. Role of nrf2 in oxidative stress and toxicity. Annual review of pharmacology and toxicology. 2013;53:401-26.

66.   Nguyen T, Nioi P, Pickett CB. The Nrf2-antioxidant response element signaling pathway and its activation by oxidative stress. The journal of biological chemistry. 2009;284(20):13291-5.

67.   Townsend GF, Lucas CC. The chemical nature of royal jelly. Biochemical journal. 1940;34(8-9):1155-62.

68.   Ramadan MF, Al-Ghamdi A. Bioactive compounds and health-promoting properties of royal jelly: A review. Journal of functional foods. 2012;4(1):39-52.

69.   Viuda-Martos M, Ruiz-Navajas Y, Fernandez-Lopez J, Perez-Alvarez JA. Functional properties of honey, propolis, and royal jelly. Journal of food science. 2008;73(9):R117-24.

70.   Blum MS, Novak AF, Taber S, 3rd. 10-Hydroxy-delta 2-decenoic acid, an antibiotic found in royal jelly. Science (New York, NY). 1959;130(3373):452-3.

71.   Ratanavalachai T, Wongchai V. Antibacterial activity of intact royal jelly, its lipid extract and its defatted extract. Thammasat international journal of science and technology. 2002;7(1):5-12.

72.   Fujiwara S, Imai J, Fujiwara M, Yaeshima T, Kawashima T, Kobayashi K. A potent antibacterial protein in royal jelly. Purification and determination of the primary structure of royalisin. The journal of biological chemistry. 1990;265(19):11333-7.

73.   Fontana R, Mendes MA, de Souza BM, Konno K, Cesar LM, Malaspina O, et al. Jelleines: a family of antimicrobial peptides from the royal Jelly of honeybees (*Apis mellifera*). Peptides. 2004;25(6):919-28.

74.   Jamnik P, Goranovic D, Raspor P. Antioxidative action of royal jelly in the yeast cell. Experimental gerontology. 2007;42(7):594-600.

75.   Azab KS, Bashandy M, Salem M, Ahmed O, Tawfik Z, Helal H. Royal jelly modulates oxidative stress and tissue injury in gamma irradiated male wister albino rats. North American journal of medicine & science 2011;3(6):268-76.

76.   Shidfar F, Jazayeri S, Mousavi SN, Malek M, Hosseini Af, Khoshpey B. Does supplementation with royal Jelly improve oxidative stress and insulin resistance in yype 2 diabetic patients? Iranian journal of public health. 2015;44(6):797-803.

77.   Mishima S, Suzuki KM, Isohama Y, Kuratsu N, Araki Y, Inoue M, et al. Royal jelly has estrogenic effects in vitro and *in vivo*. Journal of ethnopharmacology. 2005;101(1-3):215-20.

78.   Suzuki K-M, Isohama Y, Maruyama H, Yamada Y, Narita Y, Ohta S, et al. Estrogenic activities of fatty acids and a sterol isolated from royal jelly. Evidence-based complementary and alternative medicine : eCAM. 2008;5(3):295-302.

79.   Nakaya M, Onda H, Sasaki K, Yukiyoshi A, Tachibana H, Yamada K. Effect of royal jelly on bisphenol A-induced proliferation of human breast cancer cells. Bioscience, biotechnology, and biochemistry. 2007;71(1):253-5.

80.   Izuta H, Shimazawa M, Tsuruma K, Araki Y, Mishima S, Hara H. Bee products prevent VEGF-induced angiogenesis in human umbilical vein endothelial cells. BMC complementary and alternative medicine. 2009;9:45-.

81.   Oršolić N, Terzić S, Šver L, Bašić I. Honey-bee products in prevention and/or therapy of murine transplantable tumours. Journal of the science of food and agriculture. 2005;85(3):363-70.

82.   Horwitz W, Latimer GW, Association of Official Analytical Chemists I. Official methods of analysis of AOAC International. Gaithersburg (Maryland): AOAC International; 2006.

83.   Lin D, Xiao M, Zhao J, Li Z, Xing B, Li X, et al. An overview of plant phenolic compounds and their importance in human nutrition and management of type 2 diabetes. Molecules (Basel, Switzerland). 2016;21(10).

84.   Rice-Evans CA, Miller NJ, Paganga G. Structure-antioxidant activity relationships of flavonoids and phenolic acids. Free radical biology and medicine. 1996;20(7):933-56.

85.   Kahkonen MP, Hopia AI, Vuorela HJ, Rauha JP, Pihlaja K, Kujala TS, et al. Antioxidant activity of plant extracts containing phenolic compounds. Journal of agricultural and food chemistry. 1999;47(10):3954-62.

86.   Malla MY MS, Saxena RC, Mohd IM, Abrar HM and Showkat HB. Phytochemical screening and spectroscopic determination of total phenolic and flavonoid contents of eclipta alba linn. Journal of natural product and plant resources. 2013;3(2):86-91.

87.   Guedes AC, Giao MS, Seabra R, Ferreira AC, Tamagnini P, Moradas-Ferreira P, et al. Evaluation of the antioxidant activity of cell extracts from microalgae. Marine drugs. 2013;11(4):1256-70.

88.   Au WW, Heo MY, Chiewchanwit T. Toxicological interactions between nickel and radiation on chromosome damage and repair. Environmental health perspectives. 1994;102 Suppl 9:73-7.

89.   Ratanavalachai TC, Au WW. Effects of reactive oxygen species (ROS) modulators, TEMPOL and catalase, on methoxyacetaldehyde (MALD)-induced chromosome aberrations in Chinese hamster ovary (CHO)-AS52 cells. Mutation Research/Fundamental and Molecular Mechanisms of Mutagenesis. 1996;357(1):25-33.

90.   Whorton EB, Jr. Some experimental design and analysis considerations for cytogenetics studies. Environmental mutagenesis. 1985;7 Suppl 4:9-15.

91.   Nguta JM, Appiah-Opong R, Nyarko AK, Yeboah-Manu D, Addo PGA, Otchere I, et al. Antimycobacterial and cytotoxic activity of selected medicinal plant extracts. Journal of ethnopharmacology. 2016;182:10-5.

92.   Wang P, Henning SM, Heber D. Limitations of MTT and MTS-based assays for measurement of antiproliferative activity of green tea polyphenols. Plos one. 2010;5(4):e10202.

93.   Laemmli UK. Cleavage of structural proteins during the assembly of the head of bacteriophage T4. Nature. 1970;227(5259):680-5.

94.   R. Boyd M. The NCI *in vitro* anticancer drug discovery screen.1997. 23-42.

95.   Han X, Deng S, Wang N, Liu Y, Yang X. Inhibitory effects and molecular mechanisms of tetrahydrocurcumin against human breast cancer MCF-7 cells. Food & nutrition research. 2016;60:30616.

96.   Syed Abdul Rahman SN, Abdul Wahab N, Abd Malek SN. *In vitro* morphological assessment of apoptosis induced by antiproliferative constituents from the rhizomes of *Curcuma zedoaria*. Evidence-based complementary and alternative medicine. 2013;2013:14.

97.   Wongchai V, Ratanavalachai T. Seasonal variation of chemical composition of royal jelly produced in Thailand. Thammasat international journal of science and technology. 2002; 7(2):1-8.

98.   Pavel C, Balkanska R. Comparison of physicochemical parameters in royal jelly from Romania and Bulgaria. Bulletin of university of agricultural sciences and veterinary medicine Cluj-Napoca. 2013;70(1):5.

99.   Jenkhetkan W, Thitiorul S, Jansom C, Ratanavalachai T. Molecular and cytogenetic effects of Thai royal jelly: modulation through c-MYC, h-TERT, NRF2, HO-1, BCL2, BAX and cyclins in human lymphocytes *in vitro*. Mutagenesis. 2017;32(5):525-31.

100.   Liu JR, Yang YC, Shi LS, Peng CC. Antioxidant properties of royal jelly associated with larval age and time of harvest. Food and chemical toxicology. 2008;56(23):11447-52.

101.   Nagai T, Nagashima T, Myoda T, Inoue R. Preparation and functional properties of extracts from bee bread. Die Nahrung. 2004;48(3):226-9.

102.   Ratanavalachai T, Thitiorul S, Jansom C, Jenkhetkan W, Itharat A. Genotoxic and antigenotoxic activities of Thai bee pollen and its extracts in human lymphocytes by *in vitro* sister chromatid exchange assay. Natural product communications. 2017;12(7):1111-4.

103.   Inoue S, Koya-Miyata S, Ushio S, Iwaki K, Ikeda M, Kurimoto M. Royal Jelly prolongs the life span of C3H/HeJ mice: correlation with reduced DNA damage. Experimental gerontology. 2003;38(9):965-9.

104.   Kayashima Y, Yamanashi K, Sato A, Kumazawa S, Yamakawa-Kobayashi K. Freeze-dried royal jelly maintains its developmental and physiological bioactivity in Dro*sophila melanogaster*. Bioscience, biotechnology, and biochemistry. 2012;76(11):2107-11.

105.   Hiyama E, Hiyama K, Yokoyama T, Shay JW. Immunohistochemical detection of telomerase (hTERT) protein in human cancer tissues and a subset of cells in normal tissues. Neoplasia (New York, NY). 2001;3(1):17-26.

106.   Bodnar AG, Ouellette M, Frolkis M, Holt SE, Chiu CP, Morin GB, et al. Extension of life-span by introduction of telomerase into normal human cells. Science (New York, NY). 1998;279(5349):349-52.

107.   Detienne G, De Haes W, Ernst UR, Schoofs L, Temmerman L. Royalactin extends lifespan of through epidermal growth factor signaling. Experimental gerontology. 2014;60:129-35.

108.   Kamakura M. Signal transduction mechanism leading to enhanced proliferation of primary cultured adult rat hepatocytes treated with royal jelly 57-kDa protein. Journal of biochemistry. 2002;132(6):911-9.

109.   Valiollahpoor Amiri M, Deldar H, Ansari Pirsaraei Z. Impact of supplementary royal jelly on *in vitro* maturation of sheep oocytes: genes involved in apoptosis and embryonic development. Systems biology in reproductive medicine. 2016;62(1):31-8.

110.   El-Aidy WK, Ebeid AA, Sallam AE-RM, Muhammad IE, Abbas AT, Kamal MA, et al. Evaluation of propolis, honey, and royal jelly in amelioration of peripheral blood leukocytes and lung inflammation in mouse conalbumin-induced asthma model. Saudi journal of biological sciences. 2015;22(6):780-8.

111.   Ghanbari E, Nejati V, Khazaei M. Antioxidant and protective effects of royal jelly on histopathological changes in testis of diabetic rats. International journal of reproductive biomedicine. 2016;14(8):519-26.

112.   Silici S, Ekmekcioglu O, Eraslan G, Demirtas A. Antioxidative effect of royal jelly in cisplatin-induced testes damage. Urology. 2009;74(3):545-51.

113.   Malekinejad H, Ahsan S, Delkhosh-Kasmaie F, Cheraghi H, Rezaei-Golmisheh A, Janbaz-Acyabar H. Cardioprotective effect of royal jelly on paclitaxel-induced cardio-toxicity in rats. Iranian journal of basic medical sciences. 2016;19(2):221-7.

114.   Tamura T, Fujii A, Kuboyama N. Antitumor effects of royal jelly (RJ). Nihon yakurigaku zasshi Folia pharmacologica Japonica. 1987;89(2):73-80.

115.   Sugiyama T, Takahashi K, Kuzumaki A, Tokoro S, Neri P, Mori H. Inhibitory mechanism of 10-hydroxy-trans-2-decenoic acid (royal jelly acid) against lipopolysaccharide- and interferon-beta-induced nitric oxide production. Inflammation. 2013;36(2):372-8.

116.   Frohlich DA, McCabe MT, Arnold RS, Day ML. The role of Nrf2 in increased reactive oxygen species and DNA damage in prostate tumorigenesis. Oncogene. 2008;27(31):4353-62.

117.   Gharaee-Kermani M, Moore BB, Macoska JA. Resveratrol-mediated repression and reversion of prostatic myofibroblast phenoconversion. Plos one. 2016;11(7):e0158357.

118.   Jenkhetkan W, Thitiorul S, Jansom C, Ratanavalachai T. Genoprotective effects of Thai royal jelly against doxorubicin in human lymphocytes *in vitro*. Natural product communications. 2018;13:79-84.

119. Kensler TW, Wakabayashi N. Nrf2: friend or foe for chemoprevention? Carcinogenesis. 2010;31(1):90-9.

120. Yun D-K, Lee J, Keum Y-S. Finasteride increases the expression of Hemoxygenase-1 (HO-1) and NF-E2-Related Factor-2 (Nrf2) proteins in PC-3 cells: Implication of finasteride-mediated high-grade prostate tumor Occurrence. Biomolecules & therapeutics. 2013;21(1):49-53.

121. Xu D, Mei X, Xu S. [The research of 10-hydroxy-2-decenoic acid on experiment hyperlipoidemic rat]. Zhong yao cai =Zhongyaocai = Journal of Chinese medicinal materials. 2002;25(5):346-7.

122. Koya-Miyata S, Okamoto I, Ushio S, Iwaki K, Ikeda M, Kurimoto M. Identification of a collagen production-promoting factor from an extract of royal jelly and its possible mechanism. Bioscience, biotechnology, and biochemistry. 2004;68(4):767-73.

123. Hattori N, Nomoto H, Fukumitsu H, Mishima S, Furukawa S. Royal jelly and its unique fatty acid, 10-hydroxy-trans-2-decenoic acid, promote neurogenesis by neural stem/progenitor cells *in vitro*. Biomedical research. 2007;28(5):261-6.

124. Yang B, Ma YF, Liu Y. Elevated expression of Nrf-2 and ABCG2 involved in multi-drug resistance of lung cancer SP cells. Drug Research (Stuttg). 2015;65(10):526-31.

APPENDIX

REAGENTS FOR LABORATORY EXPERIMENTS

1. Reagents for SDS-Polyacrylamide gel electrophoresis (SDS-PAGE) preparation

10x running buffer (1L)

25 mM Tris	30.2 g
192 mM glycine	144 g
1% SDS	10 g

Adjust to a final volume of 1,000 mL with deionized water and keep at 4 °C until use.

1x running buffer (working solution)

10x running buffer	100 mL
Distilled water	900 mL

Stacking gel buffer (0.5 M tris-HCl, pH 6.8, 100 mL)

Tris	1.5 g
Deionized water	80.0 mL

Adjust pH into 6.8 and add deionized water to final volume 100 mL

Separating (resolving) gel buffer (1.5 M tris HCl, pH 8.8, 200 mL)

Tris	9.08 g
Deionized water	150 mL

Adjust pH 8.8 and add deionized water to a final volume 200 mL

10% APS (Ammonium per sulfate)

Ammonium persulfate	10.0 g
Deionized water	100 mL

10% SDS (Sodium dodecyl sulfate)

SDS	10.0 g
Deionized water	100 mL

Table A-1 Recipes for resolving and stacking gels

Reagents	Resolving gel		Stacking gel
	7.5%	10%	4%
30% Acrylamide/Bis solution, 29:1 (Bio-Rad)	3.75 mL	5 mL	1.98 mL
Resolving buffer	3.75 mL	3.75 mL	-
Stacking buffer	-	-	3.78 mL
10% SDS	150 µL	150 µL	150 µL
Deionized water	7.28 mL	6 mL	9 mL
10% APS	75 µL	75 µL	75 µL
TEMED	7.5 µL	7.5 µL	15 µL
Total	**15 mL**	**15 mL**	**15 mL**

2. Reagent for Western blot preparation

10x Tris-buffered saline (TBS) for 1 L:

Tris base	24 g
NaCl	88 g

Dissolve in 900 mL distilled water pH to 7.6 with HCl, Add distilled water to a final volume of 1 L.

Tris-buffered saline, 0.1% Tween 20 (TBST) for 1 L:

10x TBS 10x	100 mL
Distilled water	900 mL
Tween 20	1 mL

stripping buffer for 100 mL

10% SDS	20 mL
0.5 M Tris HCl, pH 6.8,	12.5 mL
Distilled water	67.5 mL
β-mercaptoethanol	0.8 mL

10x Towbin Buffer for 1L

25 mM Tris-HCl	30.3 g
192 M glycine	144 g
10% SDS	100 mL
adjust volume to 1 L by distill water	

1x Towbin Buffer for 1 L

10x Towbin Buffer	100 mL
methanol	200 mL
adjust volume to 1 L by distilled water	

BIOGRAPHY

Name	Miss Wantha Jenkhetkan
Date of Birth	November 7, 1984
Education Attainment	2000: Bachelor Degree (Applied Biology) Faculty of Science and Technology Phranakhon Rajabhat University, Thailand
	2007: Master Degree (Biochemistry) Faculty of Science Kasetsart University, Thailand
Scholarship	2011: A grant from Kasetsart University Research and Development Institute, and a TRF-Master Research in master degree
	2012: Teaching Assistantship Scholarship from Thamasat University
	2014: A Doctoral Research Scholarship from Thammasat University
	2015: Travel grant award from The 74th Annual Meeting of the Japanese Cancer Association

Publications

1.   Ratanavalachai T, Thitiorul S, Tanuchit S, Jenkhetkan W, Itharat A. Sakpakdeejaroen I. Synergistic genotoxic effects and modulation of cell cycle by ginger ethanolic extracts in adjunct to doxorubicin in human lymphocytes *in vitro*, Journal of the medical association of Thailand, 98 Suppl 3,S101-9, 2015.

2.   Ratanavalachai T, Thitiorul S, Jansom C, Jenkhetkan W, Itharat A. Genotoxic and antigenotoxic activities of Thai bee pollen and its extracts in human lymphocytes by *in vitro* sister chromatid exchange assay. Natural product communications. 2017; 12(7):1111-4.

3.   Jenkhetkan W, Thitiorul S, Jansom C, Ratanavalachai T. Molecular and cytogenetic effects of Thai royal jelly: modulation through c-MYC, h-TERT, NRF2, HO-1, BCL2, BAX and cyclins on human lymphocytes *in vitro*. Mutagenesis. 2017; 32 (5): 525-31.

4.   Jenkhetkan W, Thitiorul S, Jansom C, Ratanavalachai T. Genoprotective effects of Thai royal jelly against doxorubicin on human lymphocytes *in vitro*. Natural product communication. 2018; 13 (1): 79-84.

5.   Arthornthurasuk S, Jenkhetkan W, Suwan E, Chokchaichamnankit D, Srisomsap C, Wattana-Amorn P, et al. Molecular characterization and potential synthetic applications of GH1 beta-Glucosidase from higher termite *Microcerotermes annandalei*. Applied biochemistry and biotechnology. 2018, 1-18.

Oral/Poster presentation

1.   Jenkhetkan W and Kongsaeree T P. Screening and partial purification of high glucose-tolerance from termite, (Abstract; Oral presentation) The 36th Congress on Science and Technology of Thailand (STT36), p.100, October 26-28, 2010. Bangkok, Thailand.

2.   Jenkhetkan W, Thitiorul S, Itharat A and Ratanavalachai T. *In vitro* genotoxictiy and cytotoxicity of royal jelly in human lymphocytes, (Abstract; Poster presentation) World Congress on Clinical Nutrition (WCCN), p.120, December 1-3, 2014. Ubon Ratchathani, Thailand.

3.   Jenkhetkan W, Thitiorul S, Itharat A and Ratanavalachai T. Protective Effect of Royal Jelly Against Doxorubicin-induced Genotoxicity in Human Lymphocytes *in vitro*, (Abstract; Poster presentation) The 5th Asian Chromosome Colloquium (ACC5). p.121, April 29-May 1, 2015. Bangkok, Thailand.

4.   Jenkhetkan W, Thitiorul S, Itharat A and Ratanavalachai T. Genotoxic and cytotoxic activities of Royal jelly extracts and their interference with cell cycle in human lymphocytes. (Abstract; Poster presentation) The 74th Annual Meeting of the Japanese Cancer Association. p.99, October 8-10, 2015. Nagoya, Japan.

5.   Jenkhetkan W, Thitiorul S, Itharat A and Ratanavalachai T. Protective effects of royal jelly against doxorubicin in human lymphocytes *in vitro* and Its molecular mechanisms. (Abstract; Poster presentation) The 76th Annual Meeting of the Japanese Cancer Association. p.208, September 28-30, 2017. Yokohama, Japan.

6.   Jenkhetkan W, Itharat A, Kongkham S, Reungnoo S and Ratanavalachai T. Antiproliferative effects of 10-Hydroxy-2-decenoic acid against MCF-7 human breast cancer cells: modulation through cyclins, c-MYC, hTERT, BCL2/BAX, HO-1 and NRF2. (Abstract; Poster presentation) The 6th international conferences on biochemistry and molecular biology. p.92, June 20-22, 2018. Rayong, Thailand.